

**Regulation of Fetal Brain Development in Short versus Long Lived  
Mice**

---

A Thesis presented to  
The Faculty of the Graduate School  
University of Missouri-Columbia  
Division of Animal Science

---

In partial Fulfillment  
of the Requirements for the  
Degree Master of Science

---

by

MALIHA ISLAM

Dr. Susanta K. Behura, Thesis Supervisor

July 2022

The undersigned, appointed by the Dean of the Graduate School, have examined  
the thesis entitled

**Regulation of Fetal Brain Development in Short versus Long  
Lived Mice**

Presented by Maliha Islam

A candidate for the degree of Master of Science,

And hereby certify that in their own opinion it is worthy of acceptance.

---

Dr. Susanta K. Behura

---

Dr. Christine G. Elsik

---

Dr. Shawn E. Christ

## **ACKNOWLEDGEMENTS**

I would like to express my sincere appreciation and gratitude to my advisor, Dr. Behura for giving me the opportunity to pursue my master's degree under him, for his guidance and endless support throughout the process. The thorough lab techniques not only enhanced my skills but also trained me to troubleshoot and I appreciate my advisor for his patience throughout the long troubleshooting sessions. I am earnestly honored to be Dr. Behura's graduate student and will always treasure this experience.

I want to thank Dr. Elsik and Dr. Christ for serving in my committee and their enthusiasm in my research. Their expertise has truly enhanced and enriched my research. Their remarkable patience and cooperation throughout the process have been extremely helpful for me.

I express hearty appreciation to all the faculty and staff of ASRC who have shown me the support and have greeted me down the hallways every day of my time there. A huge shout out to those who helped me in each of my experiments and the endless guidance they provided throughout my research.

I have made incredible friends during my time in Mizzou, I would like to express my love and gratitude to the most wonderful friends and colleagues I have met throughout my time there. It would not be possible without them.

Most importantly, I thank my family and friends who have been there in every stage of my life and are my biggest cheerleaders. Being thousands of miles away from them has not been easy but their endless support has never been lessened by the distance and I am grateful for the love and support

## TABLE OF CONTENTS

ACKNOWLEDGEMENTS .....	ii
TABLE OF CONTENTS .....	iii
LIST OF TABLES .....	viii
LIST OF FIGURES.....	x
LIST OF ABBREVIATIONS .....	xvii
Abstract .....	xxi
Chapter 1 .....	1
Literature Review .....	1
Introduction .....	1
Developmental Aging (DevAge) theory: relevance to brain development and aging	4
Aging and brain.....	5
Role of placenta in brain development.....	7
Brain-placental axis.....	9
Early-life link with aging .....	11
Significance of using epigenetic analysis in aging related studies.....	14
Significance of using single nuclei RNA Seq.....	16

Chapter 2 .....	18
Early-life links of brain aging .....	18
<b>Abstract .....</b>	<b>18</b>
<b>Introduction .....</b>	<b>19</b>
<b>Materials and Methods .....</b>	<b>21</b>
Animals .....	21
Epigenetic clock gene profiling.....	22
Whole genome bisulfite sequencing (WGBS) .....	23
WGBS data analysis.....	23
Genomic distribution of methylation sites .....	24
RNA-seq.....	24
RNA-seq data analysis .....	25
Mutual information network analysis .....	25
Statistical analysis .....	26
<b>Results .....</b>	<b>28</b>
Epigenetic clock profiles of male and female brain.....	28
Developmental methylations and brain aging.....	29
Expression of epiclock genes in the brain.....	30
DNA Methylation of placenta and fetal brain.....	31
Expression network of epiclock and signaling genes in brain .....	33
<b>Discussion .....</b>	<b>34</b>

<b>Conclusion.....</b>	<b>38</b>
Chapter 3 .....	55
Dysregulation of fetal brain development in mice lacking Caveolin 1 .....	55
<b>Abstract.....</b>	<b>55</b>
<b>Introduction .....</b>	<b>56</b>
<b>Materials and methods.....</b>	<b>58</b>
Animal Breeding and Sample Collection.....	58
RNA Extraction.....	59
Gene expression profiling by RNA sequencing.....	60
RNA-seq Data Analysis .....	60
Single-nuclei RNA sequencing .....	61
Epigenetic clock profiling .....	63
<b>Results .....</b>	<b>64</b>
Lack of Cav-1 dysregulates fetal brain development.....	64
Functional annotation of the differentially expressed genes.....	65
DNA methylation changes in fetal brain due to lack of Cav-1 .....	67
Lack of Cav-1 leads to dysregulation of specific cell types of fetal brain .....	67
Relationship of gene expression between fetal brain and placenta.....	69
<b>Discussion .....</b>	<b>71</b>
<b>Conclusion.....</b>	<b>76</b>

Chapter 4 .....	90
Use of AKR/J mice to study early-life links of brain aging.....	90
<b>Abstract</b> .....	<b>90</b>
<b>Introduction</b> .....	<b>91</b>
<b>Methods</b> .....	<b>94</b>
Animal Breeding and Sample Collection.....	94
RNA Extraction.....	94
Gene expression profiling by RNA-seq .....	95
RNA-seq data analysis .....	95
Bulk Segregant Analysis (BSA).....	96
Single-nuclei ATAC-seq (snATAC-seq) .....	98
Data analysis of snATAC-seq: .....	99
<b>Results</b> .....	<b>100</b>
Gene expression differences during development of fetal brain of AKR/J relative to C57BL/6J .....	100
Comparative analysis of DE genes of placenta and fetal brain between AKR/J and C57BL/6J .....	105
Epigenetic clock analysis of aging brain.....	106
Identification of segregating loci linked to accelerated brain aging of AKR/J mice	107
Single-cell open chromatin profiling of brain between AKR/J vs C57BL/6J mice	108
<b>Discussion</b> .....	<b>109</b>

<b>Conclusion.....</b>	<b>115</b>
Literature Cited .....	138



## LIST OF TABLES

<b>Table 2.1</b> Number of FB (Female biased) and MB (Male biased) methylations in fetal brain and placenta in different genic and intergenic features of the genome.....	40
<b>Table 2.2</b> Methylation level (beta-value) of mouse epigenetic clock sites in fetal (GD15), postnatal (PND5), and aging (WK70) brains of female and male mice. Associated genes are also shown. ....	41
<b>Table 2.3.</b> List of early-life methylation markers predictive of brain aging in males and females. ....	42
<b>Table 2.4.</b> List of CpG sites showing sex-biased methylation in both placenta and fetal brain. The methylation level is also shown and associated genes are also listed.....	43
<b>Table 2.5.</b> Significant enrichment of specific pathways by the genes that contain either male or female biased methylation in the placenta and fetal brain. ....	45
<b>Table 2.6.</b> List of methylation levels in epiclock and pathway signaling genes showing differential crosstalk in males versus females. The brain epiclock genes which were identified as predictive markers aging and the genes associated with the GnRHR pathway are indicated. ....	46
<b>Table 3.1</b> Differentially expressed genes between GD 12.5 vs 15.5 and GD 15.5 vs 17.5 compared between <i>Cav-1</i> KO and wildtype mice (C57BL/6J).....	78
<b>Table 3.2</b> PANTHER Pathways downregulated during GD 12.5 and 15.5 in both wildtype and <i>Cav-1</i> KO mice female fetal brain.....	79

<b>Table 3.3</b> Gene Ontology biological processes downregulated on gestation days 12.5, 15.5 and 17.5 in wildtype and <i>Cav-1</i> KO female fetal brain. ....	80
<b>Table 3.4</b> Gene Ontology biological processes and PANTHER Pathways differentially expressed in female placenta of wildtype and <i>Cav-1</i> KO strain. ....	81
<b>Table 4.1</b> Gene Ontology (GO) analysis on the female fetal brain at GD 12.5, GD 15.5 and GD 17.5 of AKR/J relative to C57BL/6J. Upregulated biological processes shown as UP and downregulated as DOWN. ....	116
<b>Table 4.2</b> PANTHER Pathway analysis on the female fetal brain at GD 12.5, GD 15.5, and GD 17.5 of AKR/J relative to C57BL/6J. Upregulated biological processes shown as UP and downregulated as DOWN. ....	117
<b>Table 4.3</b> Gene Ontology (GO) analysis on Differentially Expressed Genes (DEGs) of the placenta at gestation day (GD) 15.5 of AKR/J relative to C57BL/6J. ....	118
<b>Table 4.4</b> PANTHER Pathway analysis on differentially expressed genes (DEGs) of the placenta at gestation day (GD) 15.5 of AKR/J relative to C57BL/6J. ....	119
<b>Table 4.5</b> Gene Ontology (GO) analysis of the female fetal brain-placental differentially expressed genes (DEGs) at gestation day (GD) 15.5 of AKR/J compared to C57BL/6J. ....	120
<b>Table 4.6</b> PANTHER Pathway analysis of the female fetal brain-placental differentially expressed genes (DEGs) at gestation day (GD) 15.5 of AKR/J compared to C57BL/6J. ....	121

## LIST OF FIGURES

**Figure 2.1.** **A.** Venn Diagram showing DNA age estimation, based on methylation status of epigenetic clock test, of male and female brain of 70 weeks old mice. **B.** Comparison of methylation of epiclock genes in the male and female brain at fetal stage (gestation day 15) and neonatal stage (postnatal day 5) with aged stage (week 70). **C.** Number of epiclock sites showing consistent female bias or male biased methylation among fetal, postnatal, and aging brain. **D.** Boxplot showing the pattern of variation of female biased epiclock methylation at the three stages in the brain of both sexes. **E.** Heatmap showing variation in methylation of mouse epigenetic clock in the brain of males and females at GD 15, PND5 5, and WK70. The scale on the top left shows the color codes for methylation levels. .... 47

**Figure 2.2.** Neural network modeling of epigenetic clock of brain. **A.** Epigenetic clock with female-biased methylation data was used to train a neural network model. **B.** Separately, the epigenetic clock with male-biased methylation data was used to train the neural network model. The trained models were then used reciprocal predictions of methylation of aging brain, i.e., model from male-biased epiclock data was used to predict methylation level of female aging brain (**C**), and the model from female-biased epiclock data was used to predict methylation level of male aging brain (**D**). The confusion matrix showing the number of true and false prediction relative the observed methylation data is presented in **C and D**..... 48

**Figure 2.3.** Comparison of methylation and expression variation of epiclock prediction makers of brain aging. **A.** Tanglegram showing comparison of methylation and expression patterns the epiclock predictive genes (from neural network modeling) among

the fetal, neonatal, and aging brain of both sexes. **B.** Heatmap of methylation variation of epiclock predictive genes. **C.** Heatmap of expression variation of epiclock predictive genes..... 49

**Figure 2.4.** Comparison of placenta and brain gene expression. **A.** Heatmap of expression of epiclock genes in placenta along with fetal brain, neonatal brain, and aging brain. **B.** Heatmap of expression of non-epiclock genes in placenta along with fetal brain, neonatal brain, and aging brain. **C.** CCA analysis of brain and placenta (GD15) methylation data. the genes overlapping the methylations were grouped as epiclock or non-epiclock genes. CCA was then done on each. Covariates (x=placenta and y=fetal brain of both sexes) were calculated and plotted here. .... 50

**Figure 2.5.** **A.** Boxplot showing that specific sites are methylated in a female-biased (FB) manner in both placenta and fetal brain. **B.** Boxplot showing that specific sites are methylated in a male-biased (MB) manner in both placenta and fetal brain. **C.** Bar plot showing the number of methylations female-biased and male-biased methylations within genes or in intergenic regions. The 2x2 contingency test p-value of association (sex vs. location) is shown. **D.** Venn diagram showing number of genes with either male-biased or female-biased methylation or both male as well as female biased methylation. The cartoons show location of male and female biased methylations in those genes..... 51

**Figure 2.6.** Methylation of repeat elements in placenta and fetal brain. **A.** Schematic representation of methylation of repeat elements either in genic or intergenic regions. **B.** Bar plot showing number of all methylations (sex-biased or not) in different repeat elements. Top repeats (based on number of methylation) are only shown. **C.** Number of sex biased methylations observed in both placenta and fetal brain are differentially

associated (significance level shown) with repeat elements within genes or intergenic regions. **D.** Comparison of methylation level of epiclock sites found within repeat elements among fetal, neonatal, and aged brain of both sexes. **E.** Comparison of methylation level of epiclock sites found within non-repeat elements among fetal, neonatal, and aged brain of both sexes..... 52

**Figure 2.7.** Sex-biased methylation changes among epiclock and signaling genes in the brain. **A.** Principal Component Analysis of male (M) and female (F) biased changes in methylation of epiclock and signaling genes in brain among the fetal, neonatal and aging stages. The data color codes are according to types of gene methylations described in the legend right to the plot. **B.** Circular dendrogram based on hierarchical cluster analysis of female-biased methylations. It shows co-variation of methylation of epiclock and signaling in single cluster. The leaf color in the dendrogram matches to color code description in **A.** The branch color of two clusters is shown in red and green. **C.** Circular dendrogram based on hierarchical cluster analysis of male-bias methylations. It lacks co-variation of methylation between epiclock and signaling genes. The leaf color in the dendrogram matches to color code description in **A.** The branch color of two clusters is shown in red and green..... 53

**Figure 3.1 A.** A hierarchical clustering of gene expression variation also shows that female fetal brain gene expression pattern on GD 12.5, 15.5 and 17.5 is different between the wildtype (BA, BB, BC) and *Cav-1* knockout model (CA, CB, CC). The scale of branch height is shown to the left of the cladogram. .... 82

**Figure 3.2** A principal component analysis of the gene expression variation of female fetal brain on gestation day (GD) 12.5, 15.5 and 17.5. .... 83

**Figure 3.3** Significant changes (False discovery rate < 0.05) of genes in the developing fetal brain of *Cav-1*-KO compared to wildtype C57BL/6J mice at gestation day (d) 12.5, 15.5 and 17.5. The number of upregulated genes is shown by the upward directed arrow, and number of downregulated genes are shown in downward facing arrow. .... 84

**Figure 3.4** Volcano plots showing differential expression of genes in female fetal brain between gestation 12.5, 15.5 and 17.5 compared between wildtype and *Cav-1* KO mice. In each plot, the y-axis shows the  $-\log_{10}$  of the False discovery rate (FDR) values and x-axis shows log of Fold Change (FC) values. The red color shows genes that were downregulated, and blue color shows genes upregulated between the two groups in each plot. The horizontal line above value 0 in axis represent the FDR value of 0.05, the value used to identify significance of differential expression of genes ..... 85

**Figure 3.5. A.** Changes in methylation of epigenetic clock sites of aging genes in d15 fetal brain of *Cav-1*-KO compared to WT mice. **B.** SeqMonk mouse genome browser showing a representative example of positional association between DNA methylation and chromatin occupancy of modified (lysine 3 and 4) histone 3 proteins..... 86

**Figure 3.6.** tSNE plots showing differential cluster patterns of brain cells in the fetal brain (GD15) of WT and *Cav-1* KO mice. Ret: Retinal ganglion cells, Oli: Oligodendrocytes, Mic: Microglia, Tri: Trigeminal neurons, Caj: Cajal-Retzius cells, Epe: Ependymal cells, Int: Interneurons. .... 87

**Figure 3.7 A.** A hierarchical clustering shows that the gene expression variation of female fetal brain and placenta of wildtype is different from *Cav-1* knockout model at GD 15.5. **B.** A hierarchical clustering illustrates that the placenta of female fetus of C57BL/6J is distinct from *Cav-1* KO model at gestation day 15.5. The scale of branch

height is shown to the left of the cladogram. In the figure, WTBR.1 WTBR.2 WTBR.3 indicate wildtype female fetal brain, WTPL.1, WTPL.2, WTPL.3 indicate wildtype female placenta, Cav-1.BR1, Cav-1.BR2, Cav-1.BR3 indicate *Cav-1* KO female fetal brain, Cav-1.PL1, Cav-1.PL2, Cav-1.PL3 indicate *Cav-1* KO female placenta..... 88

**Figure 3.8** Venn Diagram showing differential gene expression between brain-placenta of wildtype and *Cav-1* KO female fetus. In the figure, DOWN means downregulated genes and UP means upregulated genes..... 89

**Figure 4.1** Hierarchical Clustering Analysis of differentially expressed genes at gestation day 12.5 (A), 15.5 (B) and 17.5 (C) of female fetal brain of AKR/J mice relative to C57BL/6J mice. BA, BB, BC are fetal brains of C57BL/6J at every stage. AA, AB, AC are fetal brains of AKR/J at every stage..... 122

**Figure 4.2** Differentially expressed genes at gestation day 12.5, 15.5 and 17.5 of female fetal brain of AKR/J mice relative to C57BL/6J mice. Upregulated genes are shown by the blue upward arrow and downregulated genes shown by downward arrow. .... 123

**Figure 4.3** Volcano plot of differentially expressed genes at gestation day 12.5, 15.5 and 17.5 of female fetal brain of AKR/J mice relative to C57BL/6J mice. Red shows downregulated genes and blue shows upregulated genes. Every dot represents one gene. The plots are made with the accuracy of False Discovery Rate (FDR) 0.05 as mentioned on the plots. .... 124

**Figure 4.4** Principal Component Analysis of differentially expressed genes at gestation day 12.5, 15.5 and 17.5 of female fetal brain of AKR/J mice relative to C57BL/6J mice showing different clustering of AKR/J (solid black line) and C57BL/6J (dotted line) on

GD 12.5 and GD 15.5 and overlapping on GD 17.5. BA, BB, BC are fetal brains of C57BL/6J at every stage. AA, AB, AC are fetal brains of AKR/J at every stage. ....	125
<b>Figure 4.5</b> Hierarchical Clustering Analysis of differentially expressed genes at gestation day 15.5 (B) of female placenta of AKR/J mice (AKR.FPL1, AKR.FPL2, AKR.FPL3) relative to C57BL/6J mice (WTPL.1, WTPL.2, WTPL.3). ....	126
<b>Figure 4.6</b> Venn diagram showing the comparison of differentially expressed genes between the female brain-placenta of AKR/J and C57BL/6J mice. The upregulated brain-placental differentially expressed genes of AKR/J are shown as UP: AKR, downregulated AKR/J genes are shown as DOWN: AKR, upregulated genes of C57BL/6J are shown as UP:BL6 and downregulated genes as DOWN:BL6. ....	127
<b>Figure 4.7</b> Coordinated changes in DNA methylation of fetal brain with placenta in a sex-dependent manner (FB: female bias; MB: male bias). BR=brain, Pl=Placenta, F=female, M=male. ....	128
<b>Figure 4.8</b> BrainYEAR differences between C57BL/6J and AKR/J male and female mice. ....	129
<b>Figure 4.9</b> Cross between AKR/J and C57BL/6J generated 32 F2s. ....	130
<b>Figure 4.10</b> SNP and methylation sites in a region of mouse chromosome 14. These methylations were found in brain of fetal mice. ....	131
<b>Figure 4.11</b> Global gene expression patterns in the brain of young (Y) and old (O) mice of strain AKR/J (column names begin with A) and C57BL/6J (column names begin with B). ....	132



**Figure 4.12** tSNE clusters of brain cells based on variation of open chromatin in C57BL/6J mice. Clusters are shown in different colors. Each dot represents a brain cell. .... 133

**Figure 4.13** tSNE clusters of brain cells based on variation of open chromatin in AKR/J mice. Clusters are shown in different colors. Each dot represents a brain cell. .... 134

**Figure 4.14** Number of cells where open chromatin was identified in male (M) and female (F) brain of C57BL/6J and AKR/J mice. .... 135

**Figure 4.15** Pie chart showing proportion of transcription factor motifs in the open chromatin of the top 20 genes (based on number of peaks of genes) in male and female brain of the two strains. .... 136

**Figure 4.16** Strategy of F2 pooling for BSA-seq analysis. After phenotyping F2s for brain age (brainYEAR score from epigenetic clock analysis), mice representing both ends (low and high) in the variation of brain age, were pooled. The bulk DNA from those two pools was used for whole-genome sequencing. The sequence data was mapped to reference genome of parental mice with low brainYEAR (in this project, it is the genome of C57BL/6J which is the mouse reference genome). Mapping data was used to identify SNPs that were scored based on SNP-index for the two groups as shown. Finally, delta SNP index which is the difference between the two groups was used in sliding window analysis to identify genomic regions that control brain aging. .... 137

## LIST OF ABBREVIATIONS

<i>APOBEC</i>	Apolipoprotein B mRNA editing enzyme, catalytic polypeptide
MYA	million years ago
<i>AD</i>	Alzheimer's Disease
<i>BECon</i>	Blood–Brain Epigenetic Concordance
<i>bp</i>	Base pair
<i>BPA</i>	bisphenol A
BR	Brain
<i>C/T</i>	Cytosine (C) / thymine (T) base pairs
<i>Cav-1</i>	Caveolin 1
<i>CCA</i>	Canonical correlation analysis
<i>cDNA</i>	Complementary DNA
<i>ChiP-seq</i>	Chromatin immunoprecipitation sequencing
<i>Chr</i>	Chromosome
<i>cm</i>	Centimeter
<i>CNS</i>	Central nervous system
<i>CpG</i>	5'-Cytosinephosphate-Guanine-3'
DevAge	Developmental Age Theory
<i>DNA</i>	Deoxyribonucleic acid
<i>DOHaD</i>	Developmental Origins of Health and Diseases
<i>EDTA</i>	Ethylenediaminetetraacetic acid

<i>EM-seq</i>	Enzymatic methyl sequencing
<i>Epiclock</i>	Epigenetic Clock
<i>F</i>	Female
FB	Female Biased
<i>FDR</i>	False discovery rate
<i>FPKM</i>	Fragments per kilobase million
<i>g</i>	g force
<i>g</i>	Gram
<i>G/A</i>	Guanine (G) / adenine (A) base pairs
<i>GD</i>	Gestation Day
<i>GEO</i>	Gene expression omnibus
<i>GnRH</i>	Gonadotropin-releasing hormone
<i>GO</i>	Gene Ontology
<i>HD</i>	Huntington's Disease
<i>HOMER</i>	Hypergeometric Optimization of Motif EnRichment
KO	Knockout
<i>logFC</i>	Log fold change
<i>M</i>	Male
<i>M-value</i>	log ratio of methylated to unmethylated read counts
<i>MAPK</i>	Mitogen-activated protein kinase
MB	Male Biased
<i>MB</i>	Megabase

MI	mutual information theory
<i>MI</i>	Mutual information
<i>ml</i>	Milliliter
<i>MLV</i>	Murine Leukemia Virus
<i>MRI</i>	Magnetic resonance imaging
<i>MRMR</i>	Maximal relevance minimum redundancy
<i>mRNA</i>	Messenger RNA
<i>NES</i>	Normalized enrichment score
<i>ng</i>	Nanogram
NN	Neural network
OGT	O-linked N-acetylglucosamine transferase
<i>PANTHER</i>	Protein Analysis Through Evolutionary Relationships
<i>PCA</i>	Principal component analysis
<i>PD</i>	Parkinson's Disease
PL	Placenta
<i>PND</i>	Postnatal Day
<i>polyA</i>	Polyadenylate
<i>REST</i>	RE1-Silencing Transcription factor
<i>RNA</i>	Ribonucleic acid
<i>RNA-seq</i>	RNA sequencing
ROS	Reactive Oxygen Species
<i>SNP-index</i>	Single Nucleotide Polymorphism index

<i>SNP(s)</i>	Single nucleotide polymorphism(s)
<i>TF</i>	Transcription factor
UMAP	uniform manifold approximation and projection
<i>UTR</i>	Untranslated region
<i>WGBS</i>	Whole genome bisulfite sequencing
<i>WK</i>	Week
<i>XIC</i>	X-chromosome inactivation
$\mu$ l	Microliter

# **Regulation of Fetal Brain Development in Short-Long Living Mice**

Maliha Islam

Dr. Susanta K. Behura, Thesis Supervisor

## **Abstract**

How fetal brain development is regulated in mice with reduced life span is a primary objective of this research. Three studies were performed to investigate the fetal brain development in short and lived mice strains. The scientific premise and background of brain development and aging are provided review of literature (Chapter 1). In the first study (Chapter 2), experiments were performed to test early-life origin of brain aging. Mouse epigenetic clock (epiclock) database which represents specific genomic sites that are methylated in an age-correlated manner was profiled in three life stages: fetal (gestation day 15), postnatal (day 5), and adult (week 70) brains of male and female C57BL/6J inbred mice. Data analysis showed that the female adult brain was epigenetically younger than the male adult brain even when the chronological age (time from birth) was the same (week 70). Specific methylations in the developing brain predictive of epigenetic differences in the aging brain between sexes were identified by predictive modeling by neural network. This study also showed that gene expression of epiclock genes were similar between placenta and fetal brain. However, genes unrelated to epiclock did not show this pattern. Whole-genome bisulfite sequencing identified sites that were methylated in a coordinated manner in the placenta and in a sex-specific manner in the fetal brain. These sites showed that methylation level in the epiclock genes and genes associated with gonadotropin-releasing hormone (GnRH) signaling pathway

genes changes in a fetal-sex dependent manner both in the placenta and fetal brain. Furthermore, these methylations were maintained in the brain in the adult life stages. These findings suggested the fetal origin of sex differences in brain aging is epigenetically linked to the placenta. In the second study (Chapter 3), experiments were performed to test if reducing life span of mouse by ablating Caveolin 1 (*Cav-1*), a pro-longevity gene that codes for an abundant structural protein of plasma membrane in endothelial cells, dysregulate brain development at the fetal stage. Further relevance of studying this specific gene is that mice lacking Cav-1 show neurodegeneration and multiple hallmarks of Alzheimer's disease (AD) at an early age. As a result, most *Cav-1*-null mice die within a year. Gene expression in bulk brain tissue as well as single cells were analyzed in the *Cav-1*-null fetal brain compared to the wildtype (WT). The results of this study showed that lack of *Cav-1* leads to extensive dysregulation of genes of fetal brain at specific gestation time (day 15). Several epigenetic clock genes were differentially methylated in *Cav-1*-KO compared to WT mouse fetal brain. Single nuclei RNA sequencing identified specific glial and neuronal cells being dysregulated in the fetal brain due to the absence of *Cav-1*. In addition, methylation analysis was performed to investigate effect of *Cav-1* on epiclock genes. Based on these results, a model was proposed for fetal links of Alzheimer's symptoms in mice lacking *Cav-1*. Lastly, in the third study (Chapter 4), experiments were performed to test if reduced lifespan in mice due to murine leukemia virus induced cancer influences fetal brain development. In this experiment, gene expression pattern of fetal brain and placenta of AKR/J mice, which mostly survive for a year due to onset of cancer, was compared with C57BL/6J mice to understand molecular and cellular links between aging and leukemia. The C57BL/6J has

longer life span (> 2 years) and is refractory to AK virus that causes leukemia in AKR/J mice. The gene expression studies showed that genes related to aging and neurodegenerative diseases are differentially regulated in the fetal brain and placenta of AKR/J mice compared to that in C57BL/6J. Targeted methylation profiling of a total of 2,045 single bases of mouse genome, which are associated with mouse epigenetic clock data, showed that brain of AKR/J mice ages faster than C57BL/6J mice suggesting a link between leukemia and neuronal aging. By generating a F2 mapping population from AKR/J x C57BL/6J crosses, Bulk Segregant Analysis (BSA) was performed with the pooled DNA of F2 progenies by whole-genome sequencing to identify genetic variants associated with accelerated brain aging in AKR/J mice. Single-cell ATAC-seq (Assay for Transposase-Accessible Chromatin by sequencing) analysis further predicted that specific transcription factors are involved in the differential gene regulation of fetal brain in AKR/J mice compared to C57BL/6J mice. Together, the results of these study provide foundational knowledge to establish molecular and cellular links between reproduction and aging.



# Chapter 1

## Literature Review

### *Introduction*

An unsolved yet fundamental question in reproductive biology is how a brain develops in the fetus, and whether gestational influences on the brain during development has long-term effect on offspring health and disease. Use of animal models is helpful to perform experimental studies on fetal brain development primarily due to ethical challenges associated with the research on human fetus. The mouse is a widely used model organism for human health and disease because its genome is 99% similar to the human genome and the small size of the animal enables researchers to conduct cost-efficient studies. Mouse models have been used for preclinical studies, including drug trials, because the phenotyping of genetically engineered mice can be done at a large scale that provides valuable information on how the gene functions in human health (Vandamme, 2014). For aging related studies, *Caenorhabditis elegans* and fruit fly, *Drosophila melanogaster*, have been extensively used because of their simplicity and short lifespan. Short lifespan of mice allows researchers to study the aging mechanisms effectively. Additionally, mice have similar pathologies associated with aging that are similar to the humans. However neurodegenerative diseases do not naturally occur in mice. Fetal development from gestation day 15 to postnatal day 10 resembles the third trimester of human fetal development (Workman et al., 2013) (Bolon, 2015). Therefore,

genetically modified mice are developed to address these age-related phenomenon (Folgueras et al., 2018). Mouse models are also used to study reproductive aging in humans.

C57BL/6J mice have been increasingly used in aging and longevity studies. The 18-24 month old mice have the human age equivalency of 56-69 years old (Flurkey et al., 2007). The knockout mouse model for the gene Caveolin-1 (*Cav-1*) is an example of mouse model investigation of human aging (Hattori et al., 2006; Head et al., 2010a, 2010b; van Helmond et al., 2007; F. Wang et al., 2018). The strains of origin of *Cav-1* null mice are 129/Sv, SJL and C57BL/6J. *Cav-1* is a major structural protein called caveolae which is like a flask shaped lipid pocket of plasma membrane. It is abundant in endothelial cells but is also present in many other cell types. *Cav-1* is a known pro-longevity gene. Additionally, *Cav-1* plays a major role in the regulation of angiogenesis in mice (Chang et al., 2009). Mice lacking the *Cav-1* gene have been shown to have impaired endothelia as there are no caveolae membranes in the endothelial cells (D. S. Park et al., 2003). In mice as well as in human placenta, caveolae membranes are formed in endothelial cells and also in smooth muscle cells and mesothelial cells of the yolk sac (Mohanty et al., 2010). Ablation of *Cav-1* reduces mice lifespan by nearly 50% (D. S. Park et al., 2003). *Cav-1* null mice, though viable and fertile, show hyperproliferative and vascular abnormalities (Razani et al., 2001). At young age (3-6 month old), these mice exhibit neuronal aging which resembles > 18 months of aging in wild-type mice (Head et al., 2010c). The *Cav-1* null mice show Alzheimer's like symptoms as early as 3-6 months after birth (Head et al., 2010a). Increased amyloid beta, tau, astrogliosis and decreased

cerebrovascular volume are observed in the brain of these mice (Head et al., 2010a). As *Cav-1* plays a key role to modulate beta-secretase activity (Hattori et al., 2006), association of *Cav-1* with AD pathologies in these mice has been suggested (Head et al., 2010a).

Besides use of mouse models in studying aging related neurodegeneration, inbred mouse strain AKR/J that expresses murine leukemia viruses (MLVs) are also used to study aging related onset of leukemia. MLVs are retroviruses belonging to the gammaretroviral genus that cause cancer in mice. Endogenous MLVs integrated into the host genome are passed from one generation to the next by germ line. The AKR/J inbred mouse genome contains AK virus (AKV) as an endogenous MLV. Ecotropic expression of AKV is found in all tissues from birth in these mice (Herr & Gilbert, 1982). Leukemia progression occurs in an age-dependent manner in AKR/J mice. Onset of leukemia occurs as early as three months of age, and most of them (60 to 90%) show terminal cancer by age 10 months and die within a month or two thereafter. In an earlier study, genetic mapping identified a locus (*AKv1*) that control mouse genome susceptibility to AKV (Rowe et al., 1972). Subsequently, a second locus (*AKv2*) was identified for AKV susceptibility (Kozak & Rowe, 1980). In a relatively recent study it was shown that the Apolipoprotein B gene *Apobec3* can also be associated with AKV susceptibility to AKR/J but refractory to C57BL/6J mice (Langlois et al., 2009).

*Developmental Aging (DevAge) theory: relevance to brain development and aging*

The developmental aging (DevAge) theory proposed by Dilman (Dilman, 1971a) suggests that developmental processes have commonalities with the process that regulates aging. Genomics and systems-biology studies have revealed that DevAge is evolutionarily conserved between mice and human (de Magalhães & Church, 2005; Feltes et al., 2015a). Development of the central nervous system is a highly coordinated spatiotemporal process that includes the proliferation of glia and neurons and their migration, followed by programmed cell death, formation of synapses, myelination, and establishment of neuronal circuits. The development of the neural tube in mouse fetus begins at gestation day 9-9.5 (Greene & Copp, 2014). A histology atlas of mouse fetal brain shows that during GD 12.5 the forebrain is proliferated and expanded at a fast rate especially the medial, lateral, and caudal ganglionic sections. Also, choroid plexus first appears at this stage and the hypothalamus starts to grow bigger in the diencephalon. In addition, the olfactory (CN1) nerves grow from the multi-layered olfactory epithelium in the caudodorsal nasal cavity and hippocampi is still not developed at this stage. Moreover, the hindbrain goes through significant changes in its conformation along with differentiation of Purkinje cells start during GD 11 to 13. Simultaneously, the mantle and marginal zones of the spinal cord start growing at this stage. Also, the spinal cord expands laterally in the ventral horn more than the thoracic and lumbar divisions. The progression of fetal brain development is also shown during GD 15.5 when the six layers of the cerebral cortex are distinctive with neurons developing to make the layers superficial. Many neurons such as GABAergic inhibitory neurons develop through the

growing cerebral cortex. By GD 15.5 the pituitary stalk is also formed. Additionally in the hindbrain the population of neurons grow rapidly at this stage and the spinal cord columns are more prominent. Simultaneously at GD 15.5 the cranial nerves also are distinctive in the spinal cord. Progressively, different developmental stages occur during GD 17.5 when the forebrain is significantly developed with prominent layers. By this stage the pituitary gland gets well developed and the Rathke's pouch can be visualized as a small cleft. Also, the neurosecretory structures for hormones such as oxytocin develop in the forebrain. Moreover, in the hindbrain the Purkinje cells are well formed and in the spinal cord. The structure is very similar to the adult stage where the sympathetic nervous system starts to appear first in this stage. Most of the fetal brain development occurs before birth but the hippocampus, olfactory bulb and granule cells develop in the postnatal stages (V. S. Chen et al., 2017). In the early gestation age, the brain has more short-range connections and in the late gestation age, the brain develops to more long-range connections in different regions of the brain.

### *Aging and brain*

As the global population is aging at a higher rate than ever before (World, 2001), aging related diseases continue to be the primary contributors of morbidity and mortality among older people (Franceschi et al., 2018). Many chronic diseases of brain (Peters, 2006), kidney (Nitta et al., 2013), liver (Premoli et al., 2009), lung (Rojas et al., 2015) and heart (Steenman & Lande, 2017) impact health at old ages. Aging causes physiological and functional decline of all organs, and leads to clinical complications

such as metabolic syndrome (Bechtold et al., 2006), multiple organ failure (Neild, 2001), and decline of endocrine and immune systems (Fabbri et al., 2015). While regulation of organ aging at the molecular level is poorly understood, emerging evidence suggests that different organs age at differential rates (Ori et al., 2015; Pavanello et al., 2020; Schaum, Lehallier, Hahn, Pálovics, Hosseinzadeh, Lee, Sit, Lee, Losada, Zardeneta, Fehlmann, Webber, McGeever, Calcuttawala, Zhang, Berdnik, Mathur, Tan, Zee, Tan, Pisco, et al., 2020). Thus, understanding factors that influence organ aging at the molecular level is significant.

The brain consumes a significant proportion of energy throughout life. The brain represents approximately 2% of body weight but more than 20% of the body oxygen is used by the brain alone. As a result, aging has a distinct effect on brain compared to all other organs. The aging is the primary risk factor for neurodegenerative diseases such as Alzheimer's disease. As the brain ages in mice, rats, chimpanzees, and humans, many biological pathways alter and there is an induction of stress response genes. With aging, there is a reduction in mitochondrial gene expression which can be related to the increased stress response gene expression. Calorie restriction in mice also changes the lifespan through oxidative stress gene expression. In humans, the age-associated downregulated genes are involved in various synaptic functions needed for memory mediation and learning. In contrast, the upregulated genes include stress response, antioxidant defense, immune function, and DNA repair in many different cortical areas of aging human brain. Similar results have also been shown in rats. Moreover, studies have

shown consistent results supporting decline in the cognitive functions in mammalian brain (Yankner et al., 2008).

Brain cells are connected through a vascular network of blood vessels spreading over different sections of brains. Blood vessels in the cerebral cortex play a critical role in oxygen, glucose, and other nutrients transport in the brain. The fractional vascular volume in a ten week old adult mouse brain is  $0.018 \pm 0.004 \text{ mm}^3 \text{ per mm}^3$ , the normalized vascular length is  $0.44 \pm 0.04 \text{ m per mm}^3$ , and the mean diameter of the micro vessels is  $4.25 \pm 0.08 \text{ }\mu\text{m}$  (L.-Y. Zhang et al., 2018). In humans, the temporal correlational dynamics of different regions of the brain, called Functional Connectivity, changes with aging (Edde et al., 2021).

Risk of neurological disorders can be conditioned by sex differences in the fetal brain (Clayton, 2016; McCarthy, 2016a; Thibaut, 2016a). The brain ages differentially in males compared to females (Armstrong et al., 2019a; Goyal et al., 2019a). In humans, specific brain disorders occur in old ages at a higher frequency in one sex over the other (Young & Pfaff, 2014).

### *Role of placenta in brain development*

Viviparous female animals retain the developing eggs in their reproductive tracts where the offspring grow using maternal resources. The word placenta originally means “circular cake” and refers to a transient organ found in viviparous species. It is formed

through the apposition of the embryonic and parental tissues, resulting in physiological exchange between maternal resources and the embryo. Conversely, oviparous animals lay developing or unfertilized eggs that grow in an external environment followed by hatching. Based on phylogenetic analyses, viviparity emerged in more than 142 separate occasions during the evolution of vertebrates. The evolution of viviparity is proposed to be the result of different environmental conditions such as temperature and altitude. (Blackburn D. G., 1999).

The reproductive and developmental processes are highly diverse in animals (Ackerman, 1992). The bilaterian animals appeared ~600 million years ago (MYA) and adapted numerous strategies to reproduce and develop. Matrotrophy is one of them. Matrotrophy refers to the provision of maternal resources to progeny during reproduction and early development in placental animals. In oviparous animals, the mode of maternal nourishment is called lecithotrophy where maternal nutrients are stored in the egg that is then used for embryo development. In eutherian mammals such as humans, pigs and mice, maternal nutrients are transferred to the fetus by the placenta. There are striking differences in the feto-maternal interface among placental animals (Roberts et al., 2016). The placenta of pig is diffuse as placentation occurs all over the allantochorion. It is also epitheliochorial (Leiser & Dantzer, 1988) as there are different tissue layers that separate direct contact of the fetus from the maternal blood. On the other hand, mouse placenta is discoid and hemochorial (same as of humans) (Soares et al., 2018). The maternal blood comes in direct contact with the mouse fetus. Other animals, such as dogs and cats, have zonary placenta where the feto-maternal contact zone forms a belt around the chorionic



sac. Despite these differences, placenta plays highly conserved roles in fetal development in animals- to supply nutrient and oxygen to the fetus, collect fetal waste, and safeguard the fetus from infections and other external conditions.

### *Brain-placental axis*

Defective neuronal development due to dysfunctional placenta can lead to different neuropsychiatric disorders in childhood and later in life in humans (Kratimenos & Penn, 2019a). There is a remarkable similarity among the placental animals in the process of cortical development during fetal brain formation (Molnár & Clowry, 2012). Placental dysfunction can lead to defective neuronal development that can lead to brain disorders such as autism spectrum or attention deficit hyperactivity disorders in early childhood or chronic neuropsychiatric diseases such as schizophrenia, depression and dementia in later in life (Kratimenos & Penn, 2019c). Emerging evidence suggests that placenta plays key roles in brain development (Zeltser & Leibel, 2011). Inadequate placental support can impact developmental process of the brain and increase risk of brain diseases later in life (Gagnon, 2003). There is a remarkable coordination in gene expression between the placenta and fetal brain of mice suggesting robust regulation of the brain-placental axis (Behura, Kelleher, et al., 2019a). The brain-placental axis plays important roles in fetal programming of brain development and developmental origin of health and disease later in life (Behura, Dhakal, et al., 2019a). However, the ‘rules of life’ by which the female reproductive physiology and maternal nourishment of embryo has shaped the evolution of brain development in animals remains unsolved. Placenta originated only ~65 MYA (dos Reis et al., 2012) compared to ~600 million years of

evolution of animal brain. To understand how matrotrophy might have influenced the evolution of mammalian brain development (*aka* brain-matrotrophy axis), it is necessary to investigate brain of placental and non-placental animals. Some invertebrates such as lizards and cockroaches have placenta-like analogs (Blackburn, 2015; Dyke et al., 2014; Gao et al., 2019). By performing a large-scale comparative analysis of matrotrophy across the animal kingdom, Ostrovsky and colleagues suggested that placenta analogs in arthropods could be the simplest form of placentotrophy where specific cells, unlike a fully formed organ, may be involved in transferring nutrient from the parent to progeny (Ostrovsky et al., 2016). Whether placental analogs play role in brain development in those organisms remains unknown. Specific intracellular metabolism mechanisms are believed to be highly conserved. Serotonin transporters (SERT) play crucial roles in serotonergic control of cellular metabolism (Yabut et al., 2019). Serotonin is present in all species, and plays highly conserved roles in early developmental processes including development of brain (Bonnin et al., 2011; Rosenfeld, 2020; Turlejski, 1996). The production of serotonin (synthesized from tryptophan) is critical for reproductive processes to support protein production, fetal growth, brain development and regulation of the brain-placental axis (Badawy, 2015; Rosenfeld, 2020). The placenta synthesizes serotonin from maternal food (dietary tryptophan) which plays crucial roles in neurodevelopmental processes of the fetal brain (Velasquez et al., 2013). In mammals, dysregulation in serotone level during perinatal stage has negative impacts on brain development that lead to different behavioral disorders later in life (Shah et al., 2018).

### *Early-life link with aging*

Studies have suggested that aging and longevity processes have early-life origins (Gluckman et al., 2008; 2014; Vaiserman, 2019a). Understanding how early life developmental processes influence health and well-being later in life is an important research area that falls under the broad umbrella of research efforts collectively termed as *Developmental Origins of Health and Diseases* (DOHaD) (D. J. P. Barker, 2007; Wadhwa et al., 2009). The foundation of these research efforts is based on the Baker hypothesis (D. J. Barker & Osmond, 1986) which suggests that adverse conditions during intrauterine life and early developmental stages can cause irreversible alteration in physiology and metabolism that leads to heightened risk of diseases in adulthood. These projects not only benefit our knowledge on the early-life origins of human diseases but also bear significance to public health and society at large (Penkler et al., 2019). The story on “*How the First Nine Months Shape the Rest of Your Life*” featured on the TIME magazine cover on 04 October 2010 is an example of the public perception about the significance of this research area. Furthermore, a relatively recent article describes the broad significance of the DOHaD research as follows: “*When tracing how life environments affect health and disease, it is of utmost social and political importance...*” (Penkler et al., 2019). With the advent of DOHaD research coordination in early 2000s, diverse research themes have emerged to address basic and translational aspects of early-life origins of human health and diseases (Gage et al., 2016; Heindel & Vandenberg, 2015). This includes research on dissecting molecular mechanisms that commonly control fetal development and aging processes, which is the founding principle of the

Dilman theory of developmental-aging (DevAge) (Dilman, 1971b). Recent studies using genomics and systems-biology approaches have supported the DevAge theory, and have further revealed that the developmental-aging link is evolutionarily conserved between mouse and human (de Magalhães & Church, 2005; Feltes et al., 2015b).

Links between lifespan and reproduction have been hypothesized from studies that observed correlations between gestation times and maximum life span among different mammals, placental shape and lifespan of tall and short men, and lifespan and fertility of women. Though these studies have suggested that reproduction and lifespan may have common regulatory mechanisms, no study has directly demonstrated the functional relationship between the two. This is a major gap in our knowledge to understand placental role in offspring health and aging of the brain.

In addition, the aging brain is susceptible to several chronic diseases that occur in a sex-biased manner. Though a male fetus is generally associated with a higher risk than female fetus *in utero*, the early-life origin of sexual dimorphic aging remains a mystery. Sex differences may also influence placental function that can influence offspring health and disease. At birth, males are 4-6 weeks behind females physiologically but have higher weight than females (Copper et al., 1993). Though the growth difference is not altered by maternal diet, a male fetus shows a higher dependency on the maternal diet intake than the female fetus (Eriksson et al., 2010). This sex-biased dependency on nutrition during early development exposes male fetuses to higher risk of different obstetric problems than female fetuses. The O-linked N-acetylglucosamine transferase (OGT) plays an important role in modulating placental functions to respond to the

maternal supply and fetal demand for nutrients (Howerton et al., 2013; Howerton & Bale, 2014). OGT is expressed in the placenta in a sex-biased manner that influences fetal growth and stress response (Hart et al., 2019). Moreover, the placenta develops faster with male fetuses compared to female fetuses (Kalisch-Smith et al., 2017) suggesting sex-specific regulation of placental responses during fetal development (Rosenfeld, 2015).

Aging and longevity processes are hypothesized to have functional links to early-life developmental events (Aguilaniu, 2015a; Bianco-Miotto et al., 2017; Vaiserman, 2019a). An earlier study suggested that telomere biology plays a significant role in the fetal programming of aging processes (Entringer et al., 2018). Also, dysfunctional placenta can cause abnormal brain development leading to neurological disorders later in life (Zeltser & Leibel, 2011). Different factors associated with reproduction including gestation time (Fushan et al., 2015a), placenta development (D. J. P. Barker et al., 2011a), and fertility (Müller et al., 2002) are thought to have links with longevity. Studies have also shown that sex has a differential effect on longevity (Austad & Fischer, 2016). For example, the female brain is persistently younger than male brain at the metabolic level (Armstrong et al., 2019a; Goyal et al., 2019a). In mammals, dysregulation in serotone level during perinatal stage has negative impacts on brain development that lead to different behavioral disorders later in life (Shah et al., 2018). While the placental role in fetal programming is documented (Bronson & Bale, 2016; Denisova et al., 2020; Jansson & Powell, 2013; Koukoura et al., 2012; Kratimenos & Penn, 2019b), the role of placenta in organ aging remains unexplored.

### *Significance of using epigenetic analysis in aging related studies*

The development of placenta and the fetal brain is controlled by various epigenetic mechanisms (Nelissen et al., 2011; Petanjek & Kostović, 2012). DNA methylation, chromatin accessibility, and microRNAs, among others, play important roles in epigenetic regulation of genes in the placenta as well as fetal brain (Klemm et al., 2019; Martin et al., 2017; Mouillet et al., 2015; Nelissen et al., 2011; Petanjek & Kostović, 2012). DNA methylation plays pivotal role in epigenetic regulation of genes during development as well as aging. In the human, DNA methylation occurs in a sex-biased manner in the placenta to support fetal growth (Tekola-Ayele et al., 2019a). Methylation at discrete sets of CpG (5'-Cytosinephosphate-Guanine-3') sites, often referred to as 'epigenetic clock', have been used not only to determine the biological age of organs but also to predict life span in mice and humans (Horvath, 2013; Meer et al., 2018; Stubbs et al., 2017a). Recent studies also show that the placental epigenetic clock is a reliable predictor of gestational age (Y. Lee et al., 2019) and fetal growth (Tekola-Ayele et al., 2019b). Besides DNA methylation, chromatin accessibility to different transcription factors influences the regulation of genes associated with placenta development (Abdulghani et al., 2019). The repressor element 1 silencing transcription factor (REST), when binding to the accessible chromatin, recruits multiple corepressor complexes to influence different developmental processes (Ooi & Wood, 2007). In addition, microRNAs also act as important epigenetic modulators of genes to control developmental processes of the placenta and fetal brain (Hayder et al., 2018; Miranda,

2012), and also to regulate aging and longevity processes (Grillari & Grillari-Voglauer, 2010; Murphy, 2010). Gene regulation by circulating microRNAs during pregnancy is also known (M. Cai et al., 2017).

The major molecular and cellular hallmarks of aging are epigenetic modification, loss of proteostasis, cellular senescence, deregulated nutrient sensing, mitochondrial dysfunction, telomere attrition and stem cell exhaustion, among others (López-Otín et al., 2013). Change in DNA methylation pattern in aging cells and resulting tissue change is a process commonly known as epigenetic drift (Sierra et al., 2015). DNA methylation is a major component of epigenetic drift in aging organs, and study has shown that methylation occurs in a sex-biased manner in the placenta to support fetal growth (Tekola-Ayele et al., 2019a). Also, methylation changes of epigenetic clock are reliable predictors of biological aging of organs (Horvath, 2013; Meer et al., 2018; Stubbs et al., 2017a). DNA methylation of the placenta is also correlated with gestational age (Y. Lee et al., 2019) and fetal growth (Tekola-Ayele et al., 2019b). In human, abnormal DNA methylation of placenta is associated with Down syndrome (Jin et al., 2013). Besides methylation, the chromatin accessibility to regulatory proteins, particularly transcription factors, also influences molecular regulation of the aging processes (Jänes et al., 2018; Koohy et al., 2018; Ucar et al., 2017). REST also plays roles in controlling other biological processes including embryonic stem cell self-renewal, cellular plasticity, neuronal excitement and longevity (Gopalakrishnan, 2009; Zullo et al., 2019). In the embryonic stage, REST promotes stem cell pluripotency by suppressing neuronal genes in embryonic stem cells and blocking neuronal differentiation (Gupta et al., 2009; Singh

et al., 2008). A recent study has shown that REST controls processes of neuronal activities and acts as potent regulator of longevity (Zullo et al., 2019).

### *Significance of using single nuclei RNA Seq*

The advent of single-cell genomics has provided new insights into developmental processes including that of fetal brain (Briggs et al., 2018; Marioni & Arendt, 2017; Plass et al., 2018). Single-cell analysis provides new avenues to identify homologous cells that regulate gene expression in a similar manner in unrelated species to develop common phenotypes (Tarashansky et al., 2020). ‘Cell type homology’, which is an emerging concept in evolutionary developmental biology (Sachkova & Burkhardt, 2019), commonly refers to specific cells that use the same regulatory program to drive differentiation (Arendt et al., 2019). Evolution in molecular regulatory mechanism dictates cell type homology, a proposition (Sachkova & Burkhardt, 2019) that has been widely supported from recent single-cell functional genomics studies including regulation of cell types of microglia (Geirsdottir et al., 2019), evolution of cellular regulatory networks (Sebé-Pedrós et al., 2018), and brain development (Hu et al., 2020; Konstantinides et al., 2018; Pembroke et al., 2021). A recent study performed integrated analysis of single-cell RNA-seq (scRNA-seq) and single-cell open chromatin profiling data of cerebral organoids derived from human, chimpanzee, and macaque, and found that chromatin accessibility changes dynamically in developing brain cells that modulate gene expression between species (Kanton et al., 2019). While neural development in vertebrate animals stems from large numbers of apical and basal progenitor cells of the



neuroepithelium, these processes in fly brain arise from only a few progenitor cells. The recent spur in multimodal single-cell genomics (C. Zhu et al., 2020) is bringing new opportunities to dissect deep homology at single-cell level. As an example, integration of single-cell RNA-seq and metabolomics data provides insights into the dynamics of metabolic flux of different cell types (Damiani et al., 2019; Evers et al., 2019), and provides a new approach to translate bulk metabolomics data into single-cell metabolomics based on single-cell gene expression data (Wylter et al., 2017).

## Chapter 2

### Early-life links of brain aging

#### Abstract

Fetal programming is known to influence adult health and diseases. Whether aging is programmed at the fetal stage remains unknown. To test this hypothesis, mouse epigenetic clock (epiclock) test was performed at three life stages: fetal (gestation day 15), postnatal (day 5), and adult (week 70) brains of male and female C57BL/6J inbred mice. Data analysis showed that the female adult brain was epigenetically younger than the male adult brain even when the chronological age was the same (week 70). Specific methylation sites in the developing brain could predict the epigenetic differences in the aging brain between sexes. The epiclock genes showed similar expression pattern between placenta and fetal brain. Genes unrelated to epiclock did not show this pattern. Whole-genome bisulfite sequencing identified sites that were methylated in a sex-bias manner between placenta and fetal brain. Genes associated with the gonadotropin-releasing hormone receptor (GnRHR) pathway accumulated methylation that varied in a correlated manner with that of epiclock genes, and in a fetal-sex dependent manner between placenta and fetal brain. Evidence of transcriptional crosstalk among the epiclock and GnRHR pathway genes were found in the placenta and was maintained in

the brain throughout the adult life stages. Collectively, these findings suggested the fetal origin of sex differences in brain aging and epigenetically link to the placenta.

## **Introduction**

The link of aging with reproduction has been shown in multiple studies (Aguilaniu, 2015a; Bianco-Miotto et al., 2017; Vaiserman, 2019a). Placenta development (D. J. P. Barker et al., 2011a), Gestation length (Fushan et al., 2015a), along with fertility (Müller et al., 2002) have been suggested to have influences on aging in humans as well as animals. Furthermore, sex has been shown to influence organ aging (Austad & Fischer, 2016). Sex-specific gene expressions were found in different organs during aging (Schaum, Lehallier, Hahn, Pálovics, Hosseinzadeh, Lee, Sit, Lee, Losada, Zardeneta, Fehlmann, Webber, McGeever, Calcuttawala, Zhang, Berdnik, Mathur, Tan, Zee, Tan, Tabula Muris Consortium, et al., 2020). Interestingly, the female brain remains persistently younger than the male brain in humans (Armstrong et al., 2019a; Goyal et al., 2019a).

Placental role in fetal programming is well documented (Bronson & Bale, 2016; Denisova et al., 2020; Jansson & Powell, 2013; Koukoura et al., 2012; Kratimenos & Penn, 2019b). Recently, it has been shown that the placenta plays adaptive roles to safeguard fetal brain development from adverse conditions during the period of pregnancy (Behura, Dhakal, et al., 2019b). We showed a coordinated increase or decrease

of specific receptor and ligand genes between the placenta and fetal brain in our earlier study, suggesting they have roles in the regulation of the murine brain-placental axis (Behura, Kelleher, et al., 2019a). In addition, differential expression of different aging genes in the male and female fetal brain were evident in response to ablation of *Foxa2* which is an essential gene required for pregnancy establishment, in the uterus (Dhakal et al., 2021a). Also, we recently illustrated the sex-bias regulation of some specific genes during fetal brain development in pigs (Strawn et al., 2021). Furthermore, other studies suggested that epigenetic and metabolic changes in the fetal brain can have an impact on overall health later in life (Behura, Dhakal, et al., 2019c) remarkably elevating the risk of metabolic disorders of the brain (Dhakal et al., 2021b).

DNA methylation is a significant factor of epigenetic regulation of aging (Johnson et al., 2012; Jones et al., 2015; Rath & Kanungo, 1989; Sierra et al., 2015). Methylation, the majority of which occur in CpG (5'-Cytosine-phosphate-Guanine-3') sites, changes in a correlated manner with age. CpG methylation, a reliable predictor of biological age of different organs, can be identified using epigenetic clock (epiclock) test. In several studies, methylation changes were profiled in the brain during aging (Farré et al., 2015; Numata et al., 2012; Rath & Kanungo, 1989) and in the developing brain at fetal stages and aberrant methylation in the fetal brain was found to influence the risk of brain diseases later in life (Pidsley et al., 2014; Rachdaoui & Sarkar, 2014). The commonalities in morphometric changes that occur in the brain during developmental stages support the aging of the brain (Tammes et al., 2013). These studies have

collectively suggested that aging of the brain and the processes that regulate the development are not mutually exclusive. Mice models provided valuable insights on aging-related disorders and epigenetic regulation of brain development (Alberry & Singh, 2020; Hirabayashi et al., 2013; H. Kim et al., 2016; Niculescu et al., 2006), including the influence of sex on epigenetic regulation of brain function and development (Cortes et al., 2019; Ratnu et al., 2017; Spiers et al., 2015). However, the epigenetic relation between development and aging of brain is yet to be speculated. The present study aims to test if development and aging of brain have epigenetic connections and determine whether such links are influenced by placenta and fetal sex.

## **Materials and Methods**

### *Animals*

Adult C57BL/6J mice were mated. The day vaginal plug was observed was considered as GD 0, and on GD 15, dams were euthanized in CO<sub>2</sub> followed by cervical dislocation. We selected GD 15 because the placenta was fully developed, and the brain-placental crosstalk was confirmed during this stage (Behura, Kelleher, et al., 2019b). The placenta was carefully separated from the metrial gland and decidua, and the fetal brain was meticulously collected using curved forceps. All the samples were washed in PBS and snap-frozen in liquid nitrogen. Sex was determined by PCR (Dhakal & Soares, 2017). A total of 12 fetal brains and placenta were collected (3 replicates x 2 tissue types x 2 sexes).

We further collected three replicates of male and female brains from postnatal day 5 (PND5) and 70 weeks old mice (WK70). All animal procedures were approved by the Institutional Animal Care and Use Committee of the University of Missouri and were conducted according to the National Institute of Health Guide for the Care and Use of Laboratory Animals.

### *Epigenetic clock gene profiling*

DNA of GD15, PND5 and WK70 male and female brains were profiled for methylation status of the mouse multi-tissue epigenetic clock genes (Vaiserman, 2019b). Briefly, DNA from frozen brain samples was purified using the Quick-DNATM Miniprep Plus kit (Cat. No. D4068). EZ DNA Methylation-LightningTM Kit (Cat. No. D5030) was used to perform the bisulfite conversion, followed by enrichment for target loci and sequencing on an Illumina® HiSeq instrument. Sequence reads were identified using Illumina base calling software and aligned to the mouse reference genome (GRCm38) using *Bismark* (Krueger & Andrews, 2011) which was also used for methylation calling. Methylation level was estimated as the proportion of reads mapped to each cytosine relative to the total number mapped reads to the site. Comparison was done between the methylation data of each brain sample and the reference mouse epiclock data to estimate epigenetic age by Zymo's DNAge® predictor tool as described earlier (Coninx et al., 2020).

### *Whole genome bisulfite sequencing (WGBS)*

Genome-scale DNA methylation was profiled of GD15 female and male fetal brain and placenta. DNA was extracted using *Genra Puregene Tissue Kit* (catalog #158667, Qiagen) as per the manufacturer's instruction. Equimolar amounts of DNA from the three biological replicates were pooled for each sample and used for global methylation profiling as described earlier (Docherty et al., 2009). After bisulfite conversion of DNA, NEBNext® Ultra™ II DNA Library Prep Kit (New England Biolabs, MA) was used to generate sequencing libraries. Library preparation and sequencing were performed at the University of Missouri Genomics Technology Core. The libraries were sequenced to 20x genome coverage (150 bases sequence reads) using NovaSeq 6000.

### *WGBS data analysis*

Data analysis was performed by *Bismark* (Krueger & Andrews, 2011). Briefly, the GRCm38 genome sequences were bisulfite converted and indexed using the '*bismark\_genome\_preparation*' function. The read alignment was performed by *bowtie2* aligner implemented within *Bismark* (Langmead & Salzberg, 2012). The methylation sites were extracted using the *bismark\_methylation\_extractor* to generate methylation coverage of each sample in genome-wide manner. The coverage files contained

chromosome name, start position, end position, methylation percentage, and number of methylated, and unmethylated reads for each CpG site. We only focused on CpG sites as they represent the majority of methylations in mammalian genomes (Moore et al., 2013). The sites that had low coverage (read counts < 8) were excluded from further analysis (Y. Chen et al., 2018). The count data was converted to beta-values of methylation as described earlier (Du et al., 2010).

#### *Genomic distribution of methylation sites*

All genomic computations were performed using the *BEDTools* (Quinlan & Hall, 2010) to identify methylation in different features of genomic locations based on genome annotation (GRCm38) obtained from UCSC Genome Browser. In addition, *Awk*, *grep*, and *sed* custom codes were used whenever required to perform specific data analyses such as filtration and counting of methylation sites in different annotation features.

#### *RNA-seq*

RNA-seq was performed to profile gene expression of PND5 and WK70 brains of both sexes. The RNA-seq data of fetal brain and placenta of males and females were generated from the same strain and same gestation day in our recent study (Dhakal et al., 2021a), publicly available in the Gene Expression Omnibus database (accession # GSE157555). TRIzol (Catalog 15596026, Thermo Fisher) based protocol was used to



isolate total RNA followed by treatment with DNase I to remove genomic DNA which was further purified using a RNeasy MinElute Cleanup Kit (Qiagen). The RNA quality was checked using a Fragment Analyzer (Advanced Analytical Technologies). The RNA concentration was determined using a Qubit 2.0 Fluorometer (Life Technologies). Libraries were prepared from total RNA using the Illumina TruSeq Stranded Total RNA with Ribo-Zero Gold Library Prep Kit at the University of Missouri Genomics Technology Core. Each library was sequenced (~30 million paired end reads, 150 bases read length) using Illumina NovaSeq 6000 sequencer.

#### *RNA-seq data analysis*

RNA-seq data analysis was performed as described in our earlier works (Dhakal et al., 2021a; Strawn et al., 2021). Briefly, the quality of raw sequences was checked with FastQC followed by trimming the adaptors from the sequence reads by *cutadapt*. The *fqtrim* tool was used to perform base quality trimming (Phred score >30) by sliding window scan (6 nucleotides). The quality reads were then mapped to the mouse reference genome GRCm38 using Hisat2 aligner (D. Kim et al., 2015). Read counting from the alignment data was performed by *FeatureCounts* (Liao et al., 2014). The feature count data was then analyzed using packages in R.

#### *Mutual information network analysis*

The mutual information theory (MI) approach (Steuer et al., 2002a) was used to infer gene expression networks. MI is a measure of the information content that two variables share: a numerical value ranging from 0 to 1 depending on, intuitively, how much knowing one variable would predict the variability of the other. We calculated MIs in a pair-wise manner, both at sample and gene levels, to generate a weighted adjacency matrix by the Maximum Relevance Minimum Redundancy (MRMR) method (Radovic et al., 2017). Then mutual information network analysis was performed using *minet* (Meyer et al., 2008) followed by network visualization by *GGally*.

### *Statistical analysis*

All statistical tests were performed in *R*. Chi-Square analysis was performed to infer the significance of 2x2 contingency tests. Enrichment analysis was performed by Fisher exact tests followed by multiple corrections of *p*-values by False Discovery Rate (FDR). Comparison of variation between methylation and expression was based on beta-values of methylation (Du et al., 2010) and fragment per kilobase per million (FPKM) values of expression (Mortazavi et al., 2008). Distance calculation of methylation and expression variation was based on the *Euclidean* method. Hierarchical clustering was performed from the distance measures by *ward.D2* as the method of agglomeration. Comparison between clusters (tanglegram analysis) was performed using the package *dendextend*. The canonical correlation analysis was performed by *cancor* function of *CCA* package. In this analysis, expression of epiclock genes in the GD15 fetal brain was

treated as the dependent variable (y-values) and that of placenta was treated as the independent variable (x-values). Correlation coefficients (coefficients of x and y values) were multiplied with the respective data matrices of fetal brain and placenta to generate covariates that were used for comparison. To train neural network models by backpropagation using the weight backtracking method the *neuralnet* package was used (Riedmiller, 1994). A neural network consists of three layers: input-layer that takes training data that the model would learn, hidden-layer that uses backpropagation to optimize the weights of the input variables to train the model, output-layer that predicts variable of test data by the trained model. The methylation data of the aging brain was used as predicted values, and those of fetal and postnatal brains were used as predictor values. The trained model was used to separately predict the methylation in male and female aging brains. Finally, the observed and model-predicted values of the aging brain in both sexes were compared using *caret* to identify methylations in the developing brain that were predictive of methylations in the aging brain.

## Results

### *Epigenetic clock profiles of male and female brain*

DNA methylation of mouse epiclock genes was profiled in GD15 (gestation day 15), PND5 (postnatal day 5), and WK70 (week 70) brains of both sexes (**Table 2.1**). The methylation data were used in epigenetic age (also called DNA age) analysis (Handl et al., 2019) which showed that despite the chronological age of the animals, the female brain was biologically younger (29.6 weeks) than the male brain (38.1 weeks). The female brain showed an elevated level of methylation than the male brain for 854 sites, whereas the male brain showed higher methylation than the female brain for 1,028 sites (**Figure 2.1a**). A lower level of epiclock methylation was observed in the fetal and postnatal brain compared to the aging brain of week 70 (**Figure 2.1e**). Methylation level changed in the brain among the three life stages (fetal, postnatal, and aging) in a sex-biased manner (**Figure 2.1b**). No significant bias was observed in a 2x2 contingency analysis relative to the number of sites with either increased or decreased methylation in male and female brains between fetal and postnatal stages ( $P=0.84$ ), but a significant ( $P < 0.0001$ ) difference was observed between postnatal and aging stages. Upon aging, a greater number of sites showed increased methylation in the brain of males compared to females (**Figure 2.1b**). Furthermore, specific epiclock genes were found to be methylated in a sex-specific manner at all three life stages. A total of 245 epiclock sites showed an increased methylation in the female brain compared the male brain at fetal, postnatal, and

adult stages (**Figure 2.1c**). In contrast, an opposite pattern was observed with 187 sites (**Figure 2.1d**). Also, the median methylation level of female bias sites was consistently higher for that of the male bias sites (**Figure 2.1d**). Moreover, the female-bias sites showed an increased level of variation in methylation level than that of male-bias sites, and this pattern was consistent at the each of the stages.

### *Developmental methylations and brain aging*

Neural network (NN) modeling was used to test whether methylation changes of epiclock genes at developmental stages (fetal and postnatal) in the brain are predictors of methylation of the adult aging brain (**Figure 2.2**). NN modeling leverages training data at the input layer and learns data variation of predicted variable relative to predictors via predefined hidden layers and performs prediction of the variable of interest from a test data at the output later. The epiclock methylation status of the brain at fetal and postnatal stages was used to train a neural network (NN) model to learn the corresponding changes in methylation of the aging brain separately in males and females. To predict the methylation status of the aging brain in both sexes, the trained models were used. In the female brain, the NN converged after 778 iterative steps (number of optimizations at an error rate of less than 5%) with an average error rate of 1.69 in the female brain (**Figure 2.2a**). However, the models converged with only 175 iterations and an average error of 1.15 in the male brain (**Figure 2.2b**). This reinforces our observation that variation in epiclock methylation is relatively elevated in the female brain compared to the male

brain. The confusion matrix showing the number of true and false predictions relative to the observed data (**Figure 2.2c and d**) shows that the model identified 131 methylations in the brain that occurred in the fetal and postnatal stages and are predictive of epiclock changes in the brain upon aging. They included the 76 and 37 predictive methylations for brain aging in females and males respectively among which some are shown in **Table 2.3**.

#### *Expression of epiclock genes in the brain*

RNA was sequenced to profile gene expression of the same brain samples used for methylation analysis. Methylation changes of the predictive markers identified from *neuralnet* analysis (listed in **Table 2.3**) were compared with the expression level of the cognate genes in the brain at each stage. The tanglegram in **Figure 2.3a** showed that low methylation leads to higher expression in the fetal brain. In contrast, an increase in methylation suppressed these genes in the brain upon aging (**Figure 2.3b and c**).

We further compared expression changes of the epiclock genes in the brain relative to the placenta by hierarchical clustering (**Figure 2.4a**). The analysis showed that epiclock genes were expressed in the fetal brain more similarly with the placenta than the postnatal and aging brain. However, the genes which are not related to mouse epiclock did not show this pattern (**Figure 2.4b**). In non-epiclock genes, expression of fetal brain grouped with that of the postnatal and aging brain, and placental gene expression was

distinct. This suggested that the epigenetic clock is coordinately expressed between the fetal brain and placenta. Furthermore, canonical correlation analysis (CCA) (Zhuang et al., 2020) was performed to determine if epiclock gene expression of the fetal brain was canonically correlated with the placental one. CCA showed that covariates of expression (which is expression multiplied with the correlation coefficient) of epiclock genes in the fetal brain showed a positive correlation with the placenta (**Figure 2.4c**). However, such relationship was not present in the expression of non-epiclock genes. This corroborated our idea that epigenetic clock genes are active during pregnancy and is likely regulated in the brain-placental axis (Behura, Dhakal, et al., 2019a; Behura, Kelleher, et al., 2019a)

#### *DNA Methylation of placenta and fetal brain*

To further analyze the global methylation patterns of the placenta comparatively with fetal brain in both males and females, whole-genome bisulfite sequencing (WGBS) was performed. WGBS (available at GEO, accession# GSE157553) identified 15,269 sites and 17,028 CpG methylated sites in female-biased (FB) and male-biased (MB) manner respectively in both fetal brain and placenta (**Figure 2.5a and b**). Female-biased (FB) methylation sites had higher methylation level in the female fetal brain and placenta. In contrast, the male-biased (MB) methylation sites had higher methylation level in the male fetal brain and placenta. Several of the genomic position and methylation level of these sites are provided in **Table 2.4**. A significant bias ( $P=0.0003$ ) was observed in the relative location of these methylation sites within genes relative to intergenic regions

(**Figure 2.5c**). While some genes harbored either female-biased or male-biased methylations, genes were also identified that harbored both (**Figure 2.5d**).

The sex-biased methylations in gene bodies were predominantly found in introns and accounted for roughly 11-fold more than those found in exons (**Table 2.1**). Also, frequency of sex-biased methylations was low in the untranslated regions (UTRs). We found 630 FB and 587 MB methylations within *cis*-regulatory regions but rarely in the promoters and Refseq functional elements, which are nongenic human and mouse elements derived and validated from the literature (Farrell et al., 2022). Sex biased methylations were more frequent in CpG shores than CpG islands (**Table 2.1**). Moreover, many sex-biased methylations were identified within repeat elements, most of which were retrotransposons, both within genic and intergenic regions. We showed that the number of sex-biased methylations was significantly different between genic and intergenic repeats and methylation occurred at an elevated level in repeats compared to in non-repeat sequences (**Figure 2.6**). As these methylations occurred in both the placenta and fetal brain, the results suggest a role of heterochromatin methylation in sex-biased epigenetic regulation of fetal brain and placenta (Brown et al., 2012; Chatterjee et al., 2016; Decato et al., 2017; Spiers et al., 2015).

Functional annotation of genes harboring these methylations, showed significant enrichment of specific pathways (Fisher exact test,  $P < 9.05$ ), most of which were related to signaling. The overrepresented pathways with the highest fold enrichment are listed in



**Table 2.5.** Furthermore, genes with female-biased methylations were enriched with T cell activation, Huntington disease, FGF, and Cadherin signaling pathways. Genes with male-bias methylations were enriched with pathways of axon guidance mediated by netrin, histamine H1 receptor-mediated signaling, thyrotropin-releasing hormone receptor signaling, and heterotrimeric G-protein signaling. In addition, specific pathways were commonly enriched by genes harboring both FB and MB methylations (see **Table 2.5**).

*Expression network of epiclock and signaling genes in brain*

We identified specific epiclock genes and signaling pathway genes that were methylated in a coordinated manner in both placenta and fetal brain. Principal component analysis (PCA) of 327 sex-biased methylations that occurred in these genes (listed in **Table 2.6**) showed that these methylations occurred in single clusters with the epiclock and signaling genes (**Figure 2.7a**). Also, hierarchical cluster analysis showed that these methylations grouped together in signaling and epiclock genes but in a differential manner in males compared to females. Clustering was performed to split the dendrograms into two clusters ( $k=2$ ) which showed specific epiclock genes and signaling genes clustered in one of the clusters when those genes harbored methylation that was FB in both placenta and fetal brain. However, that pattern was not observed with MB methylations. This suggested the coordinated methylation pattern of specific epiclock genes along with specific signaling genes in both placenta and fetal brain when they harbored female-biased methylations. Thus, we wanted to know what those specific

genes were. We found that those genes included epiclock genes that were identified as predictors of brain aging from the *neuralnet* analysis and specific genes of the gonadotropin-releasing hormone receptor (GnRHR) pathway (**Table 2.6**).

Mutual information network analysis (Steuer et al., 2002b) of expression changes of those specific signaling genes and epiclock genes (**Table 2.6**) further showed that they interacted in males compared to females in a differential manner (**Figure 2.8a and b**). We further found that that the expression of these genes was mutually informative in the brain and the placenta as shown in the *Circos* plots in **Figure 2.8c and d**. The plots show that expression changes of these genes in the placenta have commonalities (shared arches) with the fetal, postnatal, and aging brain (**Figure 2.8c and d**). This suggested that crosstalk among the epiclock and GnRHR pathway genes in the placenta is epigenetically maintained in the brain throughout life in a sex-biased manner.

## **Discussion**

The epigenetic age was estimated in male and female brain of mice strain C57BL/6J. The epigenetic age of the male brain was higher than the female brain, but the chronological age was the same (70 weeks). This suggested that the biological aging of the brain is sexually dimorphic. Sexual dimorphisms of the brain have been reported in different animals, including birds (Hutchison et al., 1995), flies (Cachero et al., 2010), rodents and humans (Gorski, 1985). Particularly, sex differences in brain aging have been

investigated in several studies (Armstrong et al., 2019b; Coffey et al., 1998; Costantino & Paneni, 2020; Guebel & Torres, 2016; Rothwell et al., 2022). Our results in mice is consistent with the similar observation in humans where the female brain is known to remain younger than the male brain in a persistent manner (Goyal et al., 2019a). Studies on evolution suggest that natural selection may shape brain neoteny (youth), and such selective forces vary between and within species (Rothwell et al., 2022; Somel et al., 2009). Also, aging of the brain can vary at an individual and population levels within species (Kverková et al., 2020; Vidal-Pineiro et al., 2021). Such variation in brain aging has been studied in humans (Brewster et al., 2019). Inbred mouse strains are also known to age differentially (Yuan et al., 2009), showing evidence that sex has influences on aging (Mitchell et al., 2016).

DNA methylation changes in the brain during development and aging (L. Li et al., 2020; Numata et al., 2012; Tognini et al., 2015). Our data showed that specific CpG sites are persistently methylated in a sex-specific manner in fetal, postnatal, and old age. Mouse epigenetic clock, a reliable predictor of aging (Stubbs et al., 2017b), identified CpGs (n=275) that were methylated higher in females than males. Relatively fewer sites (n=187) showed methylation higher in males than females at all three stages. Interestingly, the female biased sites were more in number and had a higher level of methylation than male bias sites (**Figure 2.1**). This implied that the female brain may be persistently methylated at a higher level than the male brain, which supported the idea that the female brain is actively methylated to suppress genes that lead to brain

masculinization (Nugent et al., 2015). Applying the predictive modeling approach, we identified specific epiclock methylation and associated genes as predictors of brain aging in both sexes.

Methylation had an impact on the expression of epiclock genes in the brain (**Figure 2.3**). Methylation level was lower in the brain at fetal and postnatal stages compared to old age whereas expression level was higher in postnatal and old ages than in fetal stage. This contrasting pattern gave evidence to support that methylation likely suppressed gene expression at the postnatal stage in mice. An earlier study in humans has shown that at the postnatal age the brain transcriptome undergoes a significant remodeling (Somel et al., 2009). We further showed that epiclock gene expression of the fetal brain was more like that of the placenta than the neonatal or aging brain. Non-epiclock genes lacked this pattern. Expression of those genes in the fetal brain was more like the brain at postnatal and aging stages than the placenta. This suggested that transcriptional crosstalk between the placenta and fetal brain may be differentially regulated for epiclock genes compared to non-epiclock genes. This prompted us to profile global methylation of the placenta relative to the fetal brain in both sexes.

Whole-genome methylation profiling was performed with the fetal brain and placenta to account for any tissue-specific variation in DNA methylation (Horvath, 2013; Stubbs et al., 2017a; Teschendorff et al., 2020). Common methylation sites and concordance in DNA methylation between different tissues with accumulated

methylation at specific sites are known (Hannon et al., 2021). Methylation in the brain is known to have concordance with blood. Concordance in DNA methylation in mouse placenta and fetal brain in response to exposure to polychlorinated biphenyls (Laufer et al., 2021) and prenatal stress (Jensen Peña et al., 2012) were shown, suggesting possible crosstalk in epigenetic changes between the placenta and fetal brain during pregnancy. We observed from the WGBS data that the placenta and fetal brain coordinated methylation of specific CpG sites in a sex-biased manner (**Figure 2.5**). Methylation occurred in gene bodies more often than in intergenic regions, which supports earlier reports that gene body methylations play essential roles in placental functions (Lim et al., 2017; Schroeder et al., 2015). We observed that the sex-biased methylations was higher in different repeat elements including L1 retrotransposons, Alu repeats and short interspersed repeats (**Figure 2.6**) further showing evidence that repeated DNA methylation may influence physiological processes of pregnancy (Gruzieva et al., 2019) as well as aging processes of brain (Rath & Kanungo, 1989).

A key finding of this study is the evidence of crosstalk of the epigenetic clock with GnRHR pathway in the placenta and fetal brain. Our data showed CpG sites associated with specific epigenetic clock and GnRHR pathway genes (**Table 2.6**) methylated in statistically clustered patterns in both the placenta and fetal brain. The methylation pattern was different in fetuses of both sexes. Network analysis of expression of these genes further demonstrated a link between the placenta and the fetal brain that is maintained in the brain at postnatal and the aging stage. GnRH plays key roles in

mammalian reproduction by inducing luteinizing hormone (LH), and follicle-stimulating hormone (FSH). Also, it has functions in DNA modification required to express the target genes in gonadotrope (Melamed et al., 2018). Besides a role in the anterior pituitary, GnRH also plays major roles in the placenta, likely to modulate the maternal-fetal interface (Sasaki & Norwitz, 2011). Gonadotropin production varies in a sex-dependent manner during late gestation, in which fetal androgen plays a critical regulatory function in mice (Kreisman et al., 2017). Moreover, regulation of GnRH is suppressed by androgen in males, which plays pivotal roles in brain masculinization (Zuloaga et al., 2008). Suppression of genes associated with brain masculinization is mediated by DNA methylation in the female brains (Nugent et al., 2015). Multiple studies suggested that exposure to sex hormone at the fetal stage plays a leading role in sex-specific fetal programming of cellular metabolism that creates a differential risk to metabolic diseases later in life (Dearden et al., 2018; Hägg & Jylhävä, 2021), including a metabolic decline of the brain (Goyal et al., 2019b).

## **Conclusion**

To conclude, this study suggests that fetal sex influences the epigenetic crosstalk between fetal brain and placenta that is linked to the sex-biased aging program of the brain. Also, our results support the DevAge theory (Dilman, 1971c) which states that early-life developmental processes have common links to aging processes and highlight

that aging is a biological process that originates from the fetal stage and persists throughout the later stages of life.

**Table 2.1** Number of FB (Female biased) and MB (Male biased) methylations in fetal brain and placenta in different genic and intergenic features of the genome.

<b>Feature</b>	<b>FB</b>	<b>MB</b>
Exon	662	730
Intron	7594	8141
UTRs	298	331
Promoter	3	4
CpG island	1	3
CpG shore	165	175
Refseq Functional Element	14	20



**Table 2.2** Methylation level (beta-value) of mouse epigenetic clock sites in fetal (GD15), postnatal (PND5), and aging (WK70) brains of female and male mice. Associated genes are also shown.

Chromosome	Position	Name	F_BR_GD15	F_BR_PND5	F_BR_WK70	M_BR_GD15	M_BR_PND5	M_BR_WK70	Gene_name
1	32172750	1-32172750	0.001215067	0.00456621	0.001963351	0.003930818	0.001623377	0.007194245	Khdrbs2
2	18800576	2-18800576	0.010757378	0.021183346	0.098827773	0.008666004	0.024535316	0.149434704	Carlr
3	53477663	3-53477663	0.907038513	0.852130326	0.787556904	0.89785832	0.673343606	0.787661406	Proser1
4	40229898	4-40229898	0.960171017	0.95460441	0.951617604	0.955917713	0.935718617	0.970364542	Ddx58
5	21373477	5-21373477	0.541202673	0.481081081	0.653061224	0.517060367	0.527881041	0.641935484	Ccdc146
6	5297577	6-5297577	0.124763705	0.046791444	0.100478469	0.092029581	0.060928433	0.122854562	Pon2
7	19303711	7-19303711	0.045977011	0.07480315	0.218023256	0.040100251	0.05664488	0.260340633	Fosb
8	22566876	8-22566876	0.947660756	0.93729097	0.86746988	0.936261261	0.948269955	0.813284359	Slc20a2
9	21792884	9-21792884	0.269831731	0.127704117	0.180578287	0.287228405	0.13229104	0.21319797	Kank2
10	33624501	10-33624501	0.006849315	0.01594533	0.006702413	0.002945508	0.005291005	0.001297017	Clvs2
11	3160011	11-3160011	0.880535667	0.890525781	0.8820012	0.876858584	0.86722979	0.870711619	Sfi1
12	78749659	12-78749659	0.008824456	0.003913894	0.007282658	0.00562527	0.002511301	0.013949433	Mpp5
13	43559423	13-43559423	0.079320113	0.020231214	0.07768595	0.120063191	0.050955414	0.028513238	Mcur1
14	31641051	14-31641051	0.000864678	0.001610306	0.001620746	0.003407984	0.001251564	0.001645639	Hacl1
15	74751284	15-74751284	0.828838357	0.724596144	0.640053227	0.836333578	0.612273642	0.667590028	Lynx1
16	10502161	16-10502161	0.021176471	0.078947368	0.395973154	0.029761905	0.138263666	0.381132075	Ciita
17	29326177	17-29326177	0.122844828	0.197160883	0.695710456	0.182628062	0.255842558	0.677664975	Pil6
18	32430782	18-32430782	0.928981565	0.89018148	0.77815797	0.903990399	0.89468232	0.748406677	Bin1
19	6830335	19-6830335	0.011640212	0.113018598	0.369200395	0.002614379	0.103979461	0.454655381	Rps6ka4

**Table 2.3.** List of early-life methylation markers predictive of brain aging in males and females.

<b>Methylation site</b>	<b>Gene</b>	<b>Fetal brain</b>	<b>Postnatal brain</b>	<b>Aging brain</b>	<b>Neuralnet result</b>
10-54755455	Khdrbs2	0.83098592	0.799191375	0.73565381	Predictive of brain aging in female
10-121150451	Tns1	0.95439469	0.959183673	0.970037453	Predictive of brain aging in female
11-97626436	Brinp2	0.17851959	0.321721311	0.700342466	Predictive of brain aging in female
11-101165647	Clvs2	0.55225989	0.866161616	0.914498141	Predictive of brain aging in female
15-102460507	Abca7	0.64544139	0.573699422	0.670899471	Predictive of brain aging in female
1-137182659	Rhot1	0.96491228	0.913972603	0.895018747	Predictive of brain aging in male
10-79888816	Unc45b	0.67190227	0.634974533	0.773553719	Predictive of brain aging in male
10-121150433	Bcas3	0.94322344	0.896720167	0.910039113	Predictive of brain aging in male
11-48845486	Srcin1	0.42694497	0.479259259	0.716759003	Predictive of brain aging in male
13-107680956	Stard3	0.93743372	0.937759336	0.897897898	Predictive of brain aging in male

**Table 2.4.** List of CpG sites showing sex-biased methylation in both placenta and fetal brain. The methylation level is also shown and associated genes are also listed.

Name	Chromosome	Position	Gene	Brain (female fetus)	Placenta (female fetus)	Brain (male fetus)	Placenta (male fetus)	Sex bias pattern
1-4037421	1	4037421	Rpl	0.26303441	1	-0.4150375	-1.5849625	Female bias
2-3459224	2	3459224	Dclre1c	1	0.48542683	0	-0.4150375	Female bias
3-5398964	3	5398964	Zfx4	0.5849625	0.5849625	0	-0.4854268	Female bias
4-6429147	4	6429147	Nsmaf	2.169925	0.67807191	-0.4150375	0	Female bias
5-3584384	5	3584384	Rbm48	2.32192809	1.32192809	0	0	Female bias
6-4083012	6	4083012	Bet1	1	1.22239242	-0.4150375	-0.1926451	Female bias
7-3686598	7	3686598	Mboat7	1.22239242	0.73696559	-0.4150375	-0.4854268	Female bias
8-4311639	8	4311639	Elavl1	1	0.48542683	-0.5849625	-0.5849625	Female bias
9-5349702	9	5349702	Casp12	1.87446912	1	0	0	Female bias
10-3768162	10	3768162	Plekhg1	1	0.48542683	-0.5849625	-0.4150375	Female bias
11-5035886	11	5035886	Ap1b1	0.5849625	1	-1	0	Female bias
12-3477392	12	3477392	Asxl2	1.32192809	0.22239242	0	-0.4150375	Female bias
13-4512818	13	4512818	Akr1c20	1.169925	0.80735492	-1	-0.4854268	Female bias
14-8149103	14	8149103	Pxk	1.5849625	1.87446912	0	0	Female bias
15-4551977	15	4551977	Plxd3	2.32192809	0.32192809	0	0	Female bias
16-4109355	16	4109355	Crebbp	0.5849625	0.22239242	0	0	Female bias
17-3638733	17	3638733	Nox3	2.45943162	0.5849625	0	-0.4150375	Female bias
18-3385814	18	3385814	Cul2	2.32192809	1.32192809	0	-0.7369656	Female bias
19-4428639	19	4428639	Rhod	1	0.48542683	0	0	Female bias

1-3455194	1	3455194	Xkr4	-0.7369656	-2.3219281	0.5849625	0.4150375	Male bias
2-3323341	2	3323341	Nmt2	0	-1	1.32192809	0.73696559	Male bias
3-7371213	3	7371213	Pkia	0	-1	0.5849625	0.5849625	Male bias
4-3708410	4	3708410	Lyn	-0.4150375	0	2.32192809	0.73696559	Male bias
5-3363851	5	3363851	Cdk6	-0.4150375	-1.5849625	1	0.4150375	Male bias
6-3561053	6	3561053	Vps50	0	0	1.22239242	0.73696559	Male bias
7-4059197	7	4059197	Lair1	-0.4150375	-0.6780719	0.32192809	0.5849625	Male bias
8-3238770	8	3238770	Insr	0	0	1.5849625	0.73696559	Male bias
9-4749268	9	4749268	Gria4	-0.2630344	-1.4150375	0.48542683	0.4150375	Male bias
10-4663032	10	4663032	Esr1	0	0	0.73696559	0.32192809	Male bias
11-3676152	11	3676152	Morc2a	0	-1.5849625	1.80735492	0.48542683	Male bias
12-3461044	12	3461044	Asxl2	0	-0.4854268	0.5849625	0.4150375	Male bias
13-3886171	13	3886171	Net1	0	-1	1.80735492	1	Male bias
14-7929403	14	7929403	Flnb	0	-0.4854268	0.5849625	0.73696559	Male bias
15-3336130	15	3336130	Ghr	0	-1.5849625	1.32192809	1	Male bias
16-4717870	16	4717870	Nmral1	-0.7369656	-0.4150375	0.26303441	0.48542683	Male bias
17-5001488	17	5001488	Arid1b	-0.5849625	0	1.5849625	1.32192809	Male bias
18-3325440	18	3325440	Crem	0	-0.4150375	2.32192809	1	Male bias
19-3326148	19	3326148	Cpt1a	-1.169925	0	1	0.5849625	Male bias

**Table 2.5.** Significant enrichment of specific pathways by the genes that contain either male or female biased methylation in the placenta and fetal brain.

<b>Pathway</b>	<b>Number of genes</b>	<b>Fold Enrichment</b>	<b>False Discovery Rate</b>	<b>Sex bias</b>
Metabotropic glutamate receptor group I pathway	14	3.29	0.0103	Female bias
Ionotropic glutamate receptor pathway	24	2.71	0.0051	Female bias
Metabotropic glutamate receptor group III pathway	28	2.26	0.0092	Female bias
Endothelin signaling pathway	32	2.15	0.0080	Female bias
CCKR signaling map	61	2.11	0.0002	Female bias
EGF receptor signaling pathway	50	2	0.0034	Female bias
Metabotropic glutamate receptor group I pathway	15	3.37	0.0072	Male bias
Axon guidance mediated by netrin	17	2.55	0.0365	Male bias
Histamine H1 receptor mediated signaling pathway	20	2.4	0.0239	Male bias
Metabotropic glutamate receptor group III pathway	30	2.31	0.0050	Male bias
Ionotropic glutamate receptor pathway	21	2.26	0.0309	Male bias
Endothelin signaling pathway	35	2.25	0.0042	Male bias

**Table 2.6.** List of methylation levels in epiclock and pathway signaling genes showing differential crosstalk in males versus females. The brain epiclock genes which were identified as predictive markers aging and the genes associated with the GnRHR pathway are indicated.

Chromosome	Name	FBR	FPL	MBR	MPL	Gene	Gene function	Sex bias (methylation site)	Epiclock marker gene (predicted from Neuralnet)	GnRH Pathway gene
1	1-168261622	1	0.625	0.5	0.33333333	Pbx1	Signaling	Female	-	YES
1	1-191193287	1	0.77777778	0.5	0.5	Atf3	Signaling	Female	-	YES
1	1-32274727	1	1	0.5	0	Khdrbs2	Epiclock	Female	Predictive of brain aging in female	-
1	1-32459781	0.75	1	0.5	0	Khdrbs2	Epiclock	Female	Predictive of brain aging in female	-
11	11-85667778	0.57142857	1	0.5	0.375	Bcas3	Epiclock	Female	Predictive of brain aging in male	-
11	11-85775960	0.66666667	0.88888889	0.4	0.5	Bcas3	Epiclock	Female	Predictive of brain aging in male	-
1	1-168221413	0.5	0.5	1	0.66666667	Pbx1	Signaling	Male	-	YES
1	1-191208401	0.5	0.14285714	0.875	0.66666667	Atf3	Signaling	Male	-	YES
10	10-81645423	0	0.5	1	0.66666667	Ankrd24	Epiclock	Male	Predictive of brain aging in female	-
11	11-46017605	0.5	0.375	0.66666667	1	Sox30	Epiclock	Male	Predictive of brain aging in female	-
11	11-85462708	0	0.28571429	0.8	0.625	Bcas3	Epiclock	Male	Predictive of brain aging in male	-
11	11-85469852	0.33333333	0.33333333	0.8	0.8	Bcas3	Epiclock	Male	Predictive of brain aging in male	-

**Figure 2.1.** **A.** Venn Diagram showing DNA age estimation, based on methylation status of epigenetic clock test, of male and female brain of 70 weeks old mice. **B.** Comparison of methylation of epiclock genes in the male and female brain at fetal stage (gestation day 15) and neonatal stage (postnatal day 5) with aged stage (week 70). **C.** Number of epiclock sites showing consistent female bias or male biased methylation among fetal, postnatal, and aging brain. **D.** Boxplot showing the pattern of variation of female biased epiclock methylation at the three stages in the brain of both sexes. **E.** Heatmap showing variation in methylation of mouse epigenetic clock in the brain of males and females at GD 15, PND5 5, and WK70. The scale on the top left shows the color codes for methylation levels.

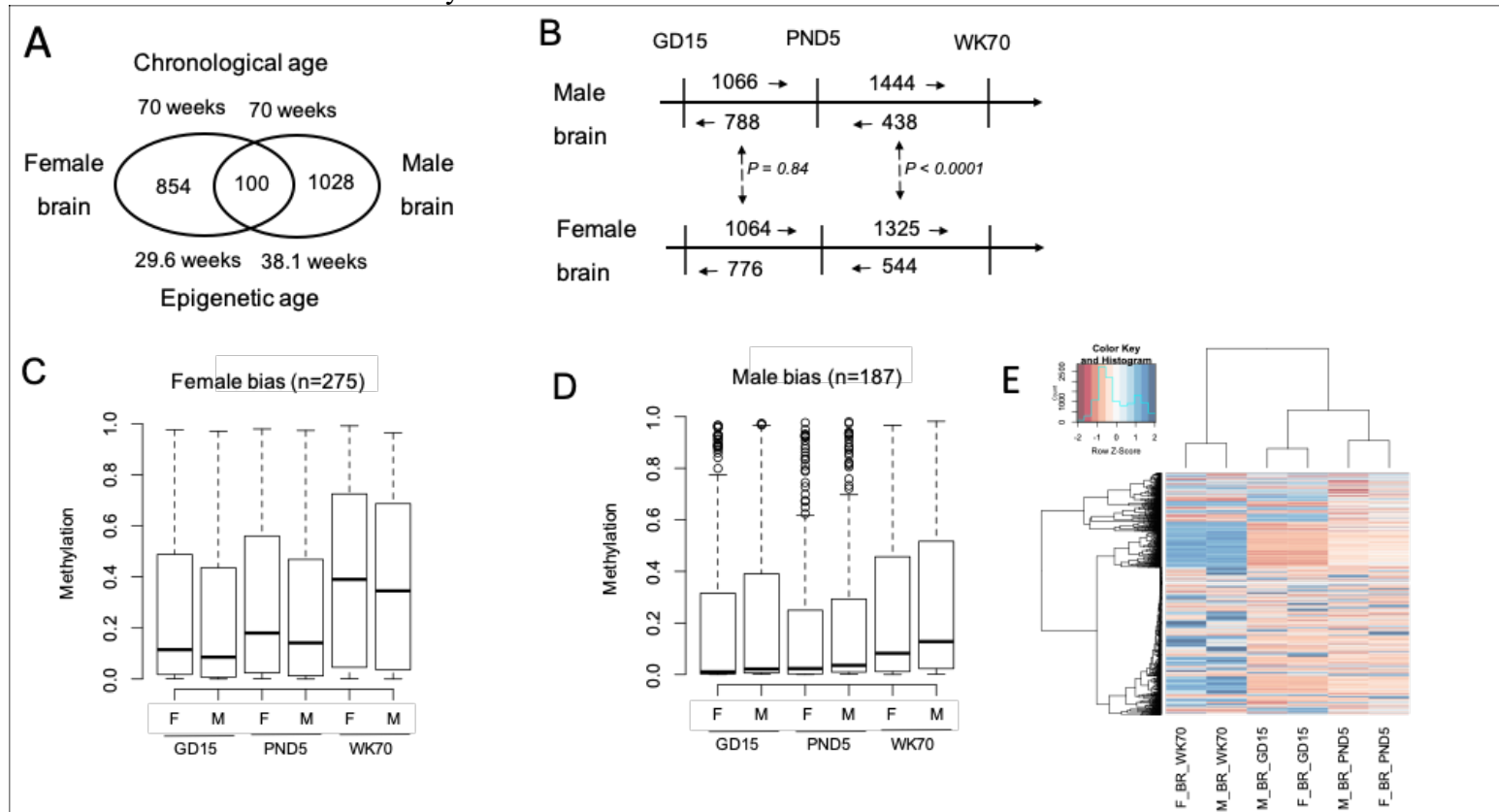


**Figure 2.2.** Neural network modeling of epigenetic clock of brain. **A.** Epigenetic clock with female-biased methylation data was used to train a neural network model. **B.** Separately, the epigenetic clock with male-biased methylation data was used to train the neural network model. The trained models were then used reciprocal predictions of methylation of aging brain, i.e., model from male-biased epiclock data was used to predict methylation level of female aging brain (**C**), and the model from male-biased epiclock data was used to predict methylation level of female aging brain (**D**). The confusion matrix showing the number of true and false prediction relative the observed methylation data is presented in **C and D**.

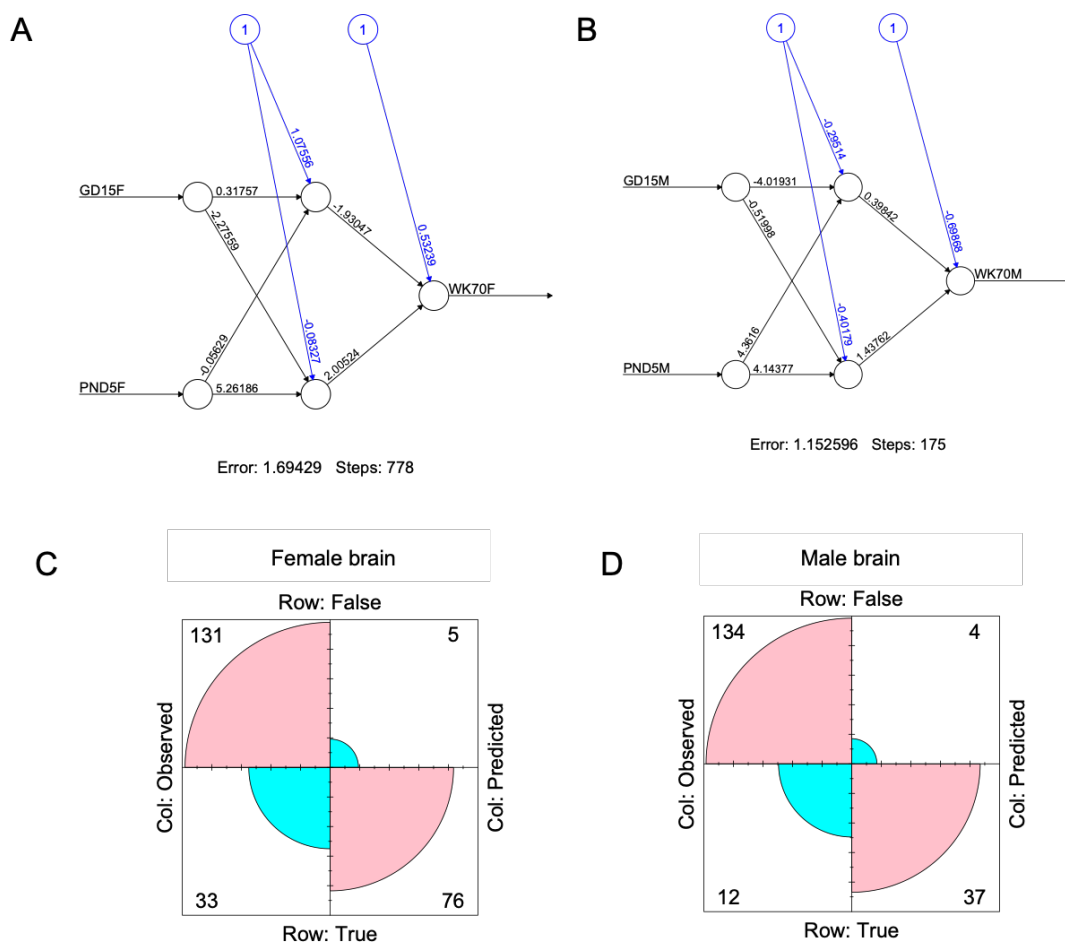




**Figure 2.3.** Comparison of methylation and expression variation of epiclock prediction makers of brain aging. **A.** Tanglegram showing comparison of methylation and expression patterns the epiclock predictive genes (from neural network modeling) among the fetal, neonatal, and aging brain of both sexes. **B.** Heatmap of methylation variation of epiclock predictive genes. **C.** Heatmap of expression variation of epiclock predictive genes.

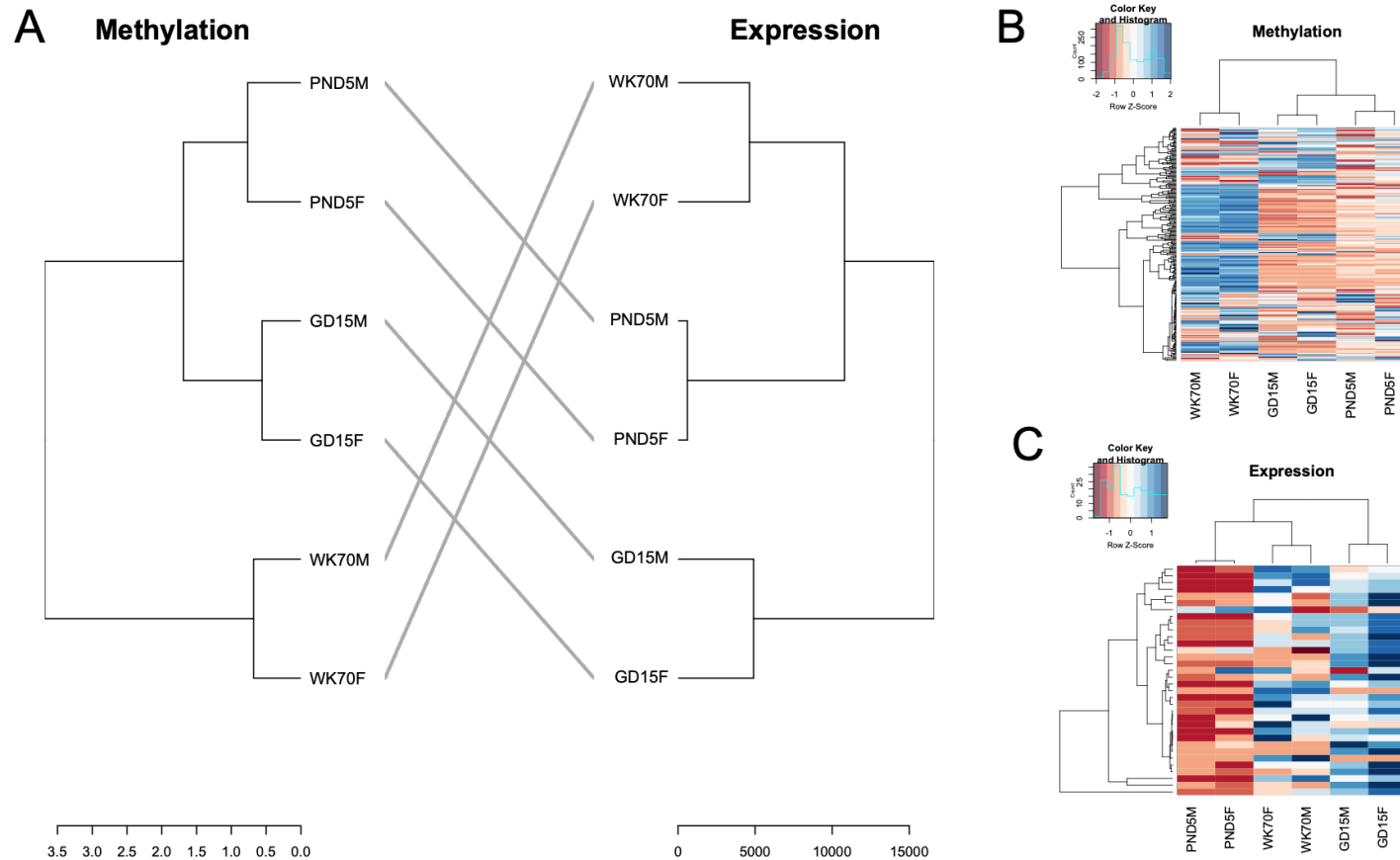


**Figure 2.4.** Comparison of placenta and brain gene expression. **A.** Heatmap of expression of epiclock genes in placenta along with fetal brain, neonatal brain, and aging brain. **B.** Heatmap of expression of non-epiclock genes in placenta along with fetal brain, neonatal brain, and aging brain. **C.** CCA analysis of brain and placenta (GD15) methylation data. the genes overlapping the methylations were grouped as epiclock or non-epiclock genes. CCA was then done on each. Covariates (x=placenta and y=fetal brain of both sexes) were calculated and plotted here.

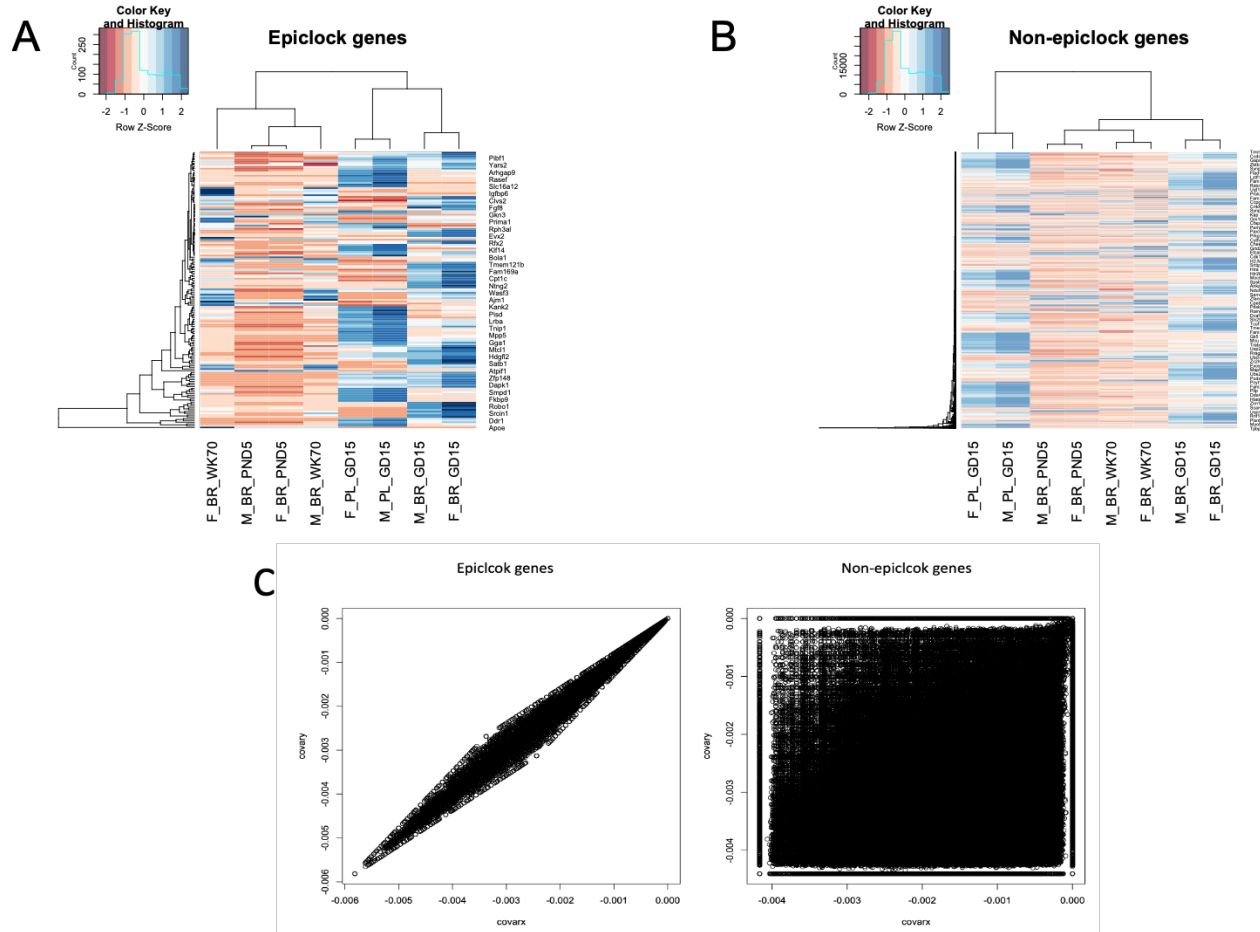


**Figure 2.5.** **A.** Boxplot showing that specific sites are methylated in a female-biased (FB) manner in both placenta and fetal brain. **B.** Boxplot showing that specific sites are methylated in a male-biased (MB) manner in both placenta and fetal brain. **C.** Bar plot showing the number of methylations female-biased and male-biased methylations within genes or in intergenic regions. The 2x2 contingency test p-value of association (sex vs. location) is shown. **D.** Venn diagram showing number of genes with either male-biased or female-biased methylation or both male as well as female biased methylation. The cartoons show location of male and female biased methylations in those genes.

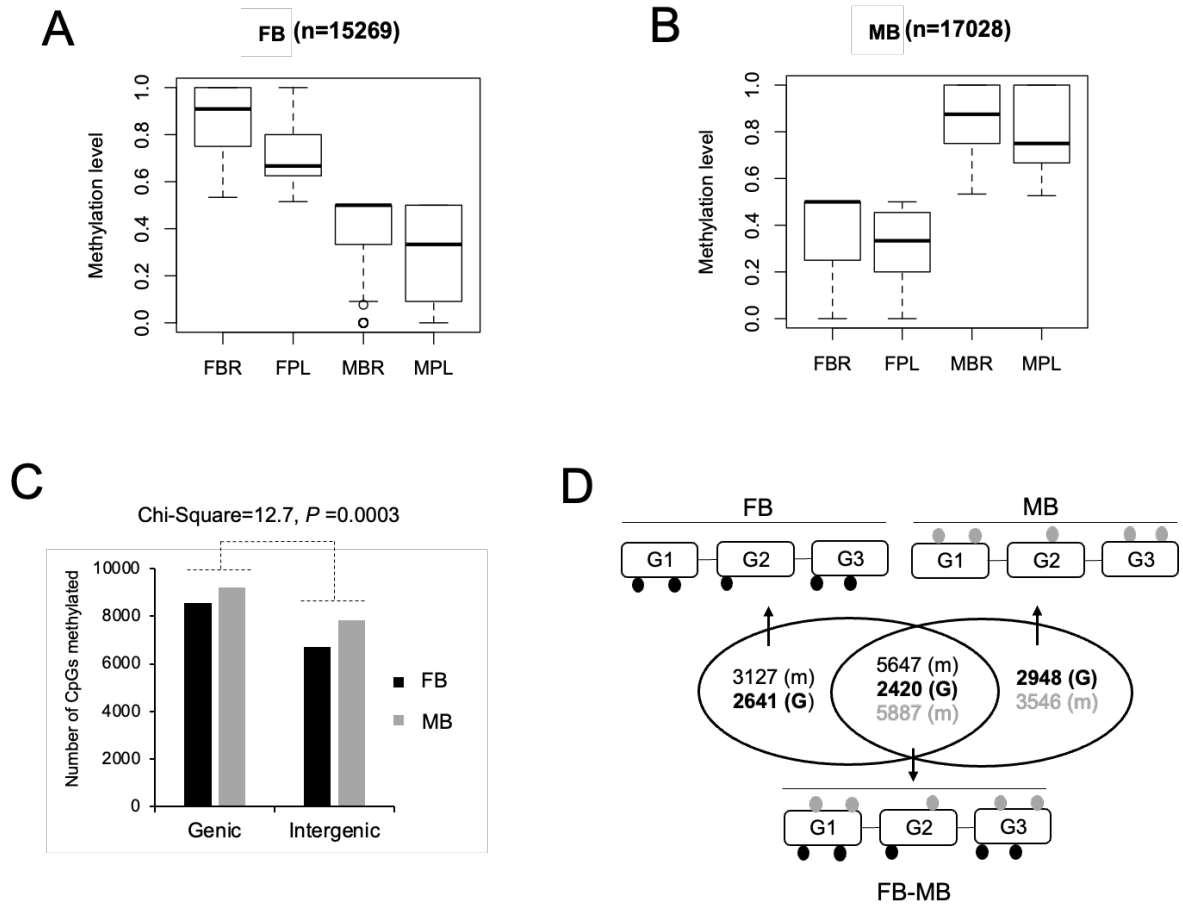


**Figure 2.6.** Methylation of repeat elements in placenta and fetal brain. **A.** Schematic representation of methylation of repeat elements either in genic or intergenic regions. **B.** Bar plot showing number of all methylations (sex-biased or not) in different repeat elements. Top repeats (based on number of methylation) are only shown. **C.** Number of sex biased methylations observed in both placenta and fetal brain are differentially associated (significance level shown) with repeat elements within genes or intergenic regions. **D.** Comparison of methylation level of epiclock sites found within repeat elements among fetal, neonatal, and aged brain of both sexes. **E.** Comparison of methylation level of epiclock sites found within non-repeat elements among fetal, neonatal, and aged brain of both sexes.

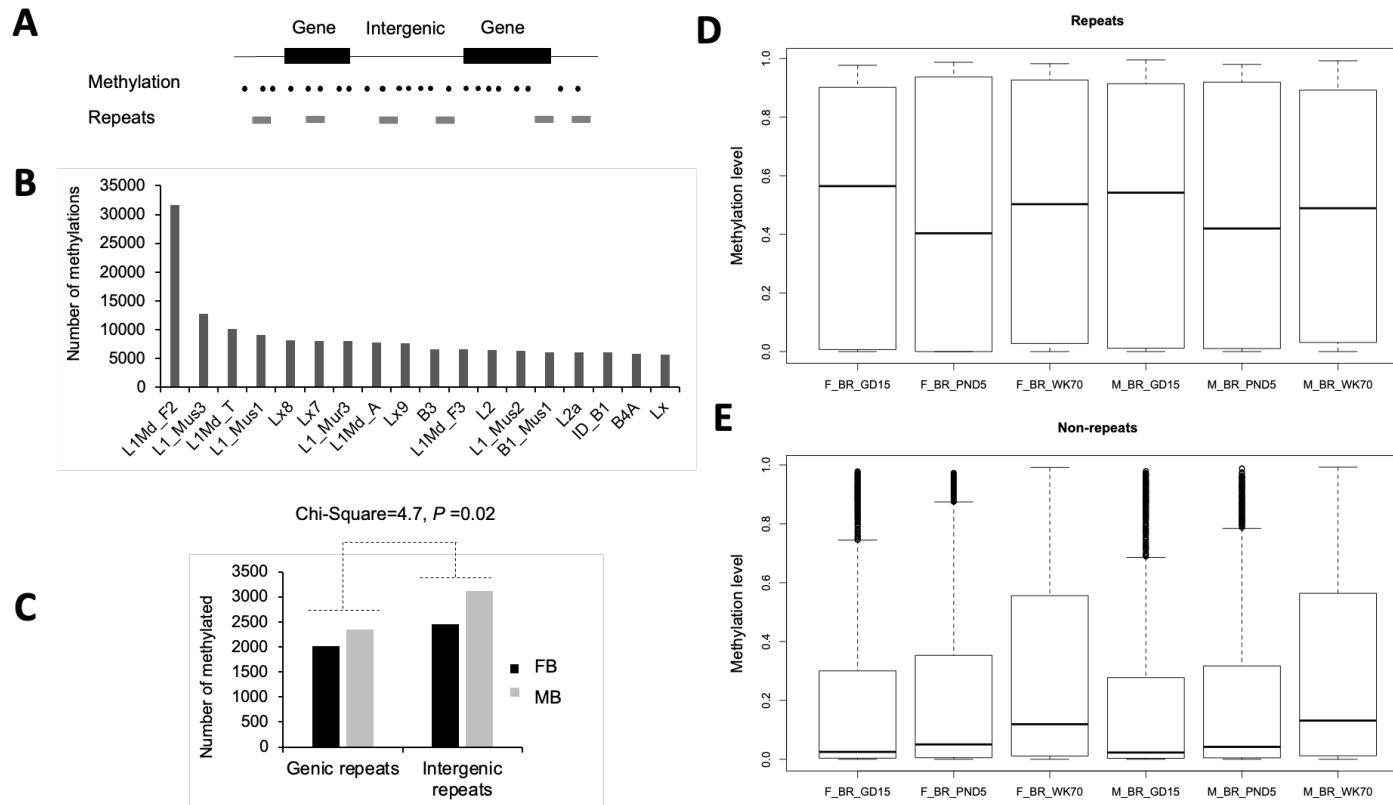


**Figure 2.7.** Sex-biased methylation changes among epiclock and signaling genes in the brain. **A.** Principal Component Analysis of male (M) and female (F) biased changes in methylation of epiclock and signaling genes in brain among the fetal, neonatal and aging stages. The data color codes are according to types of gene methylations described in the legend right to the plot. **B.** Circular dendrogram based on hierarchical cluster analysis of female-biased methylations. It shows co-variation of methylation of epiclock and signaling in single cluster. The leaf color in the dendrogram matches to color code description in **A**. The branch color of two clusters is shown in red and green. **C.** Circular dendrogram based on hierarchical cluster analysis of male-bias methylations. It lacks co-variation of methylation between epiclock and signaling genes. The leaf color in the dendrogram matches to color code description in **A**. The branch color of two clusters is shown in red and green.

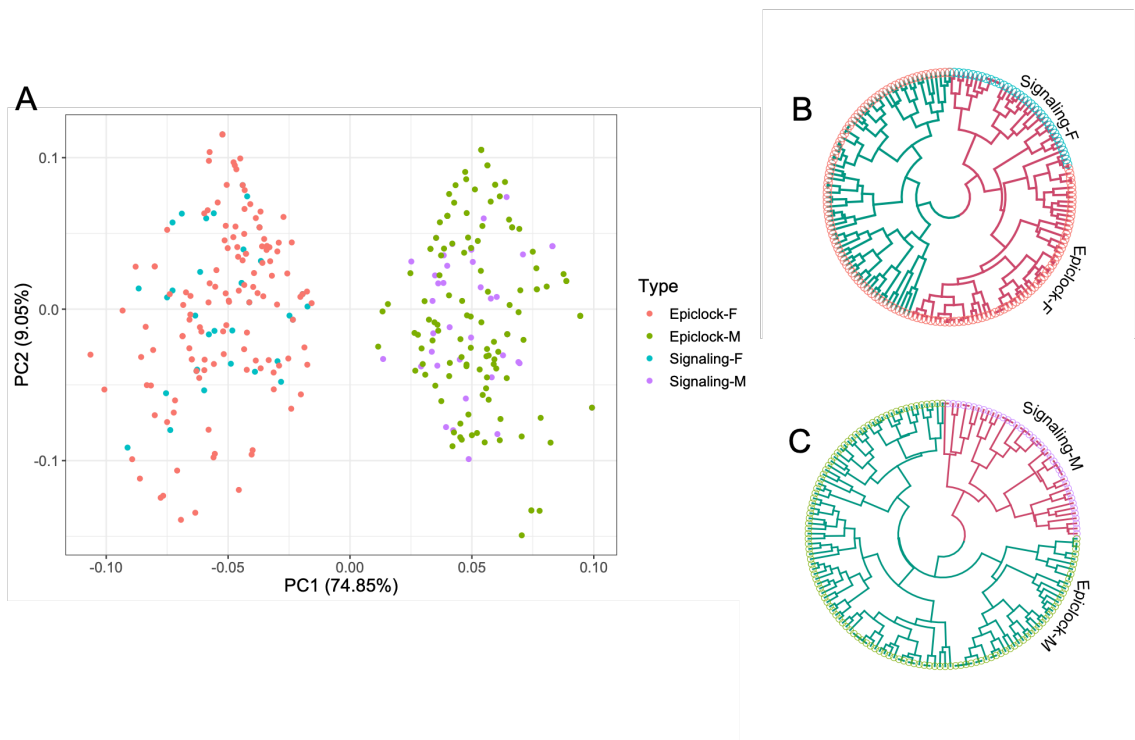
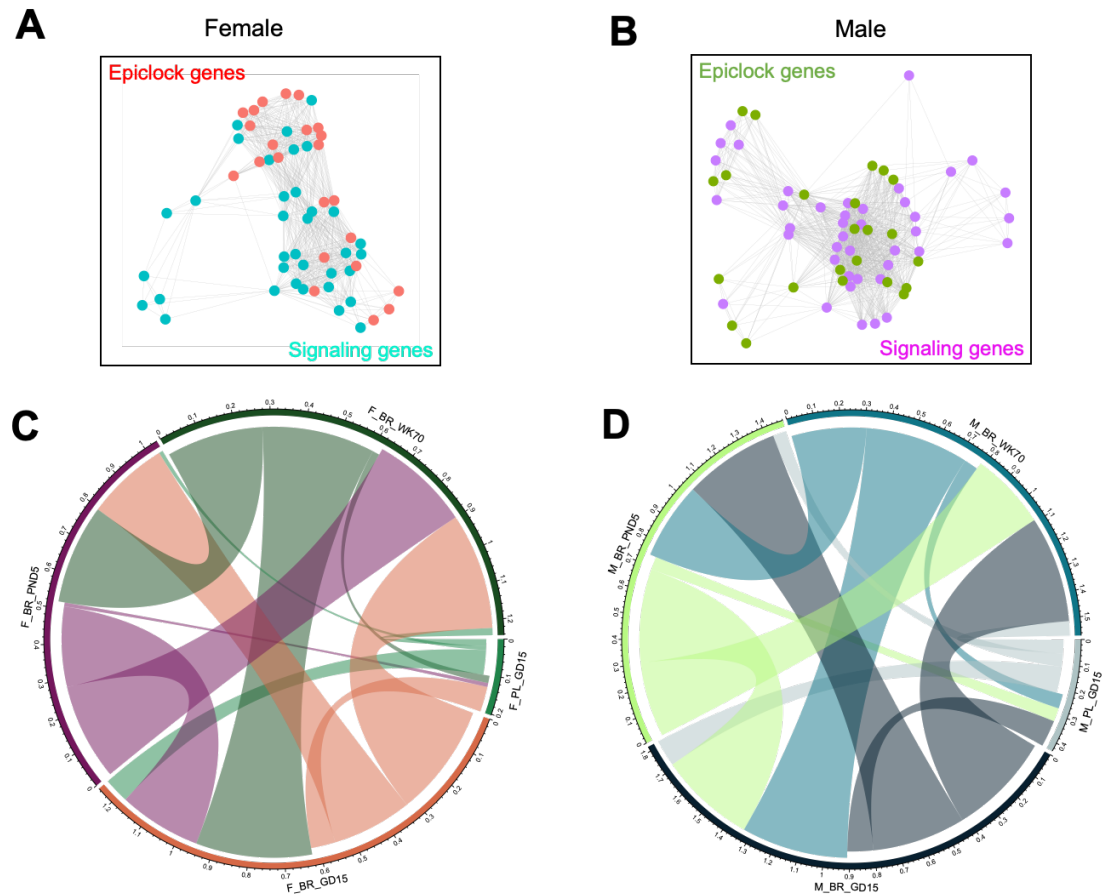


**Figure 2.8.** Crosstalk among epiclock and signaling genes. Expression network among epiclock and signaling genes associated with female-biased (A) and male-biased methylations (B). The male and female biased methylations of these genes are described in Figure 2.7A. In the network plots, genes are color coded as indicated. Network edges (interaction between genes) in both plots were inferred based on feature selection by maximum relevancy and minimum redundancy in mutual information of expression changes of the genes. C. Circos plot showing placental links with brain in the mutual information of expression among the epiclock and signaling genes (described in A). D. Circos plot showing placental links with brain in the mutual information of expression among the epiclock and signaling genes (described in B). The arches in both C and D represent the information contents in gene expression between placenta and brain (shown on the circumference of the plots, and color coded).



## Chapter 3

### Dysregulation of fetal brain development in mice lacking Caveolin 1

#### Abstract

Caveolin-1 (*Cav-1*) encodes a major component of caveolae which are flask shaped membrane invaginations found as abundant surface feature of endothelial cells. Caveolae are also found in adipocytes and embryonic notochord cells, and they are also present in many other cell types albeit at low numbers. Mice lacking *Cav-1* (Razani et al., 2001) have revealed numerous phenotypes, including reproductive ((D. S. Park et al., 2002), (Song et al., 2022), (Feng et al., 2012)) as well as neurologic ((Head et al., 2010c), (Choi et al., 2016), (Jasmin et al., 2007), (Takayasu et al., 2010)) resulting from the loss of *Cav-1*. *Cav-1* knockout (KO) mice show Alzheimer's like symptoms as early as 3-6 months after birth. Increased amyloid beta, tau, astrogliosis and decreased cerebrovascular volume are observed in the brain of these mice. As *Cav-1* plays a key role to modulate beta-secretase activity, association of *Cav-1* with Alzheimer's Disease (AD) pathologies in these mice has been suggested. This study was performed to determine changes in gene expression and DNA methylation of fetal brain due to loss of *Cav-1*. Another aim of this study was to identify brain cells dysregulated in the *Cav-1* KO compared to the wildtype fetal brain. The results of this study showed that lack of *Cav-1* leads to extensive dysregulation of genes of fetal brain development on gestation day 15. Several

epigenetic clock genes were differentially methylated in *Cav-1*-KO compared to WT mice fetal brain. Single nuclei RNA sequencing identified specific glial and neuronal cells being dysregulated in the fetal brain due to the absence of *Cav-1*. Based on these results, we propose a model for fetal links of Alzheimer's symptoms in mice lacking *Cav-1*.

## **Introduction**

A relationship between reproduction and life-span is suggested from studies that observed correlations between lifespan and gestation times among mammals (Fushan et al., 2015b), the shape of the placenta and life-span of men (D. J. P. Barker et al., 2011b), and fertility and lifespan of women (Kuningas et al., 2011). In addition, studies have further showed that lifespan and reproduction have common regulatory mechanisms that control nutrient sensing and cellular homeostasis (Aguilaniu, 2015b) (Antebi, 2013) (Templeman & Murphy, 2018) (Maklakov et al., 2008). However, there is still a significant gap in our knowledge about links between lifespan and reproduction, particularly the relationship between fetal lifespan programming and regulation of the brain-placental axis. In several studies, it has been shown that sex also influences the occurrence of specific brain diseases during old age (Thibaut, 2016b). In the uterus, a male fetus is generally associated with at higher risk of death than a female fetus (DiPietro & Voegtline, 2017). But, the effect of fetal sex on the aging process of brain remains elusive (McCarthy, 2016b).



Fetal brain development was investigated in this study using mice lacking Caveolin-1 (*Cav-1*), which is a pro-longevity gene. Additionally, *Cav-1* plays a major role in the regulation of angiogenesis in mice (Chang et al., 2009). Mice lacking the *Cav-1* gene have shown to have impaired endothelia as there are no caveolae membranes in the endothelial cells (D. S. Park et al., 2003). In mice as well as in human placenta, caveolae are formed in endothelial cells and also in smooth muscle cells and mesothelial cells of the yolk sac (Mohanty et al., 2010). Ablation of *Cav-1* reduces mice lifespan by nearly 50% (D. S. Park et al., 2003). *Cav-1* null mice, though viable and fertile, show hyperproliferative and vascular abnormalities (Razani et al., 2001). At young age (3-6 month old), these mice exhibit neuronal aging resembling > 18 months of aging in wild-type mice (Head et al., 2010c). Interestingly, our previous study showed that fetal sex has an influence on the expression of pro- and anti-longevity genes between placenta and fetal brain. Genes related to specific biological functions are known to have association with aging, including genes related to ribosome assembly (GO:0042255) (MacInnes, 2016), ribosomal small subunit biogenesis (GO:0042274) (Tiku & Antebi, 2018), rRNA processing (GO:0006364) (Tiku & Antebi, 2018), mitochondrial respiratory chain complex I assembly (GO:0032981) (Hur et al., 2014), NADH dehydrogenase complex assembly (GO:0010257) (Hur et al., 2014), ncRNA processing (GO:0034470) (S. S. Kim & Lee, 2019), regulation of programmed cell death (GO:0043067) (Shen & Tower, 2009), and response to oxidative stress (GO:0006979) (Ristow & Schmeisser, 2011).

Understanding mechanisms of fetal origin of brain diseases (Räikkönen et al., 2012; Schlotz & Phillips, 2009; Wadhwa, 2005; Weinstock, 2005) will lead to the development of novel strategies of early diagnosis of the disease. The *Cav-1* KO mice show Alzheimer's like symptoms as early as 3-6 months after birth (Head et al., 2010a). Increased amyloid beta, tau, astrogliosis and decreased cerebrovascular volume are observed in the brain of these mice (Head et al., 2010a). As *Cav-1* plays a key role in modulating beta-secretase activity (Hattori et al., 2006), association of *Cav-1* with AD pathologies in these mice has been suggested (Head et al., 2010a). Therefore, to link lifespan and reproduction we compared the genetic regulation of fetal brain development in *Cav-1* KO mice model with C57BL/6J wildtype strain and established a relationship between the fetal brain and placenta.

## **Materials and methods**

### *Animal Breeding and Sample Collection*

C57BL/6J wild-type (WT) mice and *Cav-1* KO mice were obtained from Jackson Laboratory (stock no. 000664, stock no. 007083). Adult female mice were mated with fertile males to induce pregnancy. Pregnant WT mice were euthanized on GD15. The fetal brain and placenta were collected from all implantation sites. The placenta was carefully separated from the decidua. All the samples were washed in sterile PBS and snap frozen in liquid nitrogen. Additionally, C57BL/6J and *Cav-1* KO mice were aged

under proper conditions and euthanized using CO<sub>2</sub> followed by cervical dislocation. C57BL/6J mice were collected on postnatal day 5 and 70 weeks of age and *Cav-1* null mice were collected at day 17 and 70 weeks. The organs were washed in PBS and snap frozen in liquid nitrogen. All animal procedures were approved by the Institutional Animal Care and Use Committee of the University of Missouri-Columbia and were conducted according to the *Guide for the Care and Use of Laboratory Animals* ((National Institutes of Health, Bethesda, MD, USA).

#### *RNA Extraction*

Total RNA was isolated from frozen tissue samples using an AllPrep DNA/RNA Mini Kit (Qiagen, Cat No./ID: 80204) as per the manufacturer's instruction. Each fetal brain was homogenized with 500  $\mu$ l to 1 ml RLT buffer (Qiagen, Cat No./ID: 79216) and 5  $\mu$ l 2-mercaptoethanol. Homogenization was done in a 15 ml Falcon tube using a benchtop VDI 25 tissue homogenizer (VWR). The homogenate was transferred to the mini column then centrifuged for 1 minute at  $\geq 8000 \times g$ . From the supernatant, 750  $\mu$ l was transferred into RNase/DNase-free Axygen conical tubes (Corning Axygen, 1.5ml) and mixed with 1 volume 70% ethanol to precipitate RNA. RNA was eluted in 30  $\mu$ l nuclease-free water twice for a total volume of 60  $\mu$ l. RNA from a total of 27 samples (3 gestation days, 3 biological replicates, and 2 strains) were generated. Concentration and purity of the RNA were determined using Nanodrop 1000 spectrophotometer (Thermo Fisher Scientific) before each sample was diluted to 100ng/ $\mu$ l using nuclease-free water.

### *Gene expression profiling by RNA sequencing*

Illumina sequencing libraries were generated from the total RNA of each sample. Preparation of libraries and RNA sequencing (RNA-seq) were performed by the Novogene Cooperation Inc. (8801 Folsom Blvd #290, Sacramento, CA 95826). Each library was sequenced to 20 million paired end reads of 150 bases using a NovaSeq sequencer.

### *RNA-seq Data Analysis*

RNA-seq data analysis was performed as described in our earlier works (Dhakal et al., 2021a; Strawn et al., 2021). Briefly, the quality of raw sequences was checked with FastQC followed by trimming the adaptors from the sequence reads by *cutadapt*. The *fqtrim* tool was used to perform base quality trimming (Phred score >30) by sliding window scan (6 nucleotides). The quality reads were then mapped to the mouse reference genome GRCm38 using Hisat2 aligner (D. Kim et al., 2015). Read counting from the alignment data was performed by *FeatureCounts* (Liao et al., 2014). The feature count data was then analyzed using packages in R.

### *Single-nuclei RNA sequencing*

Single nuclei from fetal brain and placenta were isolated using Pure Prep Nuclei Isolation kit (Sigma, St. Louis, MO, USA) as per manufacturer's instruction. The protocol was improvised to isolate single nuclei from frozen samples of mouse brain. Briefly, frozen brain samples after thawing were minced into small pieces and added to the lysis buffer. Using a dounce homogenizer, each sample was homogenized until the solution looked evenly mixed, which generally required 15-20 dounces. A 70 $\mu$ m cell strainer was used to filter the nuclei from the lysed cells, diluted and layered over a freshly prepared 1.8M sucrose cushion solution to collect single nuclei. After centrifugation and suspension with the kit provided storage buffer (ice cold), final purification of single nuclei was performed by filtering through a 40 $\mu$ m cell strainer. The purified nuclei were then counted using a Countess II FL Automated Cell Counter (ThermoFisher).

The freshly prepared nuclei were sent to the University of Missouri Genomics Technology Core to prepare sequencing libraries using 10X Genomics Chromium Single Cell 3' GEM, Library & Gel Bead Kit v3.1. Briefly, cell suspension concentration and viability were measured with an Invitrogen Countess II automated cell counter. Cell suspension, reverse transcription master mix, and partitioning oil were loaded on a Chromium Next GEM G chip with a cell capture target of 10,000 cells per library. Post-Chromium controller GEMs were transferred to a PCR strip tube and reverse

transcription performed on an Applied Biosystems Veriti thermal cycler at 53°C for 45 minutes. cDNA was amplified for 12 cycles and purified using Axygen AxyPrep MagPCR Clean-up beads. cDNA fragmentation, end-repair, A-tailing, and ligation of sequencing adaptors was performed according to manufacturer specifications. The final library was quantified with the Qubit HS DNA kit and the fragment size was analyzed using an Agilent Fragment Analyzer system. Libraries were pooled and sequenced on an Illumina NovaSeq to generate 50,000 reads per cell with a sequencing configuration of 28 base pair (bp) on read1 and 98 bp on read2. Each library was sequenced to a depth of 20,000 paired-end (single-indexing) reads per nucleus using NovaSeq 6000. The base call (BCL) files generated from Illumina machine were processed by Cell Ranger pipeline (v. 3.0.1) to generate the FASTQ files. The STAR aligner (Dobin et al., 2013) was used to map the reads in the FASTQ files to the mouse reference genome to generate read count data of genes expressed in the single cells.

The count data was processed by Seurat (Butler et al., 2018b) to identify expression clusters, and assign clusters to cell types. Briefly, data integration was performed by identifying integration anchors for the first 20 dimensions of data variation among the wildtype and *Cav-1 null* brain samples. The normalized integrated data was subjected to principal component analysis (PCA) followed by non-linear dimensional reduction by tSNE (t-distributed stochastic neighbor embedding) (Kobak & Berens, 2019). This approach was used to identify individual clusters of cells that were canonically correlated in gene expression between WT and *Cav-1 null* brain samples. The

'FindAllMarkers' function of Seurat was used to identify marker genes of each cluster. The marker genes were then used to annotate cell types of the expression clusters based on marker genes of brain cells curated in PanglaoDB (Franzén et al., 2019). At this step, the identified cell clusters in the integrated dataset were renamed to include information about cell type, stage (fetal, young, or adult), and strain (WT or *Cav-1*-KO) to facilitate cell identification in the downstream analyses.

### *Epigenetic clock profiling*

Mouse multi-tissue epigenetic clock genes (Vaiserman, 2019b) were profiled with DNA of wild-type gestation day 15.5, postnatal day 5, week 70 and *Cav-1* knock out GD 15.5, week 17 male and female brains using the Zymo (ZYMO RESEARCH, Irvine, CA 92614, U.S.A) DNAge® estimation service, which is based the Horvath pan-tissue clock using elastic net regression (Chew et al., 2018). Briefly, DNA from frozen brain samples was purified using the Quick-DNATM Miniprep Plus kit (Cat. No. D4068). Bisulfite conversion was performed using the EZ DNA Methylation-Lightning TM Kit (Cat. No. D5030), followed by enrichment for target loci and sequencing on an Illumina® HiSeq instrument. Sequence reads were identified using Illumina base calling software and aligned to the mouse reference genome (GRCm38) using *Bismark* (Krueger & Andrews, 2011) which was also used for methylation calling. Methylation level was estimated as the proportion of reads mapped to each cytosine relative to the total number mapped reads to the site. The methylation data of each brain sample was then compared with

mouse epiclock data to estimate epigenetic age by Zymo's DNAge® predictor tool as described earlier (Coninx et al., 2020).

## Results

### *Lack of Cav-1 dysregulates fetal brain development*

Gene expression was profiled by RNA-Seq to examine the whole transcriptome of the female fetal brains of C57BL/6J and *Cav-1* null mice at gestation day (GD) 12.5, 15.5 and 17.5. Hierarchical clustering showed that at GD 12.5 and 15.5, the female fetal brain of C57BL/6J is transcriptionally distinct from *Cav-1* knockout mice. However, at GD 17.5 the *Cav-1* knockout female fetal brain did not cluster differently from C57BL/6J due to technical errors or due to small number of differentially expressed genes. **(Figure 3.1)**. Similar results were shown between the gestation days in the Principal Component Analysis performed on wildtype and *Cav-1* KO female fetal brains **(Figure 3.2)**.

Differential expression analysis performed by *edgeR* identified genes with significant changes in the expression of the female fetal brain of C57BL/6J and *Cav-1* knockout mice at gestation days 12.5, 15.5 and 17.5. The data showed that there were greater number of upregulated and downregulated genes at GD 15.5 compared to 12.5 and 17.5 (GD 12.5: UP=186, DOWN=980; GD 15.5: UP=1648, DOWN=6306; GD17.5: UP=22, DOWN=75) **(Figure 3.3)**. The volcano plot of GD 15.5 showed a greater number



of differentially expressed genes than GD 12.5 and 17.5 (**Figure 3.4**). Moreover, there was a greater number of differentially expressed genes between GD 15.5 and 17.5 (n=5624 genes) than between GD 12.5 and GD 15.5 (n= 5192 genes) in *Cav-1* KO mice compared with wildtype, showing more regulation of genes in the later stages of gestation in mice (**Table 3.1**). Among the DEGs, between GD 12.5 and 15.5, only three genes (*Gm36952*, *7SK*, *H4c18*) were downregulated in wildtype and upregulated in *Cav-1* KO, whereas, three more genes (*Matn1*, *Six6*, *Oc90*) were upregulated in wildtype but downregulated in the knockout model. On the contrary, when GD 17.5 was compared with GD 15.5, only two genes (*Vwf*, *4930509E16Rik*) were downregulated in wildtype and upregulated in *Cav-1* KO. However, twenty-three genes (such as *Haglr*, *Alas2*, *Hbb-bt*, *Hbb-bs*, *Rpl-29*, *7SK*, *Hbba-1*, *Hba-a2*) were upregulated in wildtype but downregulated in *Cav-1* KO model.

#### *Functional annotation of the differentially expressed genes*

PANTHER pathway analysis was performed on the female fetal brain samples at gestation days 12.5, 15.5 and 17.5 of C57BL/6J compared to *Cav-1* KO mice to identify specific pathway(s) that were over-represented by the differentially expressed genes. The analysis showed that hedgehog signaling pathway, notch signaling pathway, integrin signaling pathway, cadherin signaling pathway, angiogenesis, wnt signaling pathway and Alzheimer disease presenilin pathway were downregulated in both gestation day 12.5 and 15.5 but almost double fold enriched in GD 12.5. However, some additional pathways

were downregulated at only GD 15.5 including VEGF signaling pathway, Insulin/IGF pathway-protein kinase B signaling cascade, Alzheimer disease-amyloid secretase pathway, Huntington disease, p53 pathway, PDGF signaling pathway, inflammation pathways and TGF-beta signaling pathway. On the contrary, there were no significant pathways on GD 17.5 (**Table 3.2**).

In addition to PANTHER Pathway analysis, Gene Ontology (GO) analysis was used to predict the functions of the differentially expressed genes of female fetal brain of C57BL/6J compared to *Cav-1* KO mice on gestation day 12.5, 15.5 and 17.5. Significant enrichment of 2417 GO terms were identified for genes that were downregulated at the three gestation days. During 12.5, signaling pathways were downregulated; these pathways play a role in spinal cord neuron cell fate specification, ventral spinal cord interneuron specification, and patterning along with intramembranous and direct ossification. Progressively, at GD 15.5, downregulated biological processes included spinal cord interneuron and neuron differentiation and fate commitment in ventral and dorsal sides. On the contrary, during GD 17.5, regulation of odontogenesis skeletal system morphogenesis was downregulated. Interestingly, regulation of cellular response to growth factor stimulus was downregulated during this later stage of female fetal brain development (**Table 3.3**).

When GD 17.5 was compared with GD 15.5 in both mice strains, 23 genes were upregulated in wildtype but downregulated in *Cav-1*-KO female fetal brains, among

which three GO biological processes were found to be enriched: haptoglobin binding process, oxygen carrier activity and oxygen binding process. Oxygen supply is crucial in cell development and lack of oxygen in tissues is termed as hypoxia. Low oxygen supply can result in a decline in other cellular process and can result in aging-related diseases (Yeo, 2019). Downregulation of these biological processes in *Cav-1* KO may be responsible for facilitating faster aging in them.

#### *DNA methylation changes in fetal brain due to lack of Cav-1*

Methylation profiling was performed for the known epigenetic clock sites (n=2,046) associated with aging genes in GD15.5 fetal brain *Cav-1*-KO compared to WT mice. More than 60% of these sites showed at least 2-fold changes in methylation level in *Cav-1*-KO fetal brain compared to WT mice (**Figure 3.5A**). In addition, we observed that these methylations were enriched in the chromatin regions occupied by modified histone proteins, particularly histone 3 trimethylation of lysine 3 and 4 (H3K4me3 and H3K9Me3) known in mouse brain (**Figure 3.5B**).

#### *Lack of Cav-1 leads to dysregulation of specific cell types of fetal brain*

We performed single-nuclei RNA sequencing (snRNA-seq) of GD15.5 fetal brain of WT and *Cav-1*-KO mice. Prediction of cell clusters by Seurat (Butler et al., 2018a) showed that specific glial and neuronal cells were dysregulated in the fetal brain due to

the absence of *Cav-1*. While oligodendrocytes, Cajal-Retzius cells, microglia and retinal ganglion cells showed correlated expression in the WT fetal brain, the *Cav-1*-KO fetal brain showed correlated expression among oligodendrocytes, Cajal-Retzius cells, microglia, and ependymal cells but not the retinal ganglion cells (**Figure 3.6**).

#### *Differences in gene expression between wildtype and caveolin-1 lacking placenta*

The gene expression of female placenta of wildtype was generated in a recent study which was compared against the *Cav-1* KO female placental data. The hierarchical cluster portrays how the female placenta of wildtype was clearly distinct from the placenta of the knockout female placenta (**Figure 3.7B**). Differential gene expression was further analyzed using *edgeR* which showed there were 2088 upregulated genes and 3746 downregulated genes when knockout female placenta was compared with wildtype. GO analysis of differentially expressed genes showed 934 enriched biological processes among which negative regulation of very low-density lipoprotein particle remodeling and serine-type peptidase activity were upregulated. In addition, processes, including response to methanol and chromate, were upregulated in both types of placentas. Conversely, biological processes for mitotic spindle assembly, elongation, and histone H3-K4 monomethylation (H3K4me) were downregulated in the placenta. Further analysis done using PANTHER Pathways showed that the cytoskeletal regulation by Rho GTPase, Alzheimer disease-presenilin pathway and Wnt signaling pathway were downregulated in female placenta of both strains (**Table 3.4**). In contrast, it was

previously found that the Alzheimer disease-presenilin pathway was downregulated in female fetal brain of wildtype and *Cav-1* knockout during GD 12.5 and 15.5 showing opposite regulation of this pathway in fetal brain and placenta. Furthermore, only blood coagulation pathway was upregulated in the placenta of both kinds at GD 15.5.

The gene *Rhox13* was downregulated in wildtype but upregulated in *Cav-1* KO placenta and *Gapdh* was upregulated in WT and downregulated in KO when female placenta was compared with male placenta showing there was not much difference in sex specific gene expression. Interestingly, GAPDH (glyceraldehyde-3-phosphate dehydrogenase) inhibition has been shown in the Alzheimer's disease brain. GAPDH interacts with the amyloid-beta protein precursor (A $\beta$ PP), which is a neurodegenerative disease associated protein (Butterfield et al., 2010). The downregulation of GAPDH in the placenta of *Cav-1* KO showed evidence that placenta can regulate the development of potential gene expression leading to AD in *Cav-1* brain from fetal stage.

#### *Relationship of gene expression between fetal brain and placenta*

The gene expression of GD 15.5 *Cav-1* KO female fetal brain and placenta was compared with WT using previously generated data of female fetal brain and placenta of C57BL/6J. Hierarchical clustering showed that, the female fetal brain and placenta of C57BL/6J was transcriptionally distinct from *Cav-1* knockout mice (**Figure 3.7A**).

Differential expression analysis by *edgeR* identified genes with significant changes in the expression of the female fetal brain and placenta of C57BL/6J and *Cav-1* knockout mice. The brain placental DEG lists of wildtype and *Cav-1* KO mice were compared and the results were illustrated by a Venn diagram (**Figure 3.8**). There was a total of 20,124 genes that were differentially expressed among which 6,922 genes were downregulated and 5,339 genes were upregulated in both strains. In contrast, there were only 51 genes that were downregulated in *Cav-1* KO but upregulated in wildtype, and 117 genes were upregulated in *Cav-1* KO but downregulated in wildtype.

PANTHER Pathway analysis was done on the differentially expressed genes to figure out which cellular pathways the genes represent. The analysis showed that blood coagulation, integrin signaling pathway, angiogenesis, PDGF signaling pathway and Gonadotropin-releasing hormone receptor pathway were downregulated in the brain and placenta of both strains. Additionally, upregulated in fetal brain and placenta in both strains included opioid proenkephalin, and opioid prodynorphin pathway. Moreover, some hormone releasing pathways, including oxytocin receptor mediated signaling pathway and thyrotropin-releasing hormone receptor signaling pathway were also upregulated in both strains. In addition, Alzheimer disease-amyloid secretase pathway was also upregulated in both strains.

GO analysis was done on the differentially expressed genes of the fetal brain and placenta of *Cav-1* KO and C57BL/6J mice to find out which biological processes were

associated with those genes. Among the enriched upregulated biological processes, several brain developmental processes were present, such as forebrain pattern formation, neuronal dense core vesicle exocytosis and cerebral cortex GABAergic interneuron migration. This implies that some biological processes were similarly regulated in the placenta and the fetal brain, therefore affecting the development of the brain. Moreover, biological processes including T cell mediated cytotoxicity, and positive regulation of lactation were upregulated in both strains. Conversely, among the 51 genes (such as *Illrl1*, *Atp51*, *Fgfbp1*, *Hoxc4*) and 117 genes (such as *Pttg1*, *Thbs4*, *Fasn*, *Lrp4*, *nectin1*, *Fzd8*, *Spon1*, *foxf2*, *fzd1*, *Adamts12*, *Nog*, *Ubqln2*, *Pouf31*) that were oppositely expressed in the brain and placenta included several genes.

## **Discussion**

The knockout of caveolin 1 protein showed a larger number of differentially expressed genes during GD 15.5 than other two time points. This suggested that the absence of *Cav-1* affected the developmental processes in the forebrain, hindbrain, and spinal cord. The Gene Ontology (GO) analysis also showed that the biological process associated with ventral and dorsal spinal cord neuron differentiation was downregulated during GD 15.5 in Cav-1 KO mice compared with WT mice (**Table 3.3**).

Results of hierarchical clustering in our study reflects differences in developmental stages in earlier studies. The histology atlas of mice fetal brain (V. S. Chen et al., 2017) shows that during GD 12.5 the forebrain, especially the medial, lateral,

and caudal ganglionic sections, proliferates and expands at a fast rate. Also, the choroid plexus first appears at this stage and the hypothalamus starts to grow bigger in the diencephalon. In addition, the olfactory (CN1) nerves grow from the multi-layered olfactory epithelium in the caudodorsal nasal cavity, while the hippocampus is still not developed at this stage. Moreover, the hindbrain goes through significant changes in its conformation, and differentiation of Purkinje cells start during GD 11 to 13.

Simultaneously, the mantle and marginal zones of the spinal cord start growing at this stage. The spinal cord expands laterally in the ventral horn more compared to the thoracic and lumbar divisions. The progression of fetal brain development is also shown during GD 15.5 when the six layers of the cerebral cortex are distinctive, with neurons developing to make the layers superficial. Many neurons such as GABAergic inhibitory neurons develop through the growing cerebral cortex. By GD 15.5 the pituitary stalk is also formed. Additionally, in the hindbrain the population of neurons grow rapidly at this stage and the spinal cord columns are more prominent and significantly grows.

Simultaneously at GD 15.5 the cranial nerves also are distinctive in the spinal cord.

Progressively, different developmental stages occur during GD 17.5 when the forebrain is significantly developed with prominent layers, but the hippocampus still does not develop. By this stage the pituitary gland gets well developed and the Rathke's pouch can be visualized as a small cleft. Also, the neurosecretory structures for hormones such as oxytocin develop in the forebrain. Moreover, in the hindbrain the Purkinje cells are well formed and in the spinal cord, the structure is very similar to the adult stage where the sympathetic nervous system starts to appear first in this stage (V. S. Chen et al., 2017).



Altogether, the differences in the developmental stages are well supported by earlier studies and are portrayed by our hierarchical clustering results.

In addition, at GD 17.5 GO analysis showed three downregulated biological processes in *Cav-1* KO fetal brain: haptoglobin binding process, oxygen carrier activity and oxygen binding process. Oxygen supply is crucial in cell development and lack of oxygen in tissues is called “hypoxia”. Low oxygen supply can result in a decline in other cellular process and can result in aging-related diseases (Yeo, 2019). As these biological processes are downregulated in *Cav-1* KO, these can be responsible for facilitating faster aging in them by causing a lack of oxygen in the fetal brain. Noticeably, *7SK* was downregulated in the wildtype and upregulated in the KO model during early stage, but showed opposite regulation during later stage of fetal brain development. *7SK* is a non-coding RNA that has been called the master neuron development regulator (Briese & Sendtner, 2021). We further found few other genes that are regulated differently in the KO fetal brain. During GD 12.5 and 15.5, *H4c18* was downregulated in wildtype and upregulated in *Cav-1* KO. Conversely, *Six6*, which is responsible for inducing mammalian transcription of luteinizing hormone releasing (GnRH) neurons that play a significant role in regulating mammalian fertility by maintaining hypothalamus-pituitary-gonadal (HPG) (Pandolfi et al., 2019), was downregulated in KO fetal brain and upregulated in WT, implying that the fertility of *Cav-1* fertility is also determined from the fetal stage. On the contrary, when GD 17.5 was compared with GD 15.5, *Vwf*, which is a receptor for angiogenic growth factor and plays a role in immune response in

Alzheimer's disease (Lau, Cao, et al., 2020), was downregulated in wildtype and upregulated in *Cav-1* KO, showing fetal origin of AD in *Cav-1* KO. However, *Hbba-1* and *Hba-a2*, which are shown to be downregulated in patients with variant Creutzfeldt-Jakob disease (Vanni et al., 2018), were upregulated in wildtype but downregulated in *Cav-1* KO model. These results indicate the possible link of faster aging with *Cav-1* KO mice and fetal origin of neurodegenerative diseases in mammals.

We further observed that methylation was enriched in the chromatin regions occupied by modified histone proteins, particularly histone 3 trimethylation of lysine 3 and 4 (H3K4me3 and H3K9Me3) (**Figure 3.5B**) which were identified in mice with Alzheimer's Disease (AD)-like neurodegeneration in a previous study (Gjoneska et al., 2015). In addition, meta-analysis of marker genes of brain cells (Dhakal et al., 2021a) showed that several clock genes identified from our methylation assay were markers of glia cells of fetal brain in *Cav-1*-KO mice. Moreover, our single nuclei RNA Seq has found several distinct cell clusters between the KO fetal brain and wildtype. Among which, retinal ganglion cells are known targets of Alzheimer's Disease (Bevan et al., 2020; Blanks et al., 1989; Curcio & Drucker, 1993). Association of ependymal cells with AD is also known (Gião et al., 2022; Liddelow, 2015). Our findings align with the "Glial Cell Dysregulation Hypothesis", suggesting that glial cell dysregulation is linked to functional impairment of neuronal cells in Alzheimer's Disease (von Bernhardi, 2007).

Among the upregulated genes in *Cav-1* brain and placenta and downregulated in wildtype we found *Il1rl1*, which is the receptor for IL33 (Palmer et al., 2008), and was found to improve the beta amyloid pathology in microglial cells in AD brain (Lau, Chen, et al., 2020). Additionally, *ATP5l*, which was identified as one of the major genes in creating a model for Alzheimer's and affects the dysregulated oxidative phosphorylation in mitochondria in the frontal cortex of brain (Finney et al., 2022), was also upregulated in *Cav-1* KO. Moreover, *Fgfbp1* which was found to be a Wnt/Beta-catenin-regulated gene in the endothelial cells in mouse brain to maintain blood brain barrier (Cottarelli et al., 2020), was also upregulated in the knockout brain-placenta genes along with *HOXC4*, which is a Wnt-induced spinal marker (B.-C. Liu et al., 2021). Among the 117 genes that were downregulated in *Cav-1* KO but upregulated in wildtype, there was *PTTGI* (Pituitary tumor-transforming gene), which has been associated with many oncogenic pathways; specifically low expression has been seen in low grade gliomas, meningiomas and schwannomas (Salehi et al., 2013) indicating the potential of fetal origin of oncogenes in the knockout model. In addition, *Thbs4* was also shown to have low expression levels in the female in human brain (Cagliani et al., 2013), implicating sex-biased expression. Interestingly, *LRP4* was shown to have a role in Alzheimer's, with low expression of this gene found in the postmortem brain of AD patients (H. Zhang et al., 2020). Its downregulation in the KO model clearly shows the role of brain-placental axis in fetal programming. Additional genes whose downregulation has been associated with AD were also expressed in the same manner. These include *Spon1*, which binds to the binding site of amyloid precursor protein (APP) that blocks the trigger of amyloid

genesis and reduces the amyloid beta plaque formation (S. Y. Park et al., 2020), and *Adamts12*, which is an Alzheimer's hallmark in the disease pathology (Sarnowski et al., 2022). Other brain development related genes that were downregulated in knockout in brain-placental DEG list include *Nectin 1*, which is responsible for early life stress on neuronal plasticity (C. Wu et al., 2022a); *Fzd8*, which acts in altering the cell cycle timing and size of brain in neural progenitors (Franchini & Pollard, 2015); *Foxf2*, which is responsible for blood-brain barrier breakdown (Reyahi et al., 2015); *fzd1*, which was shown to regulate neurogenesis in adult hippocampus (Mardones et al., 2016); stroke genes, such as *Nog* (Zou et al., 2019); *UBQLN2*, which has been newly associated with neurodegeneration (Renaud et al., 2019); and *Pouf31* which promotes the fate commitment of pluripotent stem cells in neurons and activates the internal neural induction programs, antagonizes extrinsic inhibitory signals in neurons (Q. Zhu et al., 2014). There is also evidence that the lack of caveolin-1 protein alters the regulation of several brain development genes in the placenta.

## **Conclusion**

The findings of this study suggest that *Cav-1* may play a role in fetal brain development in mice. Our observation of genes associated with presenilin, and amyloid secretase pathways of AD and genes associated with histone methylation and chromatin indicate that lack of *Cav-1* likely pose risk for later epigenetic alteration of brain. This double-hit mechanism (dysregulated fetal brain development and altered epigenetic states

of brain genes during aging) may be associated with early adulthood onset of AD symptoms. Moreover, our findings from the single nuclei RNA sequencing support the “Glial Cell Dysregulation Hypothesis”, suggesting that glial cell dysregulation is linked to functional impairment of neuronal cell in AD (Von Bernhardi, 2007). In conclusion, this study shows that *Cav-1* null mice can be used as a model to dissect fetal links of AD.

**Table 3.1** Differentially expressed genes between GD 12.5 vs 15.5 and GD 15.5 vs 17.5 compared between *Cav-1* KO and wildtype mice (C57BL/6J).

<b>Gestation Stage</b>	<b>Number of genes</b>
DOWN_CAV-1_12.5_15.5	1797
UP_CAV-1_12.5_15.5	634
DOWN_BL6_12.5_15.5	915
DOWN_BL6_12.5_15.5:DOWN_CAV-1_12.5_15.5	1001
DOWN_BL6_12.5_15.5:UP_CAV-1_12.5_15.5	3
UP_BL6_12.5_15.5	476
UP_BL6_12.5_15.5:DOWN_CAV-1_12.5_15.5	3
UP_BL6_12.5_15.5:UP_CAV-1_12.5_15.5	363
<b>Sum 12.5vs15.5</b>	<b>5192</b>
DOWN_CAV-1_15.5_17.5	1541
UP_Cav-1_15.5_17.5	315
DOWN_BL6_15.5_17.5	1524
DOWN_BL6_15.5_17.5:DOWN_CAV-1_15.5_17.5	846
DOWN_BL6_15.5_17.5:UP_Cav-1_15.5_17.5	2
UP_BL6_15.5_17.5	1209
UP_BL6_15.5_17.5:DOWN_CAV-1_15.5_17.5	23
UP_BL6_15.5_17.5:UP_Cav-1_15.5_17.5	164
<b>Sum 15.5vs17.5</b>	<b>5624</b>

**Table 3.2** PANTHER Pathways downregulated during GD 12.5 and 15.5 in both wildtype and *Cav-1* KO mice female fetal brain.

Pathway	Number of DEGs	Fold Enrichment	FDR	Gestation day
Hedgehog signaling pathway (P00025)	5	6.6/2.65	1.85E-03	12.5/15.5
Notch signaling pathway (P00045)	10	6.14/3.04	1.86E-05	12.5/15.5
Alzheimer disease-presenilin pathway (P00004)	22	4.57/2.18	2.49E-08	12.5/15.5
Integrin signalling pathway (P00034)	29	4.03/2.28	2.08E-09	12.5/15.5
Angiogenesis (P00005)	24	3.54/2.26	4.33E-07	12.5/15.5
Cadherin signaling pathway (P00012)	18	2.93/2.59	1.10E-04	12.5/15.5
Wnt signaling pathway (P00057)	32	2.71/2.25	1.39E-06	12.5/15.5
VEGF signaling pathway (P00056)	40	2.44	2.87E-04	15.5
Insulin/IGF pathway-protein kinase B signaling cascade (P00033)	23	2.41	9.98E-03	15.5
PDGF signaling pathway (P00047)	76	2.17	4.62E-06	15.5
Alzheimer disease-amyloid secretase pathway (P00003)	30	1.85	4.24E-02	15.5
p53 pathway (P00059)	37	1.72	4.68E-02	15.5
TGF-beta signaling pathway (P00052)	41	1.66	4.41E-02	15.5
Inflammation mediated by chemokine and cytokine signaling pathway (P00031)	95	1.49	1.03E-02	15.5

**Table 3.3** Gene Ontology biological processes downregulated on gestation days 12.5, 15.5 and 17.5 in wildtype and *Cav-1* KO female fetal brain.

<b>GO Biological Process</b>	<b>Number of DEGs</b>	<b>Fold Enrichment</b>	<b>FDR</b>	<b>GD</b>
smoothened signaling pathway involved in spinal cord motor neuron cell fate specification (GO:0021776)	3	26.41	1.90E-02	12.5
smoothened signaling pathway involved in ventral spinal cord interneuron specification (GO:0021775)	3	26.41	1.89E-02	12.5
smoothened signaling pathway involved in ventral spinal cord patterning (GO:0021910)	4	26.41	3.11E-03	12.5
intramembranous ossification (GO:0001957)	5	22.01	8.61E-04	12.5
direct ossification (GO:0036072)	5	22.01	8.59E-04	12.5
spinal cord association neuron differentiation (GO:0021527)	13	4.08	7.51E-03	15.5
ventral spinal cord interneuron differentiation (GO:0021514)	14	4.08	4.87E-03	15.5
cell fate commitment involved in pattern specification (GO:0060581)	12	4.08	1.15E-02	15.5
ventral spinal cord interneuron fate commitment (GO:0060579)	12	4.08	1.15E-02	15.5
dorsal spinal cord development (GO:0021516)	20	3.89	5.42E-04	15.5
regulation of odontogenesis of dentin-containing tooth (GO:0042487)	3	> 100	8.02E-03	17.5
regulation of odontogenesis (GO:0042481)	3	74.99	1.50E-02	17.5
negative regulation of cellular response to growth factor stimulus (GO:0090288)	4	21.36	3.48E-02	17.5
skeletal system morphogenesis (GO:0048705)	6	12.99	1.10E-02	17.5
regulation of cellular response to growth factor stimulus (GO:0090287)	6	10.44	2.31E-02	17.5



**Table 3.4** Gene Ontology biological processes and PANTHER Pathways differentially expressed in female placenta of wildtype and *Cav-1* KO strain.

<b>GO biological process</b>	<b>DEG</b>	<b>Fold Enrichment</b>	<b>FDR</b>	<b>Expression</b>
negative regulation of very-low-density lipoprotein particle remodeling (GO:0010903)	4	22.94	1.82E-02	UP
response to methanol (GO:0033986)	4	22.94	1.81E-02	UP
response to chromate (GO:0046687)	4	18.35	2.75E-02	UP
negative regulation of serine-type peptidase activity (GO:1902572)	7	17.84	3.96E-04	UP
mitotic spindle midzone assembly (GO:0051256)	7	6.69	1.97E-02	DOWN
mitotic spindle elongation (GO:0000022)	7	6.69	1.96E-02	DOWN
histone H3-K4 dimethylation (GO:0044648)	6	6.55	4.51E-02	DOWN
spindle elongation (GO:0051231)	7	5.94	2.98E-02	DOWN
histone H3-K4 monomethylation (GO:0097692)	7	5.94	2.98E-02	DOWN
<b>PANTHER Pathways</b>				
Blood coagulation (P00011)	22	9.7	2.68E-11	UP
Cytoskeletal regulation by Rho GTPase (P00016)	25	2.39	1.89E-02	DOWN
Alzheimer disease-presenilin pathway (P00004)	33	1.99	4.33E-02	DOWN
Wnt signaling pathway (P00057)	69	1.69	1.49E-02	DOWN

**Figure 3.1 A.** A hierarchical clustering of gene expression variation also shows that female fetal brain gene expression pattern on GD 12.5, 15.5 and 17.5 is different between the wildtype (BA, BB, BC) and *Cav-1* knockout model (CA, CB, CC). The scale of branch height is shown to the left of the cladogram.

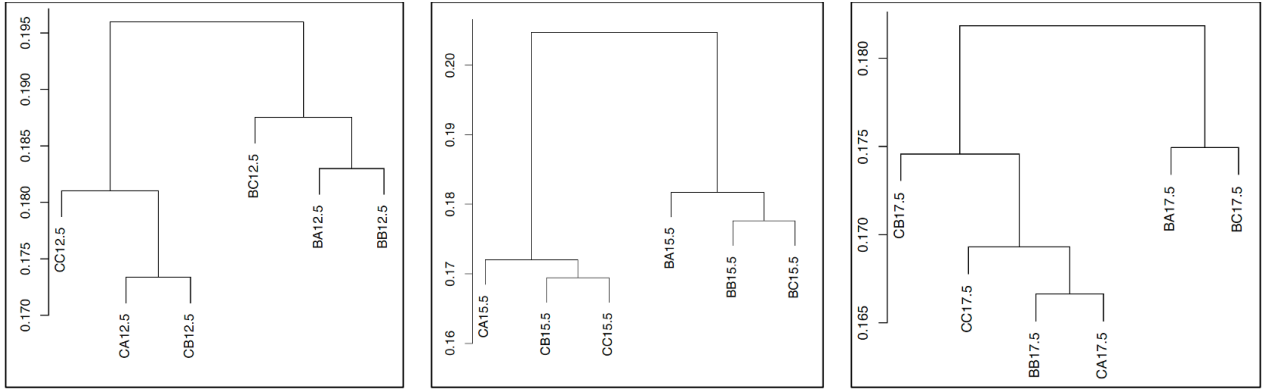


**Figure 3.2** A principal component analysis of the gene expression variation of female fetal brain on gestation day (GD) 12.5, 15.5 and 17.5.

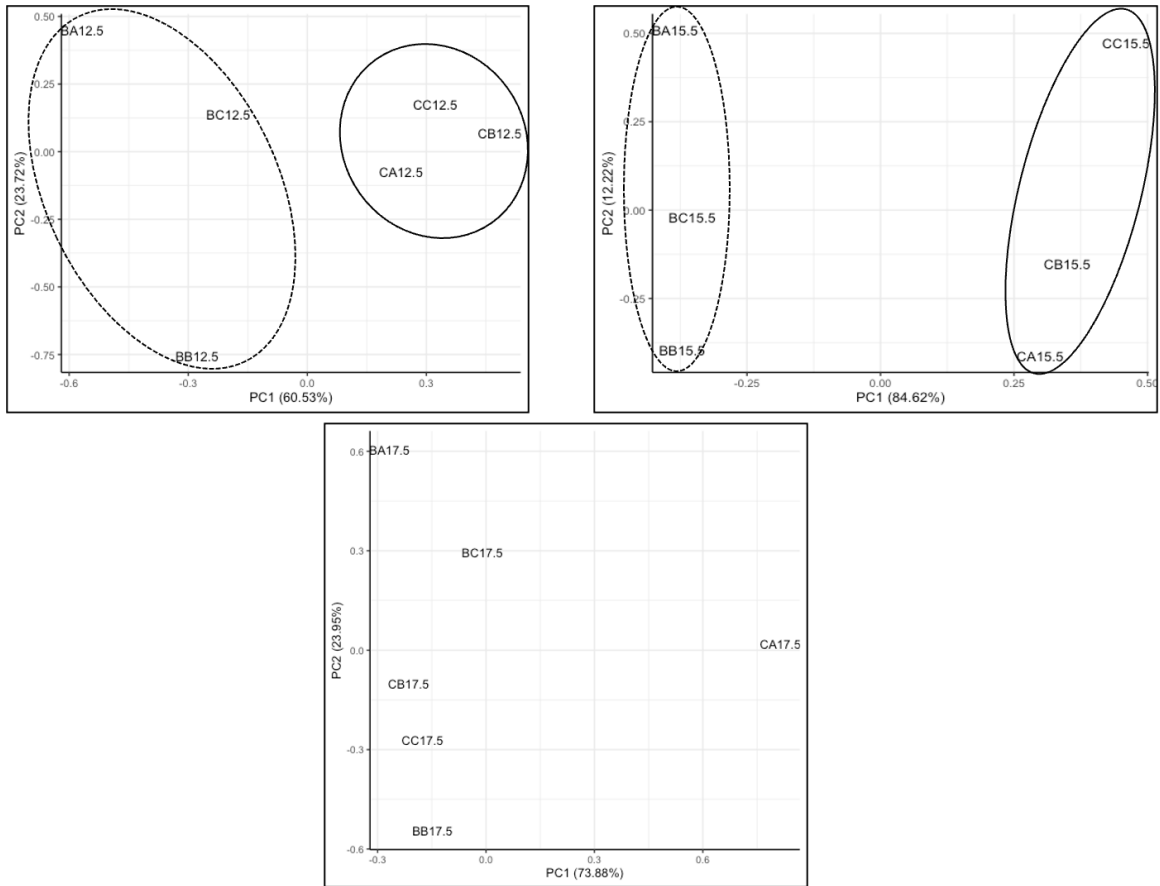


**Figure 3.3** Significant changes (False discovery rate < 0.05) of genes in the developing fetal brain of *Cav-1*-KO compared to wildtype C57BL/6J mice at gestation day (d) 12.5, 15.5 and 17.5. The number of upregulated genes is shown by the upward directed arrow, and number of downregulated genes are shown in downward facing arrow.

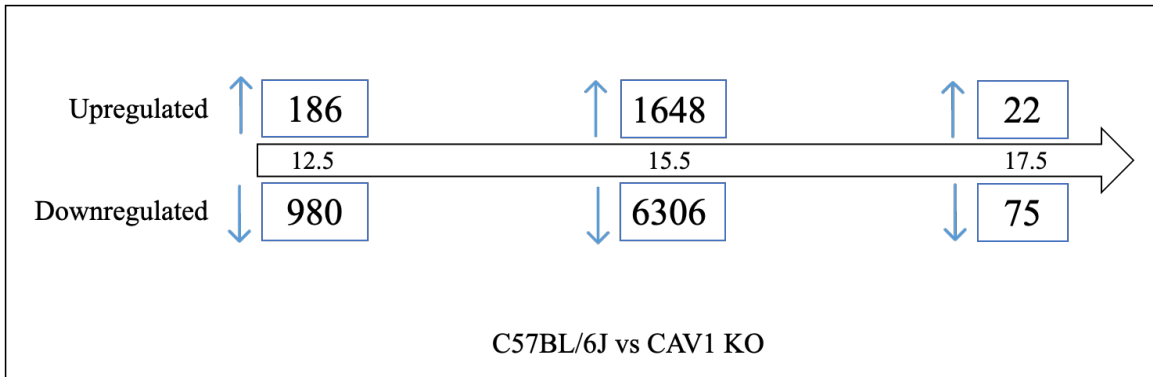


**Figure 3.4** Volcano plots showing differential expression of genes in female fetal brain between gestation 12.5, 15.5 and 17.5 compared between wildtype and *Cav-1* KO mice. In each plot, the y-axis shows the  $-\log_{10}$  of the False discovery rate (FDR) values and x-axis shows log of Fold Change (FC) values. The red color shows genes that were downregulated, and blue color shows genes upregulated between the two groups in each plot. The horizontal line above value 0 in axis represent the FDR value of 0.05, the value used to identify significance of differential expression of genes

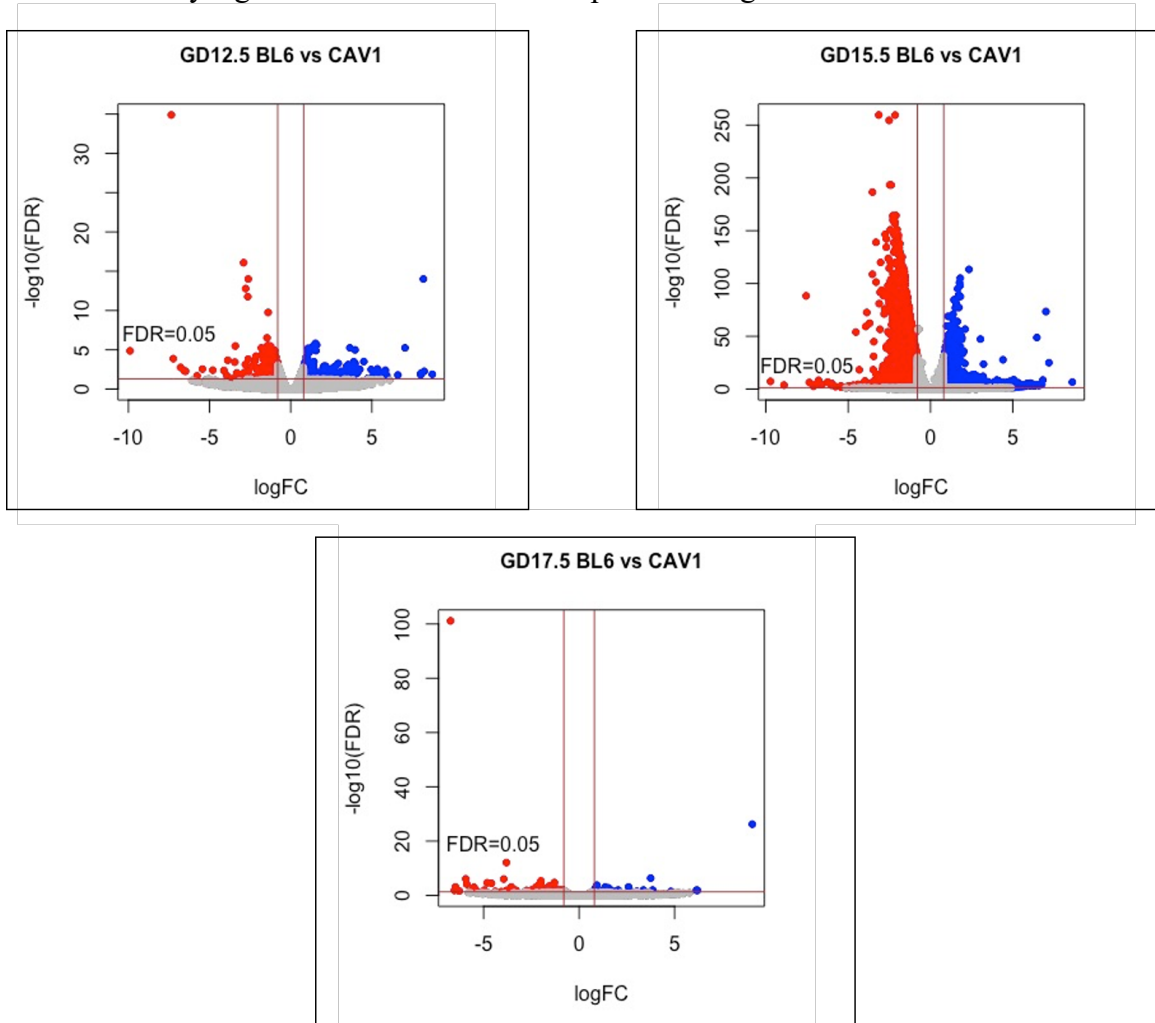


**Figure 3.5.** **A.** Changes in methylation of epigenetic clock sites of aging genes in d15 fetal brain of *Cav-1*-KO compared to WT mice. **B.** SeqMonk mouse genome browser showing a representative example of positional association between DNA methylation and chromatin occupancy of modified (lysine 3 and 4) histone 3 proteins.

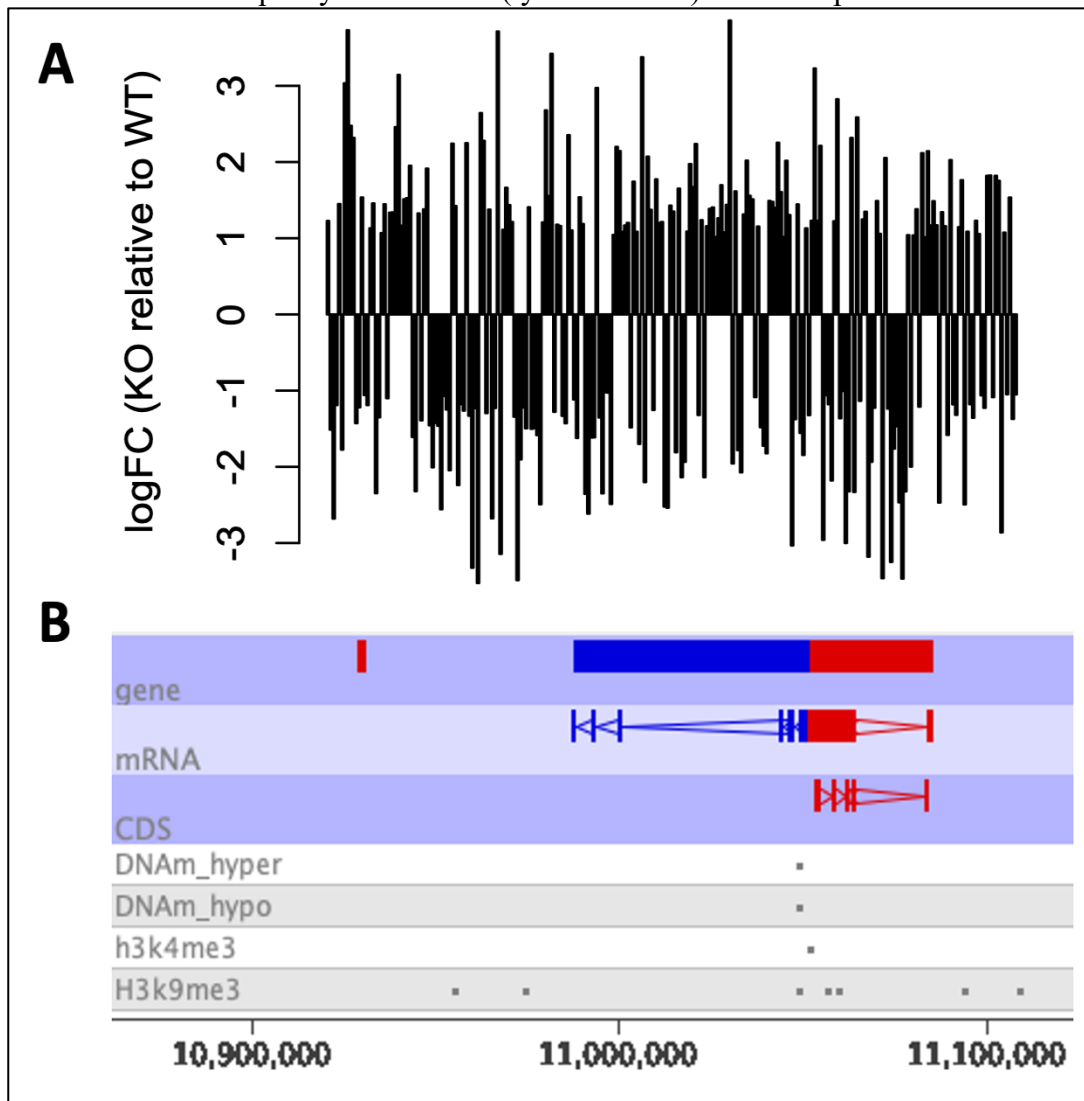


**Figure 3.6.** tSNE plots showing differential cluster patterns of brain cells in the fetal brain (GD15) of WT and *Cav-1* KO mice. Ret: Retinal ganglion cells, Oli: Oligodendrocytes, Mic: Microglia, Tri: Trigeminal neurons, Caj: Cajal-Retzius cells, Epe: Ependymal cells, Int: Interneurons.

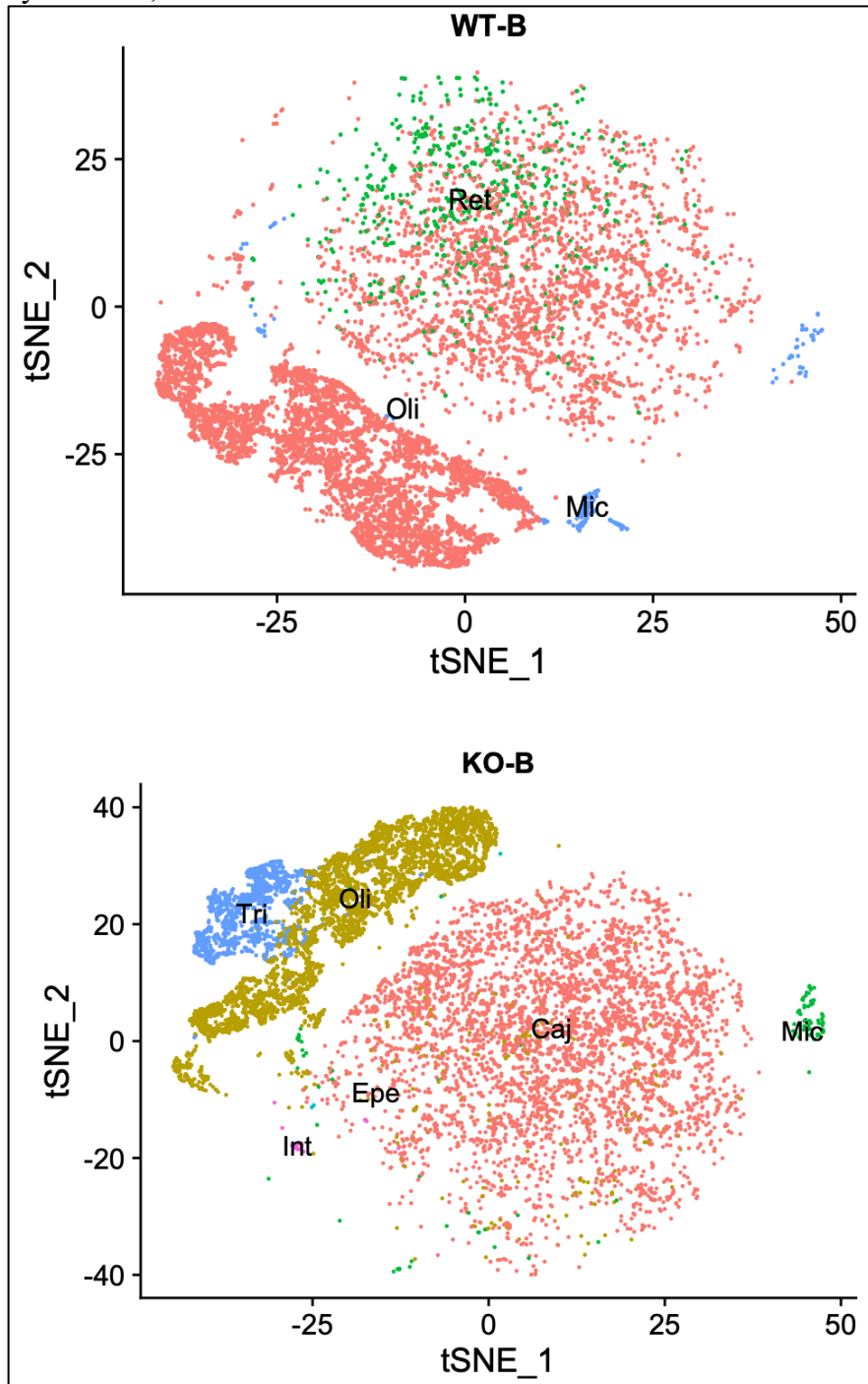


**Figure 3.7 A.** A hierarchical clustering shows that the gene expression variation of female fetal brain and placenta of wildtype is different from *Cav-1* knockout model at GD 15.5. **B.** A hierarchical clustering illustrates that the placenta of female fetus of C57BL/6J is distinct from *Cav-1* KO model at gestation day 15.5. The scale of branch height is shown to the left of the cladogram. In the figure, WTBR.1 WTBR.2 WTBR.3 indicate wildtype female fetal brain, WTPL.1, WTPL.2, WTPL.3 indicate wildtype female placenta, Cav-1.BR1, Cav-1.BR2, Cav-1.BR3 indicate *Cav-1* KO female fetal brain, Cav-1.PL1, Cav-1.PL2, Cav-1.PL3 indicate *Cav-1* KO female placenta.

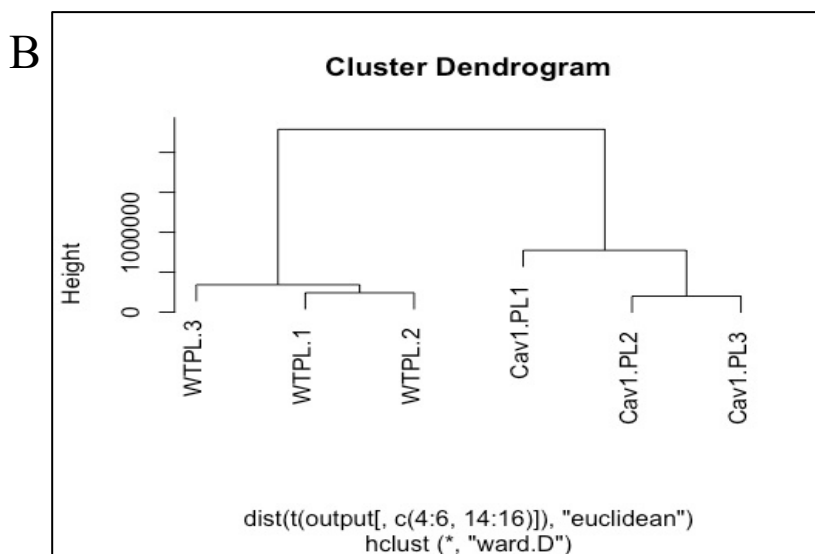
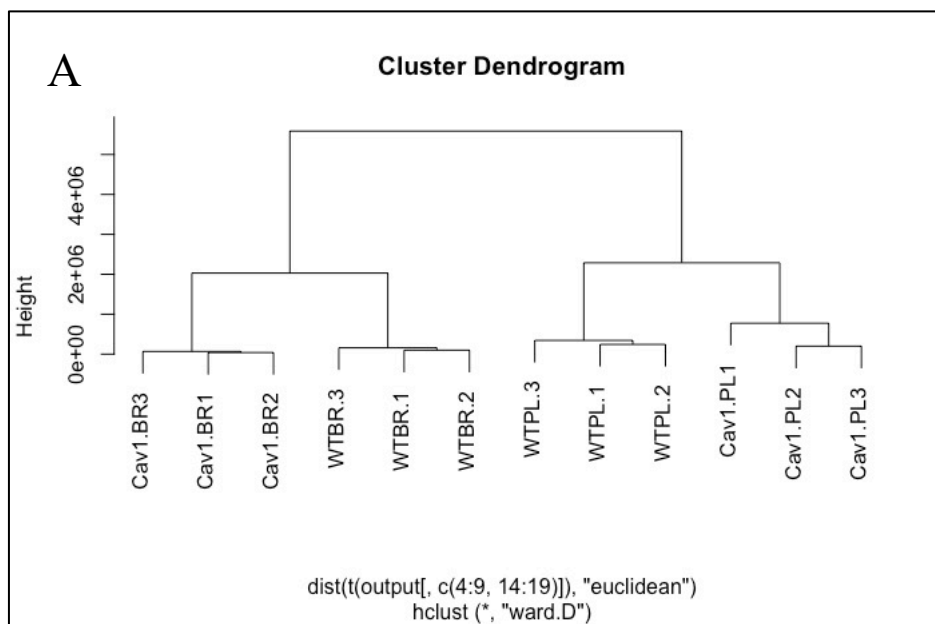
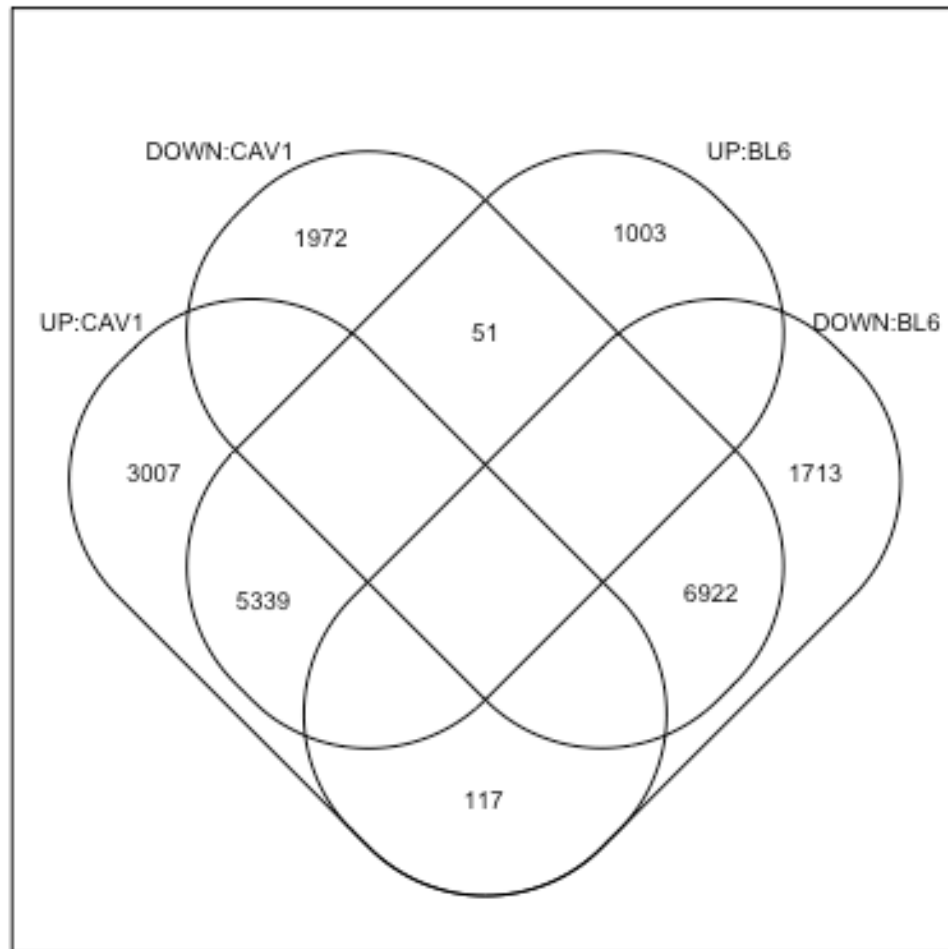




**Figure 3.8** Venn Diagram showing differential gene expression between brain-placenta of wildtype and *Cav-1* KO female fetus. In the figure, DOWN means downregulated genes and UP means upregulated genes.



## Chapter 4

### Use of AKR/J mice to study early-life links of brain aging

#### Abstract

Aging poses the primary risk for several chronic diseases including cancer, Parkinson's, and Alzheimer's diseases in human. However, links between aging and cancer or neurological diseases are not well understood. Aging causes physiological and functional decline of all organs which can lead to clinical complications such as metabolic syndrome multiple organ failure. Aging can vary among animals with different life spans. Studies have observed correlations between lifespan and gestation times among mammals. Links between lifespan and reproduction are known. AKR/J mice have endogenous AKV virus that leads to the onset of Leukemia which reduces lifespan of these mice compared to that of C57BL/6J in which AKV is absent. In this study, we compared the gene expression pattern of fetal brain and placenta of AKR/J with C57BL/6J to understand molecular and cellular links to between aging and leukemia. We show that genes related to aging and neurodegenerative diseases are regulated in specific patterns between the fetal brain and placenta of AKR/J mice. We performed targeted methylation profiling of a total of 2,045 single bases of mouse genome that are associated with the mouse epigenetic clock and showed that brain of AKR/J mice ages faster than that of C57BL/6J mice suggesting a link between leukemia and neuronal aging. By

crossing AKR/J with C57BL/6J mice, analyzing pooled DNA of F2 progenies by whole-genome sequencing as well as single-cell ATAC-seq (Assay for Transposase-Accessible Chromatin by sequencing), we further show that specific transcription factors may be involved in the differential gene regulation of fetal brain in AKR/J mice compared to C57BL/6J mice. Together, the results of this study provide foundational knowledge that will lead to establishing the link between reproduction and aging.

## **Introduction**

Aging causes decline of immune systems (Fabbri et al., 2015) that often leads to chronic diseases and progressive complications such as organ failure (Neild, 2001). Importantly, aging has the most influence on cancer incidences in humans (Berben et al., 2021). Leukemia represents different types of blood-related cancers and kills nearly 0.35 million people globally each year. In the United States alone, more than 459,000 people are living with leukemia, with 61,059 new cases being detected in year 2021 alone. Leukemia incidence is expected to rise with increase in the aging population. According to the National Cancer Institute, it is rising by 3.2% in the recent years in the United States.

Understanding the biological links between aging and leukemia (and other types of cancer) is highly important to develop intervention strategies by targeting those specific links. Several studies have shown associations between leukemia and cognitive

aging (Meyers et al., 2005). Cross-sectional study showed functional decline in cognition among people with chronic lymphatic leukemia (Williams et al., 2020). Vascular aging, particularly of bone-marrow endothelial cells, has direct influence on risk of developing leukemia (Lazzari et al., 2018). Bone-marrow is a potential source of neurons and endothelial cells for reparative processes in response to brain injury such as cerebral ischemia (Hess et al., 2002). Epigenetic changes in the DNA of blood upon aging are well known (Chew et al., 2018; Farré et al., 2015; Mori et al., n.d.; Schachtschneider et al., 2020). Striking correspondences in DNA methylation between blood and brain were shown in several studies (Edgar et al., 2017; Farré et al., 2015; Lin et al., 2018; Tylee et al., 2013; Walton et al., 2016; Wei et al., 2020). However, whether leukemia and brain aging are epigenetically related is not known.

The murine leukemia viruses (MLVs), which are the causes of cancer in mice, are retroviruses belonging to the gammaretroviral genus. Endogenous MLVs, which are passed from one generation to the next by germ line, get integrated into the host genome. AKR/J inbred mice has AKV which is an endogenous MLV. Ecotropic expression of AKV is found in all tissues from birth in AKR/J mice (Herr & Gilbert, 1982). Leukemia progression occurs in an age-dependent manner in these mice. Onset of leukemia occurs as early as three months of age, and most AKR/J mice (60 to 90%) show cancer by age 10 months and die within a month or two after the onset. In an earlier study, genetic mapping identified a locus (*AKv1*) for mouse susceptibility to AKV (Rowe et al., 1972). Subsequently, a second locus (*AKv2*) was found for AKV susceptibility (Kozak & Rowe,

1980). In a relatively recent study it was shown that the Apolipoprotein B gene *Apobec3* could also be associated with contrasting susceptibility of AKR/J and C57BL/6J mice to AKV (Langlois et al., 2009). Due to inherent susceptibility to AKV and development of leukemia, the AKR/J mice have significantly shorter lifespan (nearly three-fold less) compared to C57BL/6J mice.

Several inbred strains derived from AKR/J show different rates of aging. Some of those are prone (SAMP) and others are resistant (SAMR) to accelerated senescence. There is a high level of ectopic expression of AKV in the brain of SAMP mice but not in SAMR mice (Carp et al., 2002). Moreover, in SAMP mice, AKV is expressed abundantly in specific brain cells, primarily in neurons, astrocytes, vascular endothelium, and oligodendroglia (Jeong et al., 2002). However, SAMP and SAMR mice cannot be used in genetic mapping experiments because these mice are derived from the same inbred mice, so they lack the level of genetic polymorphisms required for mapping studies. On the other hand, AKR/J and C57BL/6J strains have extensive genetic polymorphisms (Lilue et al., 2018).

One of the aims of this study is to understand gene expression changes in the brain during fetal development of AKR/J relative to C57BL/6J mice. The second aim of this study is to identify segregating loci that are linked to differential aging of brain in AKR/J mice relative to that of C57BL/6J mice. Finally, this study also investigates

chromatin structure and identifies candidate transcription factors associated with differential gene expression in the fetal brain of AKR/J relative to C57BL/6J mice.

## **Methods**

### *Animal Breeding and Sample Collection*

C57BL/6J and AKR/J mice were obtained from Jackson Laboratory. Adult female mice were mated with fertile males of each strain to induce pregnancy. Pregnant mice were euthanized on GD15.5. The fetal brain and placenta were collected from all implantation sites. The placenta was carefully separated from the decidua. All the samples were washed in sterile PBS and snap frozen in liquid nitrogen. All animal procedures were approved by the Institutional Animal Care and Use Committee of the University of Missouri-Columbia and were conducted according to the *Guide for the Care and Use of Laboratory Animals* (National Institutes of Health, Bethesda, MD, USA).

### *RNA Extraction*

All the samples were then processed for RNA analysis. Total RNA was isolated from frozen tissue samples using an AllPrep DNA/RNA Mini Kit (Qiagen, Cat No./ID: 80204) as per the manufacturer's instruction. Each fetal brain was homogenized with 500

ul to 1 ml RLT buffer (Qiagen, Cat No./ID: 79216) and 5µl 2-mercaptoethanol. Homogenization was done in a 15 ml Falcon tube using a benchtop VDI 25 tissue homogenizer (VWR). The homogenate was transferred to the mini column then centrifuged for 1 minute at  $\geq 8000 \times g$ . From the supernatant, 750µl was transferred into RNase/DNase-free Axygen conical tubes (Corning Axygen, 1.5ml) and mixed with 1 volume 70% ethanol to precipitate RNA. RNA was eluted in 30µl nuclease-free water twice for a total volume of 60µl. RNA from a total of 27 samples (3 gestation days, 3 biological replicates, and 2 strains) were generated. Concentration and purity of the RNA was determined using Nanodrop 1000 spectrophotometer (Thermo Fisher Scientific) before each sample was diluted to 100ng/µl using nuclease-free water.

#### *Gene expression profiling by RNA-seq*

Illumina sequencing libraries were generated from the total RNA of each sample. Preparation of libraries and RNA sequencing (RNA-seq) were performed by the Novogene Cooperation Inc. (8801 Folsom Blvd #290, Sacramento, CA 95826). Each library was sequenced to 20 million paired end reads of 150 bases using a NovaSeq sequencer.

#### *RNA-seq data analysis*

RNA-seq data analysis was performed as described in our earlier works (Dhakal et al., 2021a; Strawn et al., 2021). Briefly, the quality of raw sequences was checked with FastQC followed by trimming the adaptors from the sequence reads by *cutadapt*. The *fqtrim* tool was used to perform base quality trimming (Phred score >30) by sliding window scan (6 nucleotides). The high quality reads were then mapped to the mouse reference genome GRCm38 using Hisat2 aligner (D. Kim et al., 2015). Read counting from the alignment data was performed by *FeatureCounts* (Liao et al., 2014). The feature count data was then analyzed using packages in R.

#### *Bulk Segregant Analysis (BSA)*

Our strategy of mapping genetic loci linked to brain aging in AKR/J mice is illustrated in Figure 4.16 This approach integrates BSA-seq method of QTL (quantitative trait loci) mapping (Arnold et al., 2011; Tang et al., 2018; Xia et al., 2010) with whole-genome sequencing as well as whole-genome bisulfite sequencing (WGBS) (Islam et al., 2022; Laufer et al., 2021) of F2 mapping population from AKR/J x C57BL/6J crosses. The F2s were phenotyped based on epigenetic age of brain as well as parental color coat (black: C57BL/6J and white: AKR/J). The segregating genetic variation (from whole-genome sequencing) and their allelic methylation from WGBS was used for association analysis by binomial mixed model (Fan et al., 2019).



DNA was prepared using AllPrep DNA/RNA Mini Kit (Qiagen, Cat No./ID: 80204) as per manufacturer's instruction. DNA quality and quantity was checked according to the previously used method (Islam et al., 2022). Phenotyping of brain age was based on the rate of brain aging (brainYEAR) of F2s. Based on the brainYEAR phenotype scores, two F2 pools: low brainYEAR (C57BL/6J parental phenotype) and high brainYEAR (AKR/J parental phenotype) were prepared. The two pooled F2s contained segregating alleles linked to the brainYEAR phenotypes. Bulk DNA was prepared by combining equimolar amounts of DNA from the mice of the two pools. At least 25% of the mapping population was represented in the pools to ensure segregation of rare variants in BSA-seq (Tang et al., 2018).

In BSA-seq, genome sequencing coverage should be enough to cover rare variants that might be present in the pooled DNAs. We achieved this by sequencing the libraries to genome coverage, which represents ploidy of cells multiplied with the number of individuals represented in the pool (Magwene et al., 2011; Navarro-Escalante et al., 2020), higher than the effective pool size. This roughly translates to 20x coverage in our experiment. Library preparation and sequencing were performed using Illumina NovaSeq platform at the University of Missouri Genomics Technology Core. Paired-end reads (150 bases) at 20x genome coverage were generated.

The genome sequence data was checked for quality by *FastQC*. Quality control was performed using *Trimmomatic* tool (Bolger et al., 2014). Read mapping to mouse

reference genome assembly (GRCM39) was performed using the Burrows-Wheeler Aligner (BWA) (H. Li & Durbin, 2009). Variant analysis was performed using the Genome Analysis Toolkit (GATK) with recommended best practices (Van der Auwera et al., 2013). The read alignment files (BAM format) were subjected to post-alignment steps to remove duplicates, insertion/deletion (InDel) realignment and base quality recalibration prior to SNP calling. SNP calling was performed using *Haplotypecaller* which performs genotype likelihood test for each SNP (Single nucleotide Polymorphism) in individual samples followed by a ‘joint genotyping’ analysis to identify raw SNPs. The variant recalibration step was performed to identify high quality SNPs. The SNPs generated using this approach were used to calculate *SNP-index* which is the proportion of alleles of each SNP between the two bulks. A SNP-index of ~0.5 reflects equal representation of both parents (no linkage to the phenotype). Those SNPs were excluded from the analysis. Sliding window analysis (J. Zhang & Panthee, 2020) was performed to identify genomic regions that were significantly enriched with SNPs showing *delta SNP-index* (difference in SNP-index between the two bulks) greater than zero (see **Figure 4.8**). The genotype-phenotype association tests was performed using the R package *QTLseqr*.

#### *Single-nuclei ATAC-seq (snATAC-seq)*

Single nuclei from brain samples from pooled brain of F2s were isolated using Pure Prep Nuclei Isolation kit (Sigma, St. Louis, MO, USA) as per manufacturer’s

instruction. We isolated single nuclei from flash frozen samples of mouse brain. Briefly, frozen brain samples after thawing were minced into small pieces and added to lysis buffer. Using a dounce homogenizer, the sample was homogenized until the solution looked well mixed, which generally required 15-20 dounces. A 70 $\mu$ m cell strainer was used to filter the nuclei from the lysed cells, diluted and layered over a freshly prepared 1.8M sucrose cushion solution to collect single nuclei. After centrifugation and suspension with the kit provided storage buffer (ice cold), final purification of single nuclei was performed by filtering through a 40 $\mu$ m cell strainer. The purified nuclei were then counted using a Countess II FL Automated Cell Counter (ThermoFisher). The nuclei pellet was resuspended in 10  $\mu$ l chilled nuclei buffer. Nuclei counting was performed using a Countess II FL Automated Cell Counter. The nuclei were used to prepare ATAC-seq libraries at the University of Missouri DNA core facility using the Chromium Single Cell ATAC Reagent Kit according to the manufacture's guide.

*Data analysis of snATAC-seq:*

The raw data was processed by the *Cell Ranger* pipeline. The BWA-MEM (Burrows-Wheeler Aligner Maximal Exact Matches) aligner was used to perform read mapping to the reference genome of mouse. The peak/cell and the fragment/cell count data generated from *Cell Ranger* was used to analyze open chromatin in single nuclei using the R package *Signac* (Stuart et al., 2020). First, we calculated transcriptional start site (TSS) enrichment score, nucleosome banding pattern, number of fragments in peaks,

proportion of fragments per peak, and proportion of reads in genomic blacklist regions to perform the recommended (ENCODE) quality control steps using *Signac*. The count data was then normalized by TF-IDF (term frequency-inverse document frequency) (Moussa & Măndoiu, 2018) followed by feature selection and dimension reduction. Non-linear dimension reduction and clustering was performed by UMAP (uniform manifold approximation and projection) method (Becht et al., 2018) implemented within *Signac*. Differential chromatin accessible tests (Gontarz et al., 2020) were performed to compare open chromatin regions (peaks) between cell types in each sample. Motif enrichment analysis was then performed by hypergeometric test implemented within *Signac*. The known TF motifs in the JASPAR database (*R* package *JASPAR2020*) was used to determine motif incidences within each peak. When multiple TF motifs were enriched within a peak, the motif that was closest to the peak summit was used.

## Results

### *Gene expression differences during development of fetal brain of AKR/J relative to C57BL/6J*

RNA sequencing was performed to profile gene expression of fetal brain of AKR/J mice and C57BL/6J mice (female sex used in both strains) at three gestation times (GDs 12.5, 15.5 and 15.5). Hierarchical clustering showed that the fetal brain of these two strains were transcriptionally distinct in each gestation period (**Figure 4.1**).

Differential expression (DE) analysis by *edgeR* identified 2961 genes at GD 12.5, 711 genes at GD 15.5 and 266 genes at GD 17.5 that were upregulated in AKR/J relative to C57BL/6J female fetal brain (**Figure 4.2**). While the number of upregulated genes decreased with the progression of gestation days, the downregulated genes showed a different pattern. The results showed that 3647 genes at GD 12.5, 4646 genes at GD 15.5 and 1011 genes at GD 17.5 were downregulated in AKR/J relative to C57BL/6J female fetal brain (**Figure 4.3**). The volcano plots (**Figure 4.3**) showed that the number of DEGs is the highest during early gestation which is GD 12.5. Moreover, Principal Component Analysis (PCA) showed distinct clusters indicating differences in gene expression in the fetal brains of the two strains (**Figure 4.4**).

Gene Ontology (GO) analysis of the DE genes was performed. At GD 12.5, the upregulated biological processes were proton motive force-driven mitochondrial ATP synthesis (GO:0042776), the process of NADH to ubiquinone and ubiquinol to cytochrome c in the mitochondrial electron transport (GO:0006120, GO: 0006122), NADH dehydrogenase complex assembly (GO:0010257) and mitochondrial respiratory chain complex I assembly (GO:0032981) (**Table 4.1**). In contrast, the downregulated processes were presynaptic active zone organization (GO:1990709), negative regulation of mitophagy (GO:1901525), neurotransmitter receptor diffusion trapping (GO:0099628), postsynaptic neurotransmitter receptor diffusion trapping (GO:0098970) and receptor diffusion trapping (GO:00989953). Our results show that the downregulated processes were more associated to neural development (**Table 4.1**). Moreover, there were no

significant GO terms for upregulated genes at GD 15.5, but the neural regulatory biological processes that were downregulated were maintenance of postsynaptic specialization structure (GO:0098880), regulation of synaptic membrane adhesion (GO:0099179), regulation of glutamate receptor signaling pathway (GO:19000449), regulation of modification of postsynaptic actin cytoskeleton (GO:1905274) and cerebellar granule cell differentiation (GO:0021707). On GD 17.5 the regulation of opioid receptor signaling pathway (GO:2000474), positive regulation of long-term synaptic depression (GO:1900464), regulation of postsynaptic density (GO:0099151) and specialization (GO:0099150) assembly and regulation of excitatory synapse assembly (GO:1904889) were downregulated with no significantly enriched terms for upregulated genes (**Table 4.1**).

PANTHER pathways analysis identified blood coagulation pathway (P00011) and wnt signaling pathway (P00057) enriched among the upregulated genes, and synaptic vesicle trafficking (P05734), metabotropic glutamate group I pathway (P00041), axon guidance mediated by netrin (P00009), hedgehog signaling pathway (P00025) and GABA-B receptor II signaling pathway (P05731) enriched among the downregulated genes in AKR/J compared to C57BL/6J fetal brains on GD12.5. As the brain developed to GD15.5, no specific pathway was enriched among the upregulated genes whereas the metabotropic glutamate receptor group I pathway (P00041), axon guidance mediated by netrin pathway (P00009), axon guidance mediated by semaphorins (P00007) and by Slit or Robo (P00008) and ionotropic glutamate receptor pathway (P00037), were enriched by

the downregulated genes. On GD 17.5, the GABA-B receptor II signaling pathway (P05731) was downregulated again at late gestation GD17.5 with almost double fold enrichment and the ionotropic glutamate receptor pathway (P00037) continued to be downregulated at this stage but with higher fold enrichment. Other downregulated pathways were pyridoxal phosphate salvage pathway (P02770), vitamin B6 metabolism pathway (P02787), Opioid proenkephalin pathway (P05915) with no significantly enriched upregulated pathways. The results are summarized in **Table 4.2**.

We further compared Differentially Expressed (DE) genes on GD 15.5 relative to GD 12.5. There were 15 genes that were downregulated in AKR/J but upregulated in C57BL/6J during this period. They included *Ifi202b*, *Nr1h5*, *Guca2b*, *Htra1*, *Cuzd1*, *Cdh3*, *Col4a1/2*, *Sptb*, *Hspa1a* and *Ccbe1*. In contrast, the genes that were upregulated in AKR/J but downregulated in C57BL/6J were *Kirrel2*, *Nphs1*, *Tarbp1* and *Pgk1-rs7*. We also identified genes which showed opposite expression pattern in GD 17.5 compared with GD 15.5. *Adamts3/18*, *Nos1*, *Nfix*, *Tenm2* and *Tiam2* were upregulated in AKR/J and downregulated in C57BL/6J during this period.

#### *Gene expression in the placenta between AKR/J and C57BL/6J*

RNA-seq was performed to profile gene expression of the placenta of GD15.5 female fetus of AKR/J compared to that of C57BL/6J. Hierarchical clustering showed that the placenta is transcriptionally distinct between the two strains on GD15.5 (**Figure**

**4.5).** Differential expression analysis by *edgeR* further identified 2960 upregulated and 3640 downregulated differentially expressed genes in the placenta between the two strains.

Gene Ontology (GO) analysis identified biological processes that were upregulated, such as positive regulation by host of viral transcription (GO:0043923), regulation of myoblast proliferation (GO:2000291), negative regulation of nitric oxide biosynthetic process (GO:0045019), nitric oxide metabolic process (GO:1904406) and miRNA transcription (GO:1902894). In contrast, processes related nucleobase biosynthetic process (GO:0046112), serine family amino acid biosynthetic process (GO:0009070), dopamine receptor signaling pathway (GO:0007212), negative regulation of hydrogen peroxide-induced cell death (GO:1903206) and response to reactive oxygen species (GO:1901032) were downregulated (**Table 4.3**).

PANTHER pathways analysis showed enrichment of ionotropic glutamate receptor pathway (P00037), metabotropic glutamate receptor group III pathway (P00039), p38 MAPK pathway (P05918), interleukin signaling pathway (P00036), Parkinson disease pathway (P00049), EGF receptor signaling pathway (P00018), Alzheimer disease-presenilin pathway (P00004) and Huntington disease pathway (P00029) were upregulated in AKR/J placenta. On the contrary, p53 pathway (P04393), apoptosis signaling pathway (P00006), CCLR signaling pathway (P06959) and



gonadotropin-releasing hormone receptor pathway (P06664) were significantly enriched among the downregulated pathways in AKR/J placenta (**Table 4.4**).

*Comparative analysis of DE genes of placenta and fetal brain between AKR/J and C57BL/6J*

The Venn diagram in **Figure 4.6** shows a comparative distribution of DE genes of placenta and fetal brain between AKR/J and C57BL/6J mice. The figure shows that there were 6252 genes commonly downregulated and 5321 genes commonly upregulated in the fetal brain relative to the placenta in both the strains. However, there were 11 genes that were downregulated in AKR/J but upregulated in C57BL/6J fetal brain relative to respective placenta. Another, 172 genes showed the opposite expression pattern.

Gene Ontology analysis (**Table 4.5**) identified significant enrichment of biological processes for upregulated genes in both strains such as spinal cord association neuron differentiation (GO:0021527), forebrain dorsal/ventral pattern formation (GO:0021798), gamma-aminobutyric acid secretion (GO:0014051), clustering of voltage-gated potassium channels (GO:0045163) and presynaptic dense core vesicle exocytosis (GO:0099525). The commonly downregulated processes showed enrichment of natural killer cell mediated cytotoxicity (GO:0042270), positive regulation of lactation (GO:1903487), cellular response to lipoteichoic acid (GO:0071223), T cell mediated cytotoxicity (GO:0001913) and skin morphogenesis (GO:0043489).

PANTHER pathway analysis (**Table 4.6**) identified 31 pathways that were enriched among the upregulated DE genes. They included endogenous cannabinoid signaling pathway (P05730), ionotropic glutamate receptor pathway (P00037), metabotropic glutamate receptor group III pathway (P00039), GABA-B receptor II signaling pathway (P05731) and cadherin signaling pathway (P00012). On the other hand, only 8 pathways were enriched among the downregulated genes in the fetal brain of both strains. They included blood coagulation pathway (P00011), integrin signaling pathway (P00034), cytoskeletal regulation by Rho GTPase (P00016), apoptosis signaling pathway (P00006) and angiogenesis pathway (P00005) among others (**Table 4.6**).

#### *Epigenetic clock analysis of aging brain*

Epigenetic clock analysis, which is an assay based on the principles of Horvath pan-tissue clock (Chew et al., 2018), was performed (Zymo DNAge®, Irvine, CA) by profiling methylation of the 2,045 CpG sites of epigenetic clock genes (Stubbs et al., 2017a) in the male and female brain of AKR/J and C57BL/6J mice at fetal, postnatal and old stages (**Figure 4.7**). The methylation data was then used to estimate brain age by elastic net regression by Zymo's DNAge® predictor tool (Coninx et al., 2020). The rate of brain aging was calculated using a novel score called brainYEAR (YEAR: Year-wise Epigenetic Age Rise) that estimates rate of increase of brain biological age per year of chronological age. The brainYEAR = 1 means that brain ages according to chronological ages, and brainYEAR < 1 means slow biological aging, often referred to as SuperAger

(Harrison et al., 2012; Kwak et al., 2018; Rogalski et al., 2013). On the other hand, brainYEAR > 1 means accelerated aging of brain. The brainYEAR analysis showed that brain of AKR/J mice aged in an accelerated manner, nearly 2x fold, compared to that of C57BL/6J mice (**Figure 4.8**).

#### *Identification of segregating loci linked to accelerated brain aging of AKR/J mice*

Crosses were performed between AKR/J female and C57BL/6J male mice (8 weeks old) to generate 32 F2s (**Figure 4.9**). The genome sequences of AKR/J and C57BL/6J differ by ~6.8 million single nucleotide polymorphisms (SNPs). We analyzed those SNPs relative to the sites methylated in the fetal brain of C57BL/6J mice generated by whole-genome bisulfite sequencing in our earlier work (Islam et al., 2022). The analysis identified a total of 37,424 SNPs where the reference alleles were methylated in the fetal brain of C57BL/6J mice. An additional 192,522 SNPs were found within 100 bp (with median distance 28 bp) of the methylation sites in the fetal brain. A representative genome browser image in **Figure 4.10** shows positional correspondences between SNPs and brain methylation sites.

#### *Gene expression studies of aging brain of AKR/J compared to C57BL/6J mice*

We performed RNA sequencing of brain from AKR/J and C57BL/6J mice of both sexes at young and old ages. The brain of AKR/J mice at young age showed a reduced

level of gene expression compared to brain of C57BL/6J mice at old age (**Figure 4.11**) suggesting that genes in the brain of AKR/J mice at a young age may function same way as those in C57BL/6J mice at an old age.

*Single-cell open chromatin profiling of brain between AKR/J vs C57BL/6J mice*

Single-nuclei ATAC seq analysis identified open chromatin in 13,908 cells of AKR/J male brain, 14,185 cells of AKR/J female brain, 15,930 cells of C57BL/6J male brain and 6,946 cells of C57BL/6J female brain. Cluster analysis followed by non-linear dimension reduction showed variation in fragment counts that mapped to the open chromatin revealing different clusters (**Figure 4.12 & 4.13**). The number of the peaks representing the open chromatin represented 36% of cells of AKR/J male brain, 36.2 % cells of AKR/J female brain, 34.1% cells of C57BL/6J male brain and 39.4% of C57BL/6J female brain. The number of single cells with open chromatin varied between the two strains. Only 1608 cells harbored common open chromatin regions between the brain cells of both strains and both sexes (**Figure 4.14**). Also, there were brain cells that had open chromatin in a strain-specific manner. These were relatively less in AKR/J mice compared to C57BL/6J brain. Genes associated with the open chromatin regions were analyzed. Comparison of the top 20 genes for enrichment of binding motifs of transcription factor (TF) showed similar proportions of TF motifs in both the strains (**Figure 4.15**) indicating that same TFs may bind to the open chromatin regions of the fetal brain cells in both the AKR/J and C57BL/6J mice.

## Discussion

In this study, we sequenced RNA from fetal brain of C57BL/6J and AKR/J. Our results show differential gene expression in the fetal brain of AKR/J compared to C57BL/6J mice at gestation day 12.5, 15.5 and 17.5. Our results support the previous studies which showed that the mouse fetal brain goes through changes over the gestation period (V. S. Chen et al., 2017). It has been shown that during GD 12.5, the fetal forebrain is proliferated and expanded at a fast rate especially the medial, lateral, and caudal ganglionic sections with the choroid plexus appearing at this stage and the hypothalamus starting to grow bigger in the diencephalon. Simultaneously, the spinal cord start growing at this stage. At this stage, GABAergic inhibitory neurons develop through the growing cerebral cortex. On GD 15.5, the hindbrain the population of neurons grows rapidly at this stage and the spinal cord columns are more prominent and starts growing rapidly. On GD 17.5, the neurosecretory structures for hormones such as oxytocin develop in the forebrain while the hindbrain the Purkinje cells are well formed (V. S. Chen et al., 2017).

Gene Ontology analysis identified over-represented biological processes of Differentially Expressed (DE) genes of the fetal brains of both strains at different gestation days (GD 12.2, 15.5, 17.5). The upregulated processes at GD 12.5 were mitochondrial ATP Synthase activity, mitochondrial electron transport activity, proton

motive force-driven ATP synthesis activity, NADH dehydrogenase activity (one of the major electron donors in oxidative phosphorylation (Ying, 2008)). Interestingly, increase of mitochondrial oxidative metabolism has been recognized as a metabolic hallmark for leukemia (Byrd et al., 2013) (Kuntz et al., 2017) (E. A. Lee et al., 2015) (Sriskanthadevan et al., 2015) (Suganuma et al., 2010) (Nelson et al., 2021), which suggests that the hallmark is present in the early gestational fetal brain in AKR/J mice. ATP synthase has been further shown to be the target of lipid oxidative damage in human brain and in aging and it is considered as anti-aging therapeutic target (Jové et al., 2019). Mitochondria are one of the most significant sources of Reactive Oxygen Species (ROS) in the brain known as mitochondrial ROS (mtROS) and they are the center for major cellular functions, most importantly ATP synthesis through oxidative phosphorylation which produces ROS as well (Stefanatos & Sanz, 2018). Altogether, these findings coincide with our results. Moreover, during GD 15.5 glutamate receptor signaling pathway was downregulated in the fetal brain. It has been shown before that over 40% of the synapses in the neurons are glutamergic and it is firmly regulated in the neurons, astrocytes, and endothelial cells via metabolite exchange. Strikingly, in an Alzheimer's disease brain the amyloid beta pathology can reduce the glutamate uptake in astrocytes that can lead to swelling of neurones, membrane integrity destruction and cell death (Conway, 2020). It has also been shown that glutamate concentrations were lower in the AD patients in the posterior cingulate cortex (Fayed et al., 2011) (Gimse et al., 2019). These differentially regulated cellular processes suggest that the fetal brain programming can be different

based on the potential of faster aging in the adult stage and can show hallmarks of aging related diseases before the diseases are expressed in older age.

Our results from PANTHER pathway analysis are also consistent with the previous findings. During GD 12.5 hedgehog signaling pathway was downregulated in the female fetal brain of AKR/J relative to C57BL/6J. Previous studies showed that depletion of this pathway reduces the lifespan, dopaminergic neuron integrity and locomotor activity in AD drosophila which is a disease model for human amyloid beta in the glia cells, indicating that the Hedgehog signaling pathway is essential for lifespan deduction (Rallis et al., 2020). Moreover, glutamate receptor pathways were also downregulated at all gestation days, which is consistent with the GO analysis of our results, and was also shown to be decreased in AD brain (Fayed et al., 2011). Simultaneously, at GD 15.5 the axon guidance by *netrin-1* was downregulated, which can result in compromised transmission excitatory synapses and LTP at Schaffer collateral synapses (Glasgow et al., 2020). Progressively at GD 17.5 fetal brain, the pyridoxal phosphate salvage pathway was downregulated. It was previously shown to be a major cofactor of different metabolic enzymes including amino acid metabolism with change with age (Bode & van den Berg, 1991) (de Lucia et al., 2021). Furthermore, downregulation of Vitamin B6 metabolism at this stage supports the previous study that Vitamin B6 has a negative correlation with brain function during aging (Nwanaji-Enwerem et al., 2021). The GABABergenic receptor II signaling, which has a role in depression at advanced age (Lissemore et al., 2018), was also downregulated in AKR/J

relative to C57BL/6J. Interestingly, the pathway is also related to the opioid proenkephalin pathway which causes nervous disorders (Monstein et al., 1986).

The role of the placenta is significant in brain development during gestation. The differentially expressed genes in AKR/J placenta relative to C57BL/6J at GD 15.5 are related to aging related diseases that are regulated in the placenta. Our results showed the p38 MAPK pathway was upregulated in the placenta. This pathway regulates CryaB and has been found in increased levels in the brain cortex with progression of AD (Muraleva et al., 2019). Moreover, interleukin signaling pathway was upregulated as well. In a previous study it has been shown that IL-6 activation in placenta can block maternal immune activation which is a risk factor of autism (W.-L. Wu et al., 2017). Furthermore, gonadotropin-releasing hormone receptor pathway, which is shown to be linked with neurodegenerative pathophysiology (L. Wang et al., 2010), was downregulated. Additionally, serine biosynthetic process, which is previously shown to be impaired in AD mice and patients (Le Douce et al., 2020), was downregulated. Our data shows downregulation of dopamine receptor signaling pathway. Interestingly, in Parkinson's disease progression loss of dopamine occurs due to dysfunctional dopamine signaling which is also the central symptom for Huntington's disease (Klein et al., 2019). Moreover, nitric oxide metabolic process, which is known for its production of ROS that is one of the causes of neurodegenerative diseases such as Parkinson's disease (Hannibal, 2016), was upregulated in the placenta. Our data further indicated that production of ROS in the placenta is likely due to the downregulation of the pathways: negative regulation of



hydrogen peroxide included cell death and negative regulation of response to ROS. Hydrogen peroxide included cell death is known to promote the production of ROS (Premratanachai et al., 2020). Altogether, our results show that placenta has a role in programming the fetal brain in regulating the production of ROS in the female fetal brain of AKR/J relative to C57BL/6J.

Our data further identified genes that were differentially expressed between the fetal brain of AKR/J compared to C57BL/6J at different gestation times. *Tarbp1*, which has DNA methylation sites that were linked to the ADHD symptoms in adults and children (Weiß et al., 2021), was upregulated in AKR/J but downregulated in C57BL/6J during brain development from GD 12.5 to 15.5. Also, *Pgkl-rs7*, which codes for phosphoglycerate kinase (PGK), is an important enzyme for glycolysis and has been associated with the PGK activity in patients with Parkinson's Disease (Fujino et al., 2021), was upregulated in AKR/J fetal brain in our study. Strikingly, during the mid to late stage of gestation several genes (*Adamrs3*, *Nos-1*, *Adamts18*, *Tenm2*), related to neuronal diseases, were upregulated in AKR/J but downregulated in C57BL/6J. *Adamts3* (A disintegrin and metalloproteinase with thrombosin motifs-3) is an inactivator of Reelin, which an extracellular matrix protein secreted by Cajal-Retzius cells and is reduced in brain with schizophrenia symptoms (Tsuneura et al., 2021). *Nos-1* is strongly associated with Schizophrenia as well through its production nitric oxide (Cui et al., 2010). In addition, *Adamts18* is generally found in the brain of people 72-74 years old. Lack of this gene in mice causes reduction in levels of depression like behavior in

wildtype littermates (R. Zhu et al., 2019). Moreover, specific CpG methylation sites in *Tenm2* has positive relation with neonatal infection (Everson et al., 2020). Therefore, many genes associated with Schizophrenia, AD, PD and Huntington diseases were uniquely regulated in AKR/J fetal brain.

Comparison of differentially expressed genes (DEG) in the fetal brain and placenta between the two strains generated lists of genes which we call “brain-placental DEGs”. *Nectin1* and *Ankdd1b* were downregulated in AKR/J brain and placenta. Previous study shows that reduced level of *Nectin1* in the mice is linked to cognitive and structural abnormalities along with early-life stress related cognitive disorders (C. Wu et al., 2022b). Additionally, *Ankdd1b* is related to migraine and a number of other brain related diseases (Yang et al., 2018). In contrast, specific genes were upregulated in the AKR/J brain placental DEGs but downregulated in C57BL/6J. They included *Rpl10*, which is highly expressed in the hippocampus of mice with autism (Klauck et al., 2006); *Cxcl2* that promotes the transport and proliferation of Acute Myeloid Leukemia (AML) cells (L. Li et al., 2021); *Rpl34-As1*, which is expressed in the tumor grade glioma tissues (D. Zhang et al., 2021); *Hoxa-as3*, which is activated in glioma patients (F. Wu et al., 2017); *Malat1*, which promotes inflammation in Parkinson’s disease (L.-J. Cai et al., 2020); and *Kcnq1ot1*, which controls blood-brain barrier function (N. Liu et al., 2021). The contrasting regulation of these genes in AKR/J brain placenta compared to C57BL/6J further enforces our suggestion that fetal brain programming is different in the mice with naturally selected shorter life span. Furthermore, the epigenetic clock analysis on brain of

AKR/J and C57BL/6J mice at different life-stages showed that brain ages faster in AKR/J mice compared to that of C57BL/6J mice.

## **Conclusion**

The findings of this study show that fetal brain development in AKR/J mice is differentially regulated compared to C57BL/6J mice. Specific epigenetic (methylation and chromatin structure) changes are likely linked to the transcriptomic differences in the brain development of these mouse strains. The study has generated foundational resources to further delineate epigenetic mechanisms of fetal links to neuronal aging in leukemic AKR/J mice.

**Table 4.1** Gene Ontology (GO) analysis on the female fetal brain at GD 12.5, GD 15.5, and GD 17.5 of AKR/J relative to C57BL/6J. Upregulated biological processes shown as UP and downregulated as DOWN.

GO biological process complete	DEG	Fold Enrichment	FDR	GD
proton motive force-driven mitochondrial ATP synthesis (GO:0042776)	34	9.31	6.58E-16	12.5_UP
mitochondrial electron transport, NADH to ubiquinone (GO:0006120)	13	8.83	1.44E-05	12.5_UP
proton motive force-driven ATP synthesis (GO:0015986)	34	8.61	3.57E-15	12.5_UP
mitochondrial electron transport, ubiquinol to cytochrome c (GO:0006122)	6	7.83	4.06E-02	12.5_UP
NADH dehydrogenase complex assembly (GO:0010257)	26	7.74	8.11E-11	12.5_UP
mitochondrial respiratory chain complex I assembly (GO:0032981)	26	7.74	7.92E-11	12.5_UP
presynaptic active zone organization (GO:1990709)	6	7.09	3.03E-02	12.5_DOWN
negative regulation of mitophagy (GO:1901525)	6	7.09	3.03E-02	12.5_DOWN
neurotransmitter receptor diffusion trapping (GO:0099628)	9	6.38	4.62E-03	12.5_DOWN
postsynaptic neurotransmitter receptor diffusion trapping (GO:0098970)	9	6.38	4.61E-03	12.5_DOWN
receptor diffusion trapping (GO:0098953)	9	6.38	4.60E-03	12.5_DOWN
maintenance of postsynaptic specialization structure (GO:0098880)	7	5.57	3.01E-02	15.5_DOWN
regulation of synaptic membrane adhesion (GO:0099179)	7	5.57	3.01E-02	15.5_DOWN
regulation of glutamate receptor signaling pathway (GO:1900449)	7	5.57	3.01E-02	15.5_DOWN
regulation of modification of postsynaptic actin cytoskeleton (GO:1905274)	8	5.57	1.63E-02	15.5_DOWN
cerebellar granule cell differentiation (GO:0021707)	9	5.01	1.35E-02	15.5_DOWN
regulation of opioid receptor signaling pathway (GO:2000474)	3	31.7	2.34E-02	17.5_DOWN
positive regulation of long-term synaptic depression (GO:1900454)	6	17.29	6.07E-04	17.5_DOWN
regulation of postsynaptic density assembly (GO:0099151)	7	15.85	1.90E-04	17.5_DOWN
regulation of long-term synaptic depression (GO:1900452)	8	13.35	1.10E-04	17.5_DOWN
regulation of excitatory synapse assembly (GO:1904889)	7	13.05	4.57E-04	17.5_DOWN
regulation of postsynaptic specialization assembly (GO:0099150)	7	12.33	5.93E-04	17.5_DOWN

**Table 4.2** PANTHER Pathway analysis on the female fetal brain at GD 12.5, GD 15.5, and GD 17.5 of AKR/J relative to C57BL/6J. Upregulated biological processes shown as UP and downregulated as DOWN.

PANTHER Pathways	DEG	Fold Enrichment	FDR	GD
Blood coagulation (P00011)	16	5.22	1.17E-04	12.5_UP
Wnt signaling pathway (P00057)	4	0.22	1.33E-02	12.5_UP
Synaptic vesicle trafficking (P05734)	18	4.11	3.58E-04	12.5_DOWN
Metabotropic glutamate receptor group I pathway (P00041)	13	3.84	3.52E-03	12.5_DOWN
Axon guidance mediated by netrin (P00009)	16	3.24	3.88E-03	12.5_DOWN
Hedgehog signaling pathway (P00025)	9	3.19	3.53E-02	12.5_DOWN
GABA-B receptor II signaling (P05731)	16	3.06	4.74E-03	12.5_DOWN
Metabotropic glutamate receptor group I pathway (P00041)	17	3.94	5.83E-04	15.5_DOWN
Axon guidance mediated by semaphorins (P00007)	11	2.92	3.03E-02	15.5_DOWN
Axon guidance mediated by Slit/Robo (P00008)	13	2.89	2.68E-02	15.5_DOWN
Axon guidance mediated by netrin (P00009)	18	2.86	6.07E-03	15.5_DOWN
Ionotropic glutamate receptor pathway (P00037)	25	2.84	6.66E-04	15.5_DOWN
Pyridoxal phosphate salvage pathway (P02770)	2	31.7	3.94E-02	17.5_DOWN
Vitamin B6 metabolism (P02787)	3	23.77	1.05E-02	17.5_DOWN
GABA-B receptor II signaling (P05731)	8	6.85	1.56E-03	17.5_DOWN
Ionotropic glutamate receptor pathway (P00037)	9	5.82	1.43E-03	17.5_DOWN
Opioid proenkephalin pathway (P05915)	6	5	2.11E-02	17.5_DOWN

**Table 4.3** Gene Ontology (GO) analysis on Differentially Expressed Genes (DEGs) of the placenta at gestation day (GD) 15.5 of AKR/J relative to C57BL/6J.

GO Analysis	DEG	Fold Enrichment	FDR	GD
positive regulation by host of viral transcription (GO:0043923)	10	4.38	1.63E-02	UP
regulation of myoblast proliferation (GO:2000291)	9	4.19	3.25E-02	UP
negative regulation of nitric oxide biosynthetic process (GO:0045019)	11	4.1	1.40E-02	UP
negative regulation of nitric oxide metabolic process (GO:1904406)	11	4.1	1.40E-02	UP
negative regulation of miRNA transcription (GO:1902894)	12	3.89	1.19E-02	UP
nucleobase biosynthetic process (GO:0046112)	11	3.93	2.54E-02	DOWN
serine family amino acid biosynthetic process (GO:0009070)	10	3.8	4.58E-02	DOWN
dopamine receptor signaling pathway (GO:0007212)	15	3.14	1.98E-02	DOWN
negative regulation of hydrogen peroxide-induced cell death (GO:1903206)	13	3.04	4.65E-02	DOWN
negative regulation of response to reactive oxygen species (GO:1901032)	13	3.04	4.64E-02	DOWN

**Table 4.4** PANTHER Pathway analysis on differentially expressed genes (DEGs) of the placenta at gestation day (GD) 15.5 of AKR/J relative to C57BL/6J.

PANTHER Pathways	DEG	Fold Enrichment	FDR	GD
Ionotropic glutamate receptor pathway (P00037)	18	2.74	1.09E-02	UP
Metabotropic glutamate receptor group III pathway (P00039)	25	2.7	4.03E-03	UP
p38 MAPK pathway (P05918)	14	2.55	4.45E-02	UP
Interleukin signaling pathway (P00036)	29	2.48	5.75E-03	UP
Parkinson disease (P00049)	27	2.1	1.75E-02	UP
EGF receptor signaling pathway (P00018)	38	2.08	4.76E-03	UP
Alzheimer disease-presenilin pathway (P00004)	33	1.94	1.37E-02	UP
Huntington disease (P00029)	39	1.9	1.21E-02	UP
p53 pathway (P00059)	30	2.07	3.33E-02	DOWN
Apoptosis signaling pathway (P00006)	40	1.96	1.37E-02	DOWN
CCKR signaling map (P06959)	50	1.86	1.23E-02	DOWN
Gonadotropin-releasing hormone receptor pathway (P06664)	71	1.84	1.71E-03	DOWN

**Table 4.5** Gene Ontology (GO) analysis of the female fetal brain-placental differentially expressed genes (DEGs) at gestation day (GD) 15.5 of AKR/J compared to C57BL/6J.

GO biological process complete	DEG	Fold Enrichment	FDR	Expression
spinal cord association neuron differentiation (GO:0021527)	13	6.13	4.32E-04	UP
forebrain dorsal/ventral pattern formation (GO:0021798)	7	6.13	2.44E-02	UP
gamma-aminobutyric acid secretion (GO:0014051)	6	6.13	4.76E-02	UP
clustering of voltage-gated potassium channels (GO:0045163)	6	6.13	4.76E-02	UP
presynaptic dense core vesicle exocytosis (GO:0099525)	6	6.13	4.75E-02	UP
protection from natural killer cell mediated cytotoxicity (GO:0042270)	11	3.93	2.89E-02	DOWN
regulation of lactation (GO:1903487)	28	3.93	2.81E-05	DOWN
cellular response to lipoteichoic acid (GO:0071223)	10	3.93	4.29E-02	DOWN
response to lipoteichoic acid (GO:0070391)	10	3.93	4.29E-02	DOWN
positive regulation of lactation (GO:1903489)	27	3.93	4.20E-05	DOWN
T cell mediated cytotoxicity (GO:0001913)	12	3.63	2.83E-02	DOWN
embryonic skeletal system morphogenesis (GO:0048704)	5	30.86	1.08E-02	AKR/J UP C57BL/6J DOWN
embryonic skeletal system development (GO:0048706)	5	22.99	2.20E-02	AKR/J UP C57BL/6J DOWN



**Table 4.6** PANTHER Pathway analysis of the female fetal brain-placental differentially expressed genes (DEGs) at gestation day (GD) 15.5 of AKR/J compared to C57BL/6J.

PANTHER Pathways	DEG	Fold Enrichment	FDR	Expression
Endogenous cannabinoid signaling (P05730)	16	3.92	9.17E-04	UP
Ionotropic glutamate receptor pathway (P00037)	31	3.88	9.07E-07	UP
Metabotropic glutamate receptor group III pathway (P00039)	42	3.73	1.59E-08	UP
GABA-B receptor II signaling (P05731)	22	3.64	1.52E-04	UP
Cadherin signaling pathway (P00012)	96	3.63	1.78E-18	UP
Blood coagulation (P00011)	36	2.72	6.65E-04	DOWN
Integrin signalling pathway (P00034)	101	2.09	8.64E-07	DOWN
Cytoskeletal regulation by Rho GTPase (P00016)	38	1.87	4.65E-02	DOWN
Apoptosis signaling pathway (P00006)	58	1.84	8.84E-03	DOWN
Angiogenesis (P00005)	80	1.76	1.98E-03	DOWN

**Figure 4.1** Hierarchical Clustering Analysis of differentially expressed genes at gestation day 12.5 (A), 15.5 (B) and 17.5 (C) of female fetal brain of AKR/J mice relative to C57BL/6J mice. BA, BB, BC are fetal brains of C57BL/6J at every stage. AA, AB, AC are fetal brains of AKR/J at every stage.

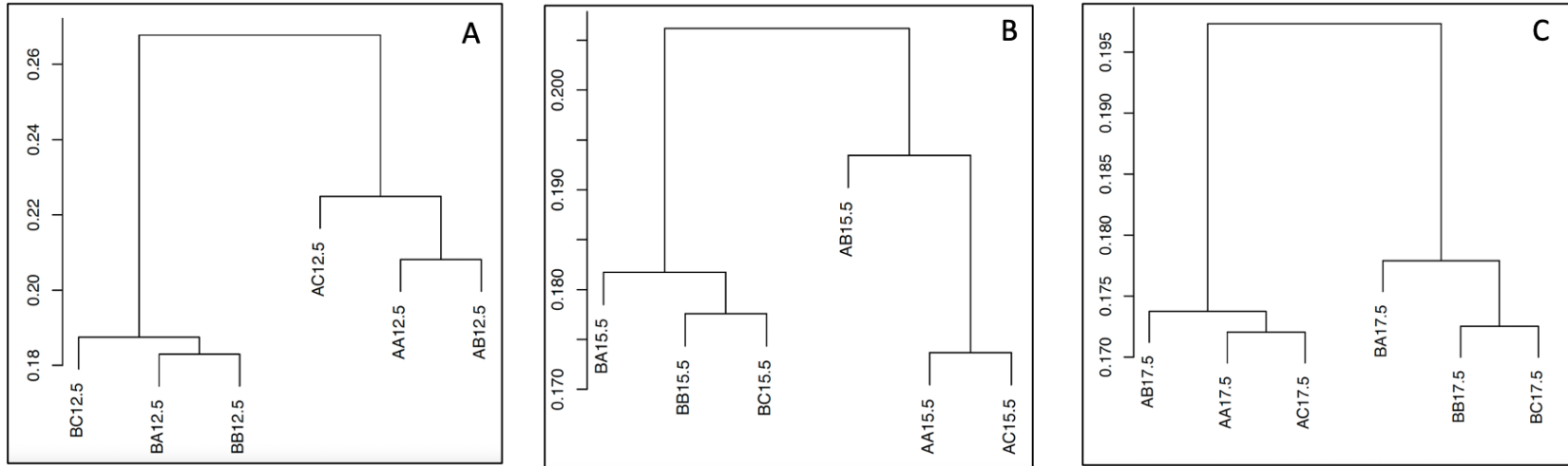


**Figure 4.2** Differentially expressed genes at gestation day 12.5, 15.5 and 17.5 of female fetal brain of AKR/J mice relative to C57BL/6J mice. Upregulated genes are shown by the blue upward arrow and downregulated genes shown by downward arrow.

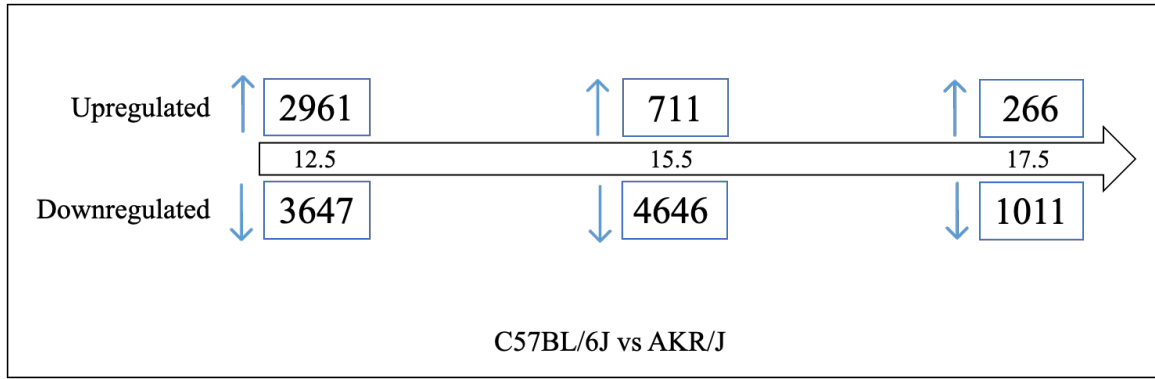


**Figure 4.3** Volcano plot of differentially expressed genes at gestation day 12.5, 15.5 and 17.5 of female fetal brain of AKR/J mice relative to C57BL/6J mice. Red shows downregulated genes and blue shows upregulated genes. Every dot represents one gene. The plots are made with the accuracy of False Discovery Rate (FDR) 0.05 as mentioned on the plots.

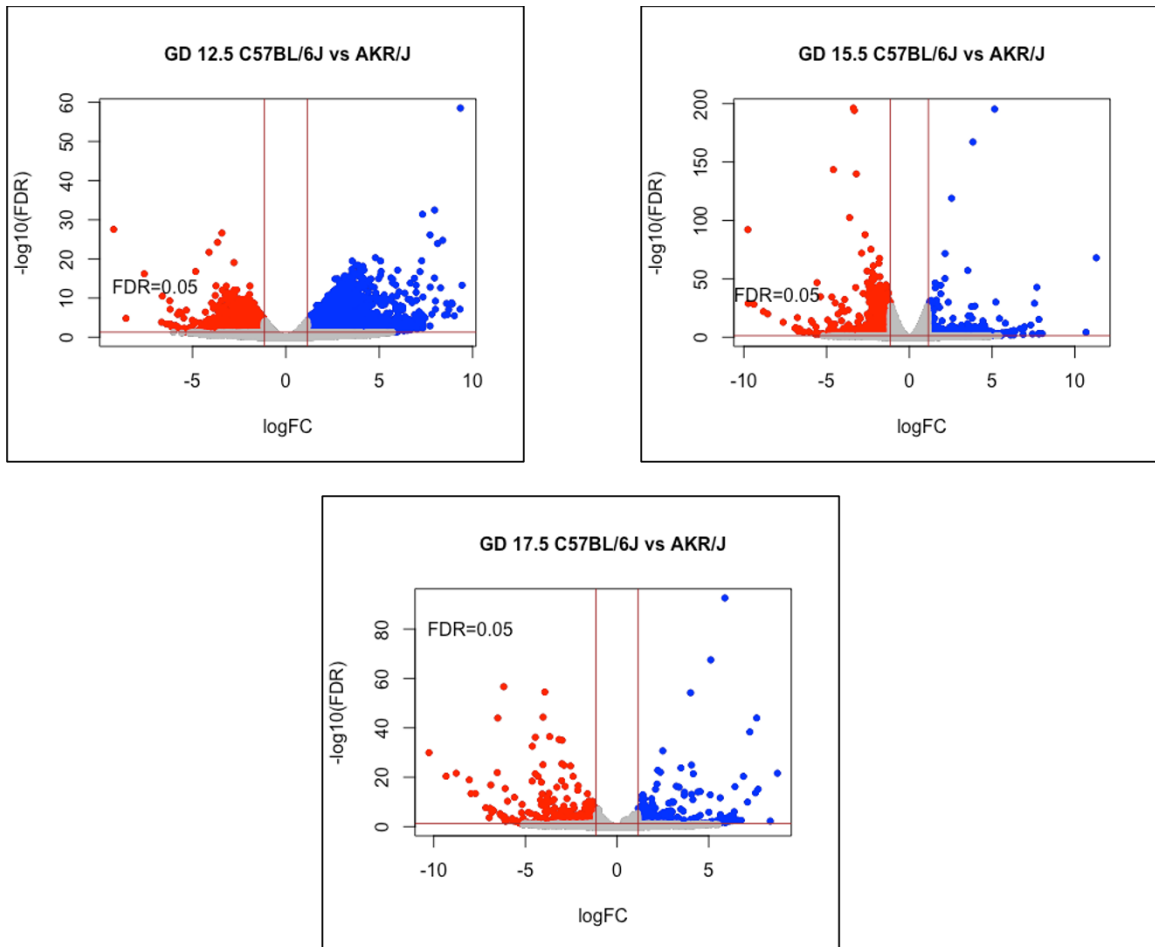


**Figure 4.4** Principal Component Analysis of differentially expressed genes at gestation day 12.5, 15.5 and 17.5 of female fetal brain of AKR/J mice relative to C57BL/6J mice showing different clustering of AKR/J (solid black line) and C57BL/6J (dotted line) on GD 12.5 and GD 15.5 and overlapping on GD 17.5. BA, BB, BC are fetal brains of C57BL/6J at every stage. AA, AB, AC are fetal brains of AKR/J at every stage.

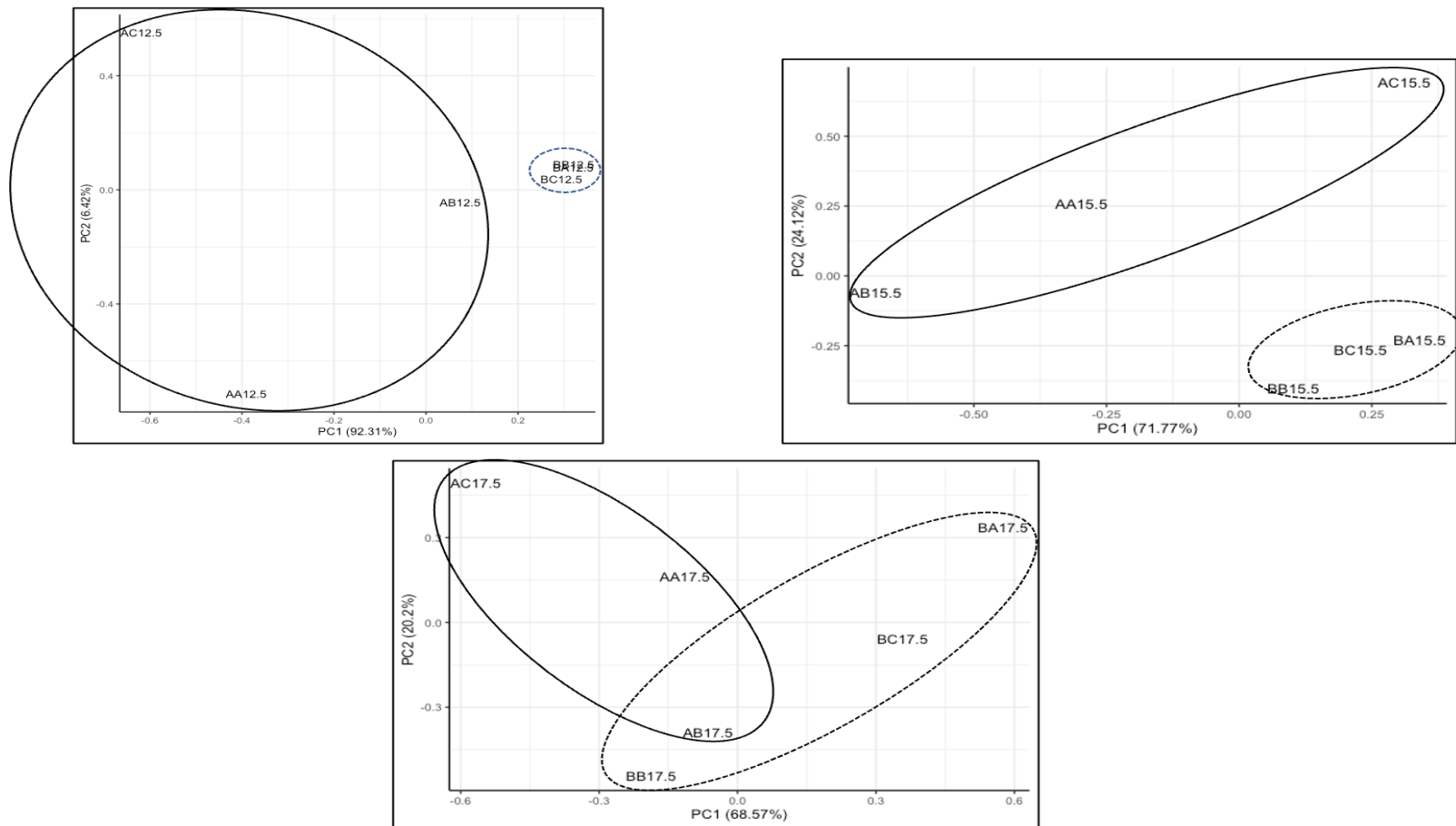


**Figure 4.5** Hierarchical Clustering Analysis of differentially expressed genes at gestation day 15.5 (B) of female placenta of AKR/J mice (AKR.FPL1, AKR.FPL2, AKR.FPL3) relative to C57BL/6J mice (WTPL.1, WTPL.2, WTPL.3).

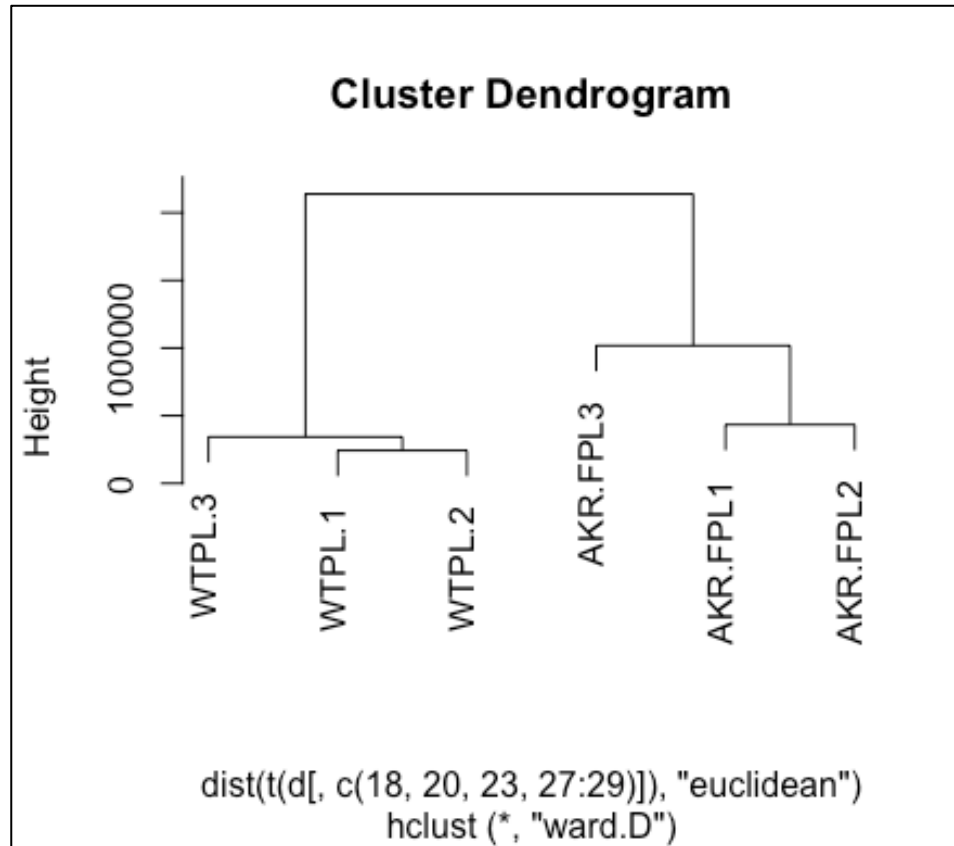


**Figure 4.6** Venn diagram showing the comparison of differentially expressed genes between the female brain-placenta of AKR/J and C57BL/6J mice. The upregulated brain-placental differentially expressed genes of AKR/J are shown as UP: AKR, downregulated AKR/J genes are shown as DOWN: AKR, upregulated genes of C57BL/6J are shown as UP:BL6 and downregulated genes as DOWN:BL6.

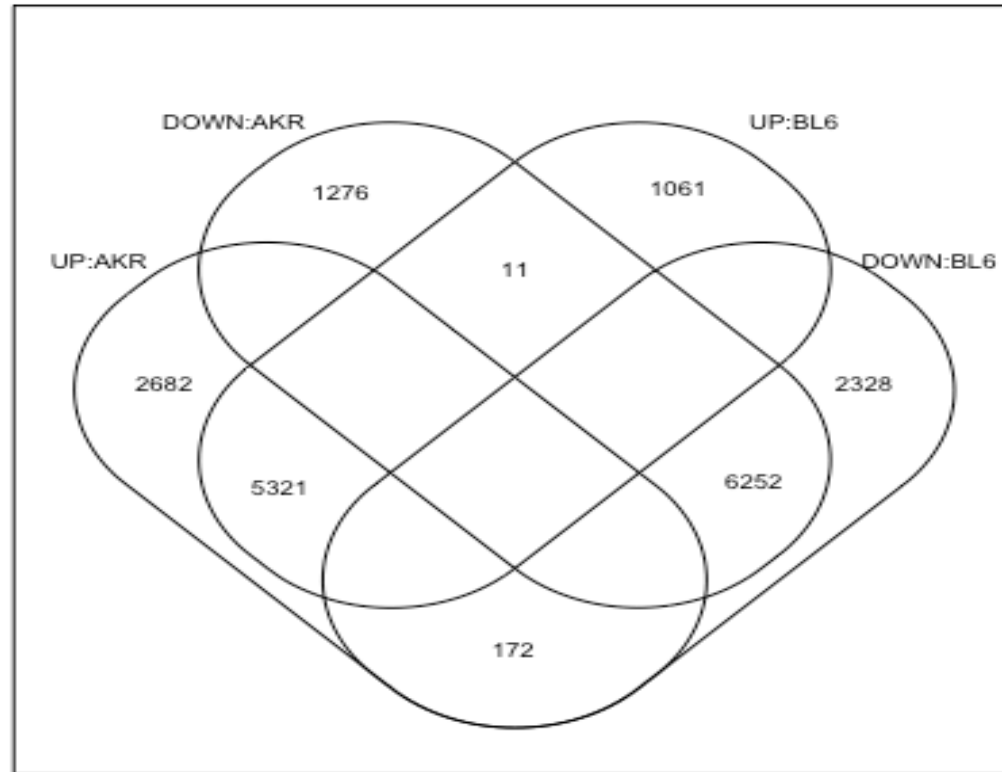


**Figure 4.7** Coordinated changes in DNA methylation of fetal brain with placenta in a sex-dependent manner (FB: female bias; MB: male bias). BR=brain, Pl=Placenta, F=female, M=male.

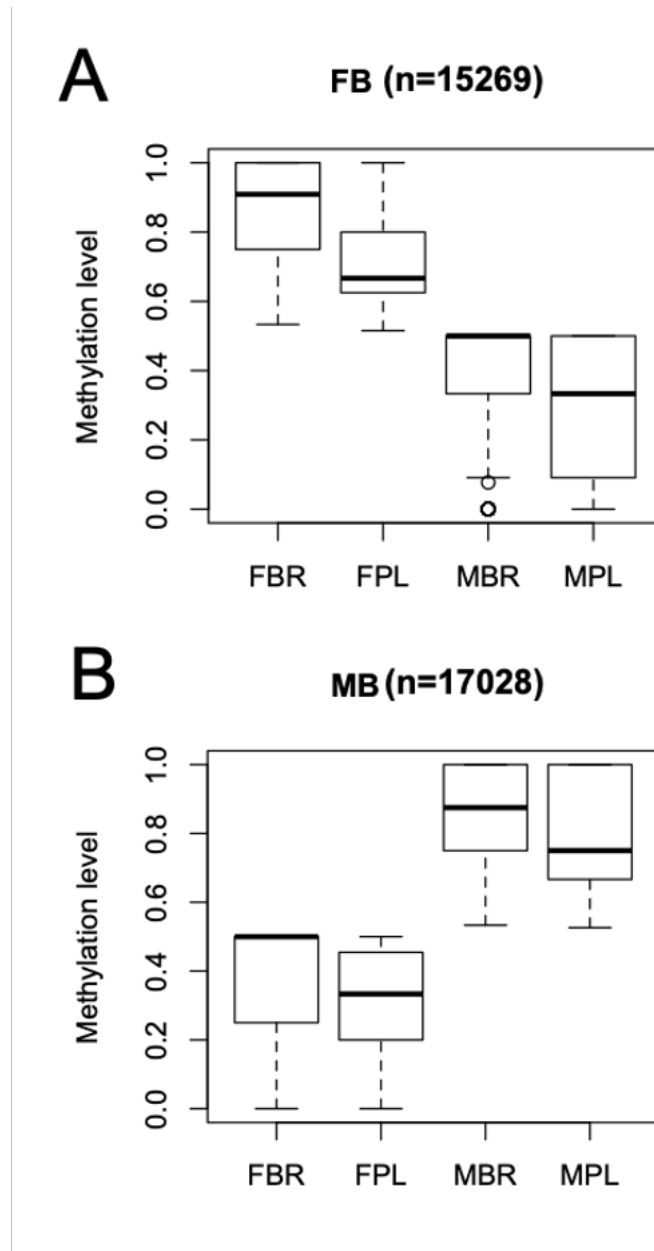




**Figure 4.8** BrainYEAR differences between C57BL/6J and AKR/J male and female mice.

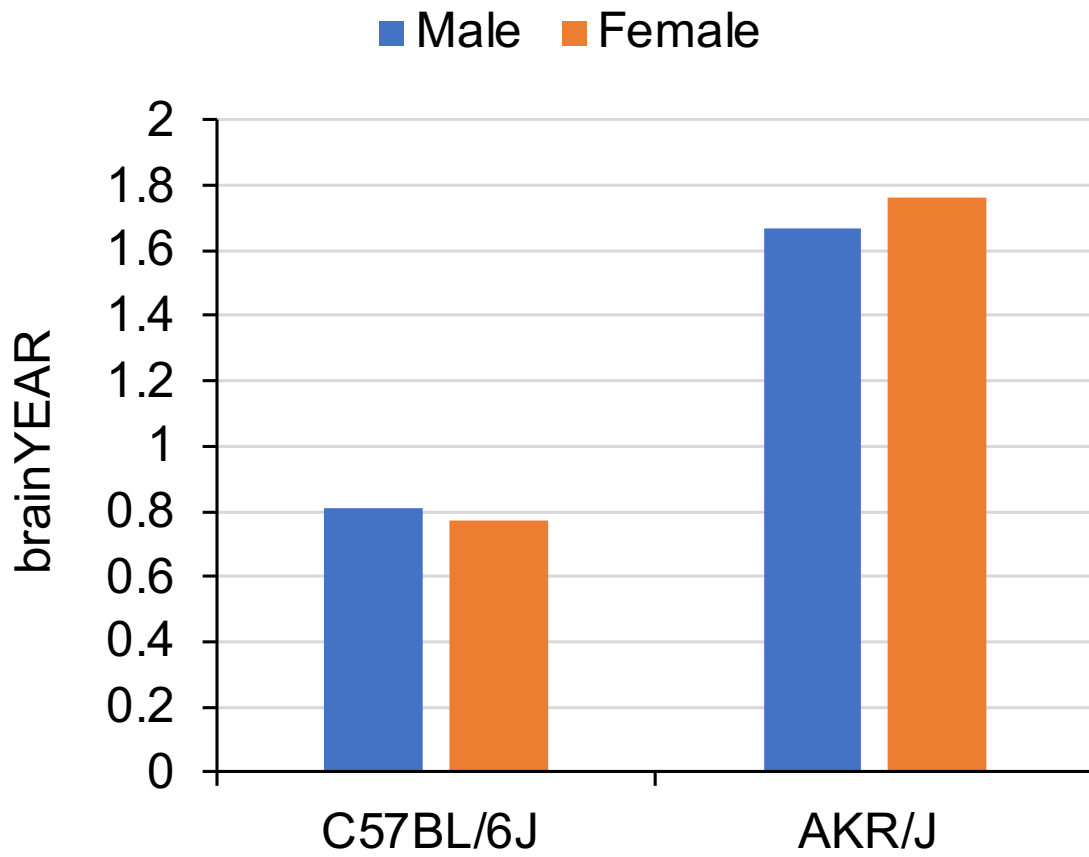


**Figure 4.9** Cross between AKR/J and C57BL/6J generated 32 F2s.

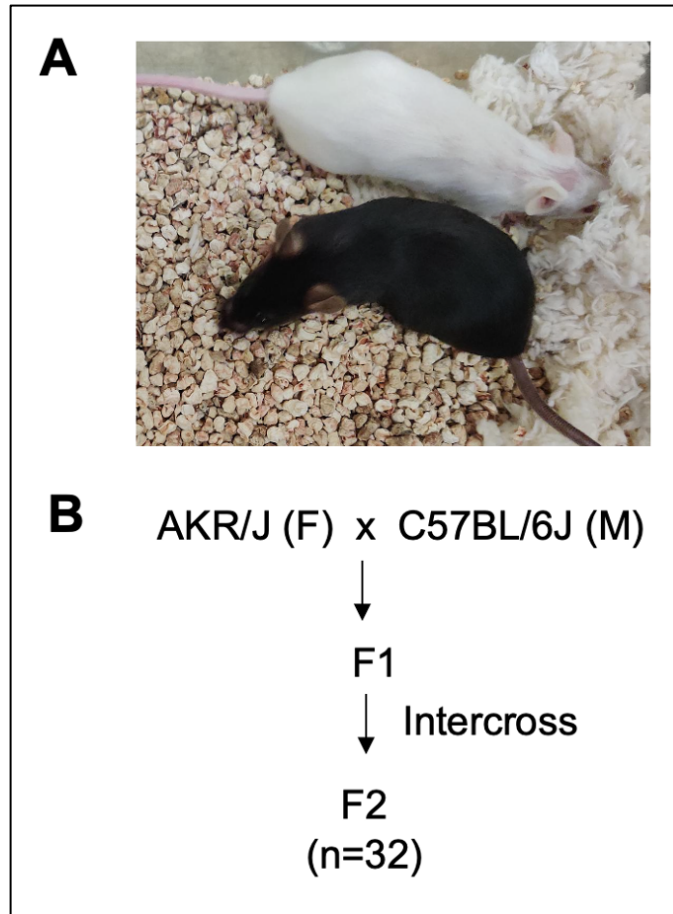


**Figure 4.10** SNP and methylation sites in a region of mouse chromosome 14. These methylations were found in brain of fetal mice.

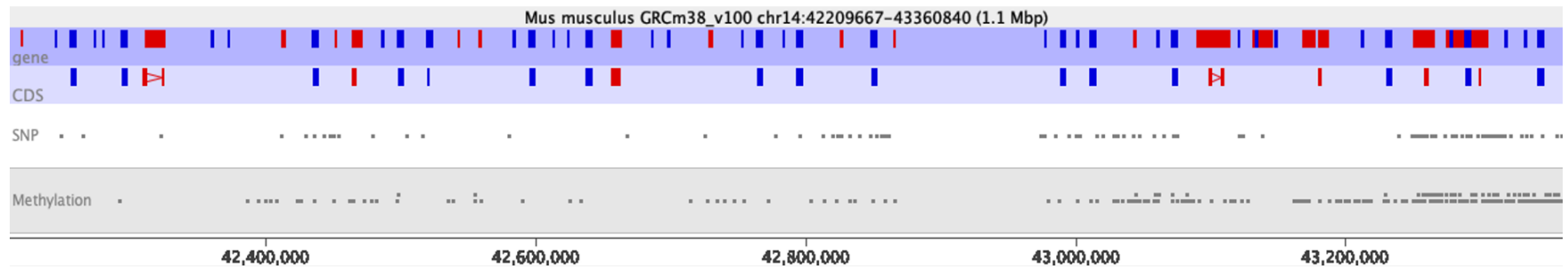


**Figure 4.11** Global gene expression patterns in the brain of young (Y) and old (O) mice of strain AKR/J (column names begin with A) and C57BL/6J (column names begin with B).

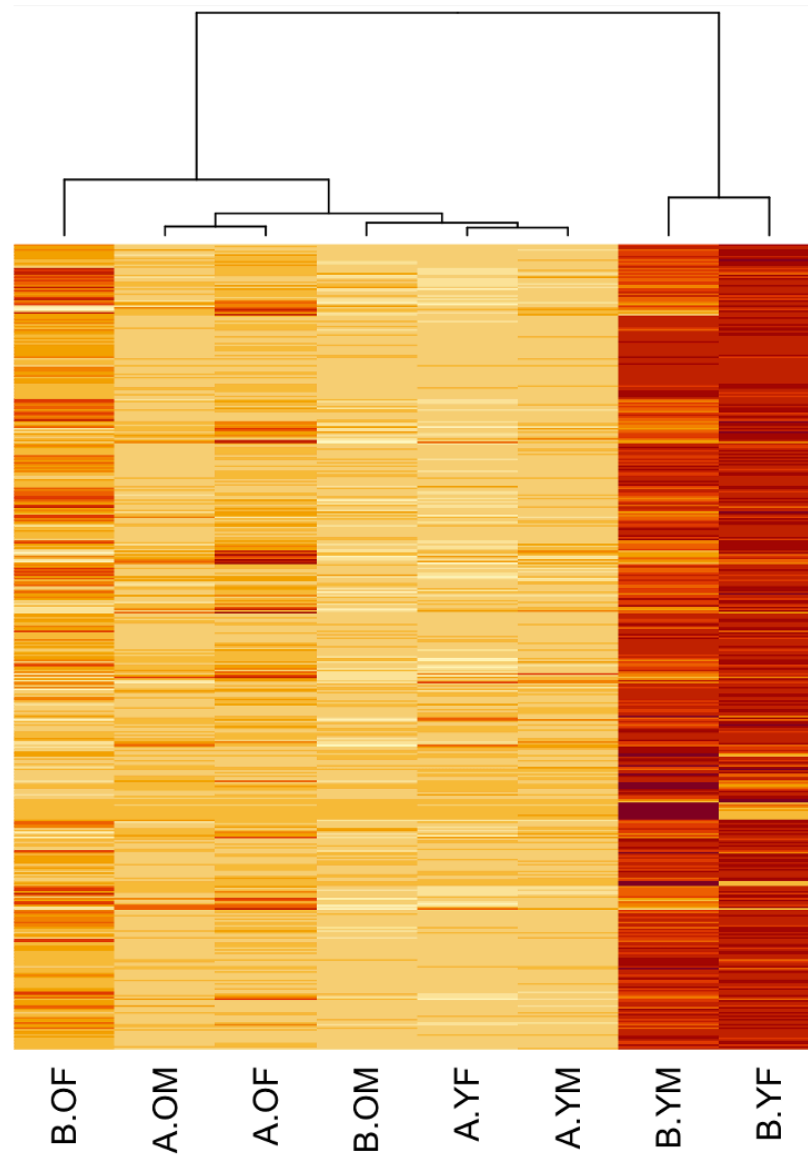


**Figure 4.12** tSNE clusters of brain cells based on variation of open chromatin in C57BL/6J mice. Clusters are shown in different colors. Each dot represent a brain cell.

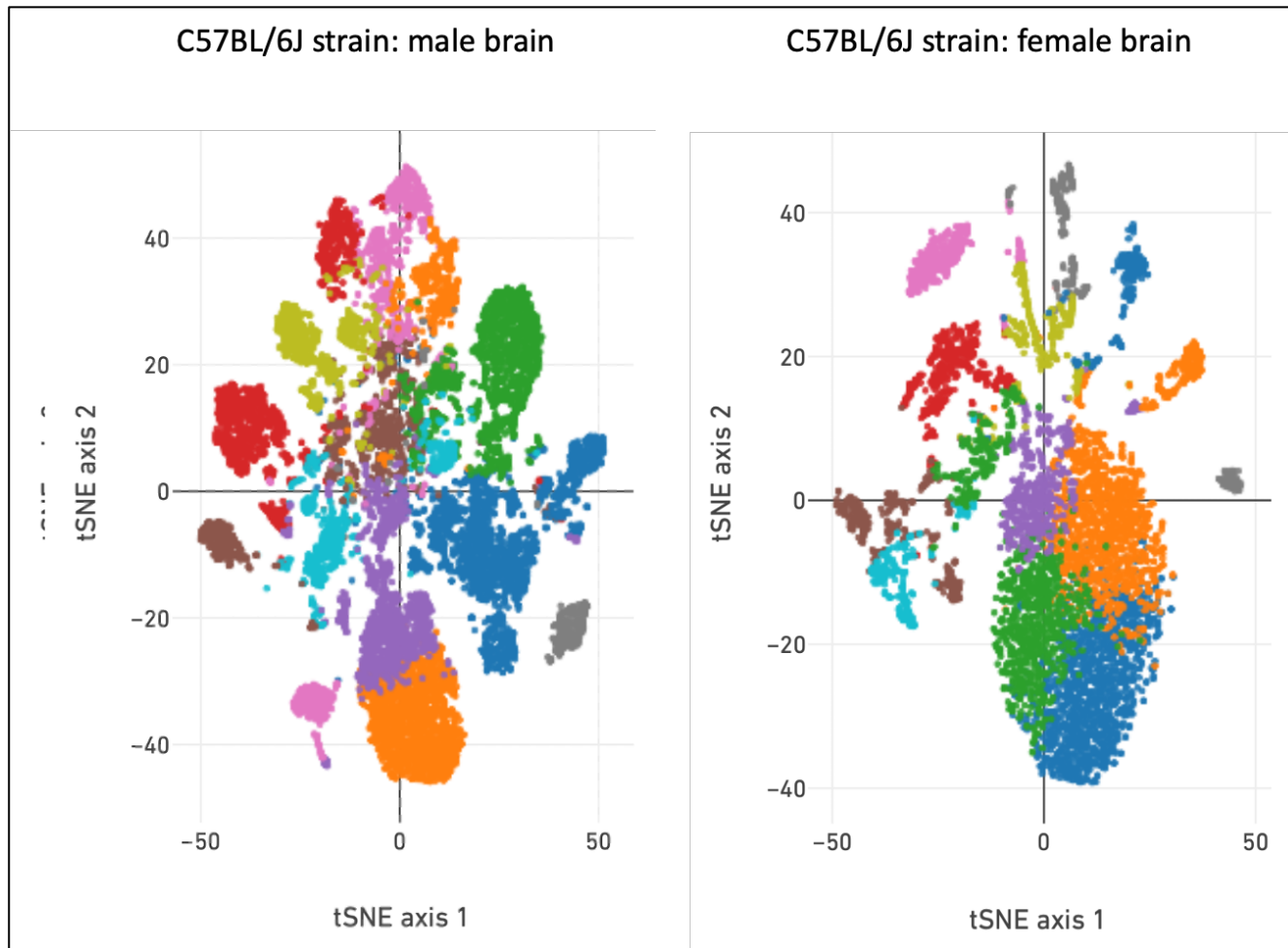


**Figure 4.13** tSNE clusters of brain cells based on variation of open chromatin in AKR/J mice. Clusters are shown in different colors. Each dot represent a brain cell.

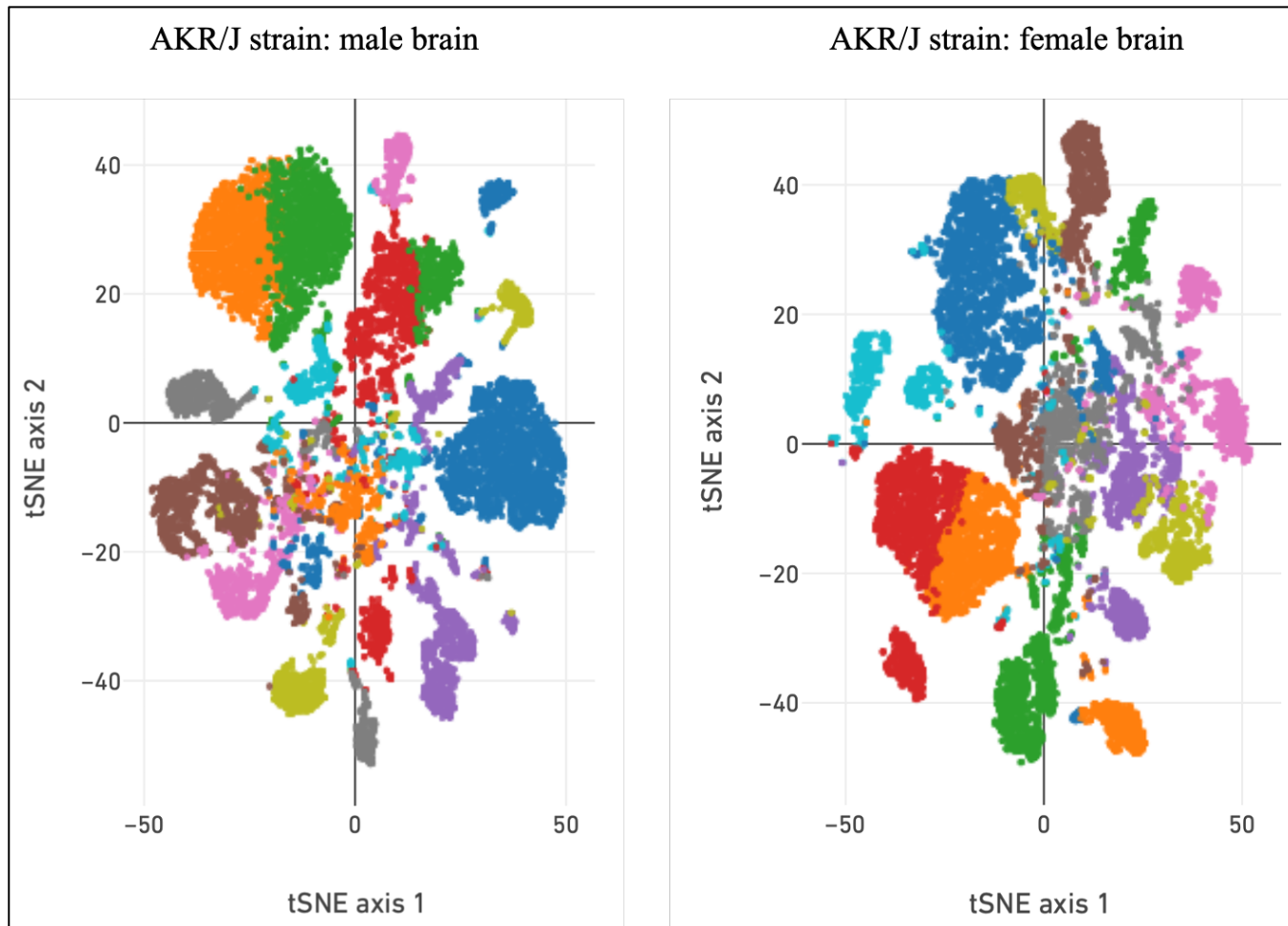


**Figure 4.14** Number of cells where open chromatin were identified in male (M) and female (F) brain of C57BL/6J and AKR/J mice.

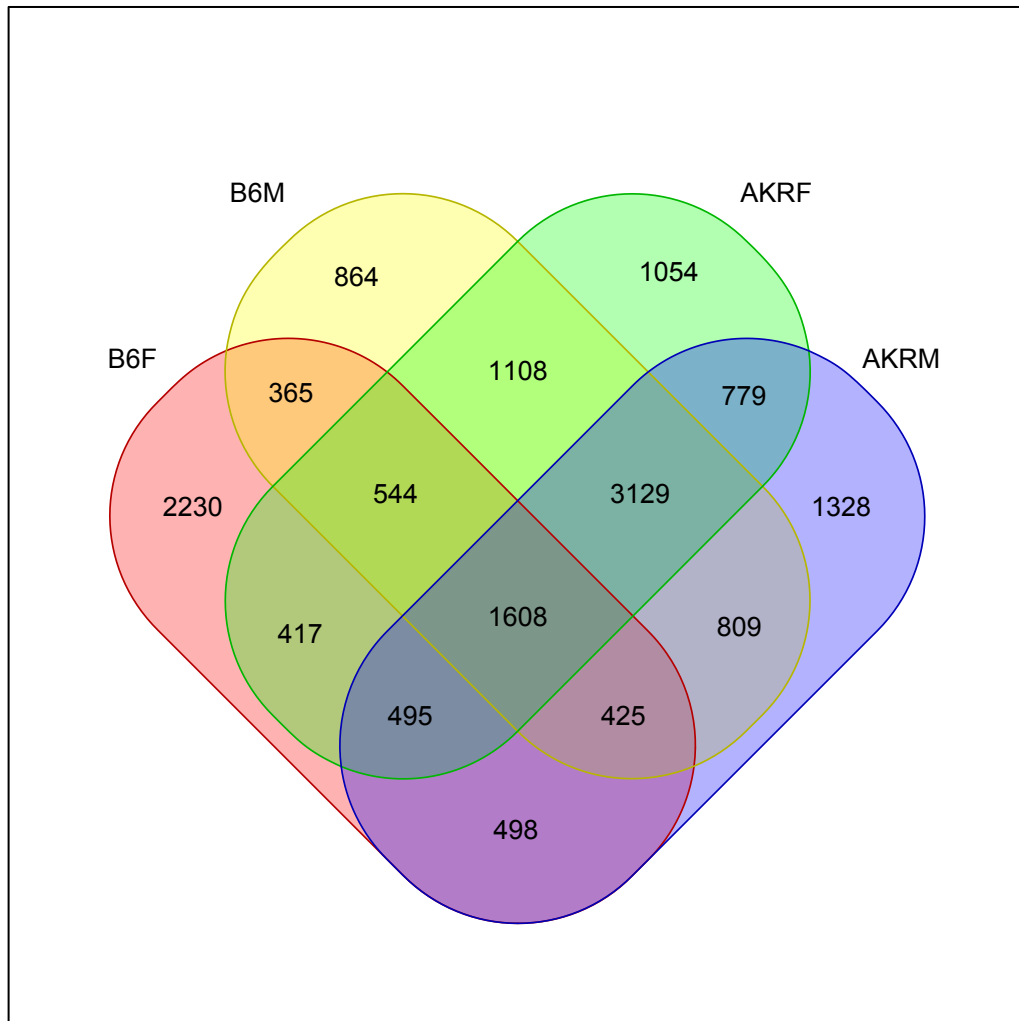


**Figure 4.15** Pie chart showing proportion of transcription factor motifs in the open chromatin of the top 20 genes (based on number of peaks of genes) in male and female brain of the two strains.

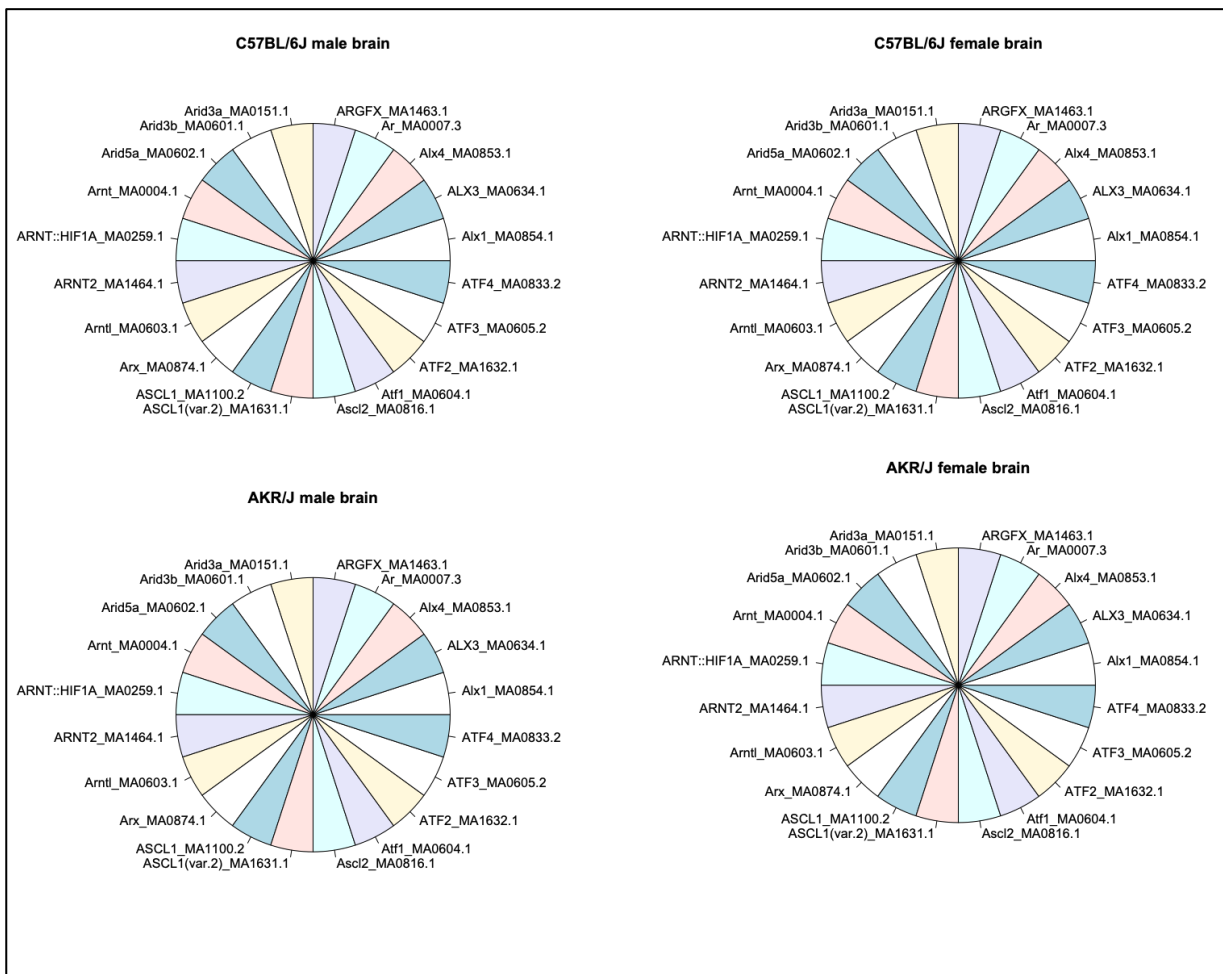
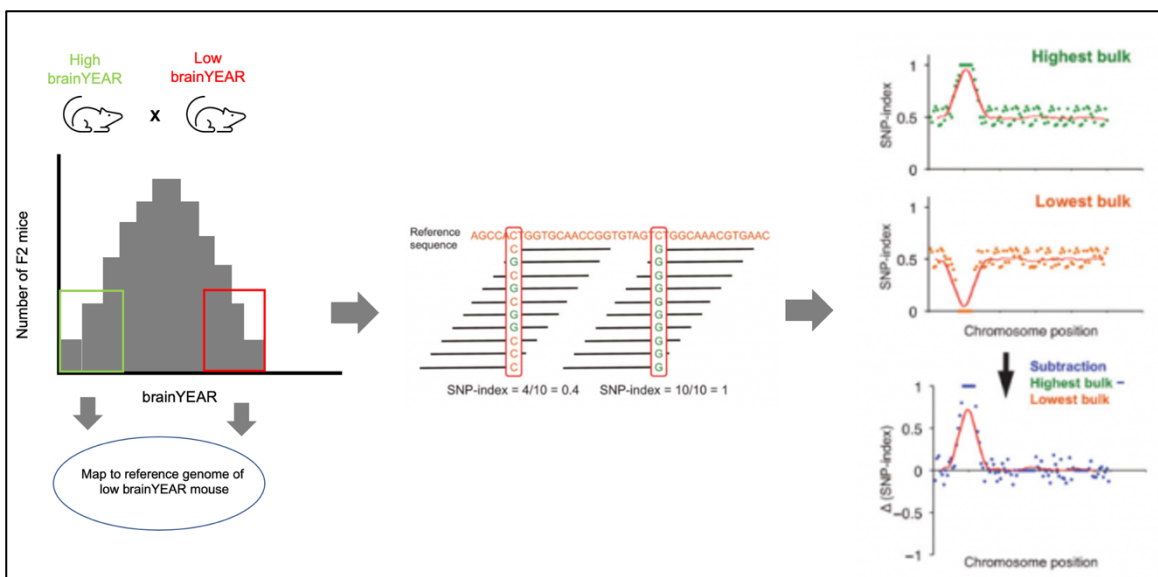




**Figure 4.16** Strategy of F2 pooling for BSA-seq analysis. After phenotyping F2s for brain age (brainYEAR score from epigenetic clock analysis), mice representing both ends (low and high) in the variation of brain age, was pooled. The bulk DNA from those two pools was used for whole-genome sequencing. The sequence data was mapped to reference genome of parental mice with low brainYEAR (in this project, it is the genome of C57BL/6J which is the mouse reference genome). Mapping data was used to identify SNPs that was scored based on SNP-index for the two groups as shown. Finally, delta SNP index which is the difference between the two groups was used in sliding window analysis to identify genomic regions that control brain aging.



## Literature Cited

- Abdulghani, M., Jain, A., & Tuteja, G. (2019). Genome-wide identification of enhancer elements in the placenta. *Placenta*, *79*, 72–77.  
<https://doi.org/10.1016/j.placenta.2018.09.003>
- Ackerman, S. (1992). The Development and Shaping of the Brain. In *Discovering the Brain*. National Academies Press (US).  
<https://www.ncbi.nlm.nih.gov/books/NBK234146/>
- Aguilaniu, H. (2015a). The mysterious relationship between reproduction and longevity. *Worm*, *4*(2), e1020276. <https://doi.org/10.1080/21624054.2015.1020276>
- Aguilaniu, H. (2015b). The mysterious relationship between reproduction and longevity. *Worm*, *4*(2), e1020276. <https://doi.org/10.1080/21624054.2015.1020276>
- Alberry, B. L. J., & Singh, S. M. (2020). Hippocampal DNA Methylation in a Mouse Model of Fetal Alcohol Spectrum Disorder That Includes Maternal Separation Stress Only Partially Explains Changes in Gene Expression. *Frontiers in Genetics*, *11*, 70. <https://doi.org/10.3389/fgene.2020.00070>
- Antebi, A. (2013). Regulation of longevity by the reproductive system. *Experimental Gerontology*, *48*(7), 596–602. <https://doi.org/10.1016/j.exger.2012.09.009>
- Arendt, D., Bertucci, P. Y., Achim, K., & Musser, J. M. (2019). Evolution of neuronal types and families. *Current Opinion in Neurobiology*, *56*, 144–152.  
<https://doi.org/10.1016/j.conb.2019.01.022>

- Armstrong, N. M., An, Y., Beason-Held, L., Doshi, J., Erus, G., Ferrucci, L., Davatzikos, C., & Resnick, S. M. (2019a). Sex differences in brain aging and predictors of neurodegeneration in cognitively healthy older adults. *Neurobiology of Aging*, *81*, 146–156. <https://doi.org/10.1016/j.neurobiolaging.2019.05.020>
- Armstrong, N. M., An, Y., Beason-Held, L., Doshi, J., Erus, G., Ferrucci, L., Davatzikos, C., & Resnick, S. M. (2019b). Sex differences in brain aging and predictors of neurodegeneration in cognitively healthy older adults. *Neurobiology of Aging*, *81*, 146–156. <https://doi.org/10.1016/j.neurobiolaging.2019.05.020>
- Arnold, C. N., Xia, Y., Lin, P., Ross, C., Schwander, M., Smart, N. G., Müller, U., & Beutler, B. (2011). Rapid Identification of a Disease Allele in Mouse Through Whole Genome Sequencing and Bulk Segregation Analysis. *Genetics*, *187*(3), 633–641. <https://doi.org/10.1534/genetics.110.124586>
- Austad, S. N., & Fischer, K. E. (2016). Sex Differences in Lifespan. *Cell Metabolism*, *23*(6), 1022–1033. <https://doi.org/10.1016/j.cmet.2016.05.019>
- Badawy, A. A.-B. (2015). Tryptophan metabolism, disposition and utilization in pregnancy. *Bioscience Reports*, *35*(5). <https://doi.org/10.1042/BSR20150197>
- Barker, D. J., & Osmond, C. (1986). Infant mortality, childhood nutrition, and ischaemic heart disease in England and Wales. *Lancet (London, England)*, *1*(8489), 1077–1081. [https://doi.org/10.1016/s0140-6736\(86\)91340-1](https://doi.org/10.1016/s0140-6736(86)91340-1)
- Barker, D. J. P. (2007). The origins of the developmental origins theory. *Journal of Internal Medicine*, *261*(5), 412–417. <https://doi.org/10.1111/j.1365-2796.2007.01809.x>

- Barker, D. J. P., Osmond, C., Thornburg, K. L., Kajantie, E., & Eriksson, J. G. (2011a). The lifespan of men and the shape of their placental surface at birth. *Placenta*, 32(10), 783–787. <https://doi.org/10.1016/j.placenta.2011.07.031>
- Barker, D. J. P., Osmond, C., Thornburg, K. L., Kajantie, E., & Eriksson, J. G. (2011b). The lifespan of men and the shape of their placental surface at birth. *Placenta*, 32(10), 783–787. <https://doi.org/10.1016/j.placenta.2011.07.031>
- Becht, E., McInnes, L., Healy, J., Dutertre, C.-A., Kwok, I. W. H., Ng, L. G., Ginhoux, F., & Newell, E. W. (2018). Dimensionality reduction for visualizing single-cell data using UMAP. *Nature Biotechnology*. <https://doi.org/10.1038/nbt.4314>
- Bechtold, M., Palmer, J., Valtos, J., Iasiello, C., & Sowers, J. (2006). Metabolic syndrome in the elderly. *Current Diabetes Reports*, 6(1), 64–71. <https://doi.org/10.1007/s11892-006-0054-3>
- Behura, S. K., Dhakal, P., Kelleher, A. M., Balboula, A., Patterson, A., & Spencer, T. E. (2019a). The brain-placental axis: Therapeutic and pharmacological relevancy to pregnancy. *Pharmacological Research*, 149, 104468. <https://doi.org/10.1016/j.phrs.2019.104468>
- Behura, S. K., Dhakal, P., Kelleher, A. M., Balboula, A., Patterson, A., & Spencer, T. E. (2019b). The brain-placental axis: Therapeutic and pharmacological relevancy to pregnancy. *Pharmacological Research*, 149, 104468. <https://doi.org/10.1016/j.phrs.2019.104468>
- Behura, S. K., Dhakal, P., Kelleher, A. M., Balboula, A., Patterson, A., & Spencer, T. E. (2019c). The brain-placental axis: Therapeutic and pharmacological relevancy to

pregnancy. *Pharmacological Research*, 149, 104468.

<https://doi.org/10.1016/j.phrs.2019.104468>

Behura, S. K., Kelleher, A. M., & Spencer, T. E. (2019a). Evidence for functional interactions between the placenta and brain in pregnant mice. *FASEB Journal: Official Publication of the Federation of American Societies for Experimental Biology*, 33(3), 4261–4272. <https://doi.org/10.1096/fj.201802037R>

Behura, S. K., Kelleher, A. M., & Spencer, T. E. (2019b). Evidence for functional interactions between the placenta and brain in pregnant mice. *FASEB Journal: Official Publication of the Federation of American Societies for Experimental Biology*, 33(3), 4261–4272. <https://doi.org/10.1096/fj.201802037R>

Berben, L., Floris, G., Wildiers, H., & Hatse, S. (2021). Cancer and Aging: Two Tightly Interconnected Biological Processes. *Cancers*, 13(6), 1400. <https://doi.org/10.3390/cancers13061400>

Bevan, R. J., Hughes, T. R., Williams, P. A., Good, M. A., Morgan, B. P., & Morgan, J. E. (2020). Retinal ganglion cell degeneration correlates with hippocampal spine loss in experimental Alzheimer's disease. *Acta Neuropathologica Communications*, 8(1), 216. <https://doi.org/10.1186/s40478-020-01094-2>

Bianco-Miotto, T., Craig, J. M., Gasser, Y. P., van Dijk, S. J., & Ozanne, S. E. (2017). Epigenetics and DOHaD: From basics to birth and beyond. *Journal of Developmental Origins of Health and Disease*, 8(5), 513–519. <https://doi.org/10.1017/S2040174417000733>

- Blackburn, D. G. (2015). Evolution of vertebrate viviparity and specializations for fetal nutrition: A quantitative and qualitative analysis. *Journal of Morphology*, 276(8), 961–990. <https://doi.org/10.1002/jmor.20272>
- Blanks, J. C., Hinton, D. R., Sadun, A. A., & Miller, C. A. (1989). Retinal ganglion cell degeneration in Alzheimer's disease. *Brain Research*, 501(2), 364–372. [https://doi.org/10.1016/0006-8993\(89\)90653-7](https://doi.org/10.1016/0006-8993(89)90653-7)
- Bode, W., & van den Berg, H. (1991). Pyridoxal-5'-phosphate and pyridoxal biokinetics in aging Wistar rats. *Experimental Gerontology*, 26(6), 589–599. [https://doi.org/10.1016/0531-5565\(91\)90076-x](https://doi.org/10.1016/0531-5565(91)90076-x)
- Bolger, A. M., Lohse, M., & Usadel, B. (2014). Trimmomatic: A flexible trimmer for Illumina sequence data. *Bioinformatics (Oxford, England)*, 30(15), 2114–2120. <https://doi.org/10.1093/bioinformatics/btu170>
- Bolon, B. (Ed.). (2015). *Pathology of the developing mouse: A systematic approach*. CRC Press, Taylor & Francis Group.
- Bonnin, A., Goeden, N., Chen, K., Wilson, M. L., King, J., Shih, J. C., Blakely, R. D., Deneris, E. S., & Levitt, P. (2011). A transient placental source of serotonin for the fetal forebrain. *Nature*, 472(7343), 347–350. <https://doi.org/10.1038/nature09972>
- Brewster, P., Barnes, L., Haan, M., Johnson, J. K., Manly, J. J., Nápoles, A. M., Whitmer, R. A., Carvajal-Carmona, L., Early, D., Farias, S., Mayeda, E. R., Melrose, R., Meyer, O. L., Zeki Al Hazzouri, A., Hinton, L., & Mungas, D. (2019). Progress and future challenges in aging and diversity research in the

- United States. *Alzheimer's & Dementia: The Journal of the Alzheimer's Association*, 15(7), 995–1003. <https://doi.org/10.1016/j.jalz.2018.07.221>
- Briese, M., & Sendtner, M. (2021). Keeping the balance: The noncoding RNA 7SK as a master regulator for neuron development and function. *BioEssays*, 43(8), 2100092. <https://doi.org/10.1002/bies.202100092>
- Briggs, J. A., Weinreb, C., Wagner, D. E., Megason, S., Peshkin, L., Kirschner, M. W., & Klein, A. M. (2018). The dynamics of gene expression in vertebrate embryogenesis at single-cell resolution. *Science (New York, N.Y.)*, 360(6392). <https://doi.org/10.1126/science.aar5780>
- Bronson, S. L., & Bale, T. L. (2016). The Placenta as a Mediator of Stress Effects on Neurodevelopmental Reprogramming. *Neuropsychopharmacology: Official Publication of the American College of Neuropsychopharmacology*, 41(1), 207–218. <https://doi.org/10.1038/npp.2015.231>
- Brown, J. D., Piccuillo, V., & O'Neill, R. J. (2012). Retroelement demethylation associated with abnormal placentation in *Mus musculus* x *Mus caroli* hybrids. *Biology of Reproduction*, 86(3), 88. <https://doi.org/10.1095/biolreprod.111.095273>
- Butler, A., Hoffman, P., Smibert, P., Papalexi, E., & Satija, R. (2018a). Integrating single-cell transcriptomic data across different conditions, technologies, and species. *Nature Biotechnology*, 36(5), 411–420. <https://doi.org/10.1038/nbt.4096>

- Butler, A., Hoffman, P., Smibert, P., Papalexi, E., & Satija, R. (2018b). Integrating single-cell transcriptomic data across different conditions, technologies, and species. *Nature Biotechnology*, *36*(5), 411–420. <https://doi.org/10.1038/nbt.4096>
- Butterfield, D. A., Hardas, S. S., & Lange, M. L. B. (2010). Oxidatively modified glyceraldehyde-3-phosphate dehydrogenase (GAPDH) and Alzheimer's disease: Many pathways to neurodegeneration. *Journal of Alzheimer's Disease: JAD*, *20*(2), 369–393. <https://doi.org/10.3233/JAD-2010-1375>
- Byrd, J. C., Furman, R. R., Coutre, S. E., Flinn, I. W., Burger, J. A., Blum, K. A., Grant, B., Sharman, J. P., Coleman, M., Wierda, W. G., Jones, J. A., Zhao, W., Heerema, N. A., Johnson, A. J., Sukbuntherng, J., Chang, B. Y., Clow, F., Hedrick, E., Buggy, J. J., ... O'Brien, S. (2013). Targeting BTK with Ibrutinib in Relapsed Chronic Lymphocytic Leukemia. *New England Journal of Medicine*, *369*(1), 32–42. <https://doi.org/10.1056/NEJMoa1215637>
- Cachero, S., Ostrovsky, A. D., Yu, J. Y., Dickson, B. J., & Jefferis, G. S. X. E. (2010). Sexual Dimorphism in the Fly Brain. *Current Biology*, *20*(18–4), 1589–1601. <https://doi.org/10.1016/j.cub.2010.07.045>
- Cagliani, R., Guerini, F. R., Rubio-Acero, R., Baglio, F., Forni, D., Agliardi, C., Griffanti, L., Fumagalli, M., Pozzoli, U., Riva, S., Calabrese, E., Sikora, M., Casals, F., Comi, G. P., Bresolin, N., Cáceres, M., Clerici, M., & Sironi, M. (2013). Long-standing balancing selection in the THBS4 gene: Influence on sex-specific brain expression and gray matter volumes in Alzheimer disease. *Human Mutation*, *34*(5), 743–753. <https://doi.org/10.1002/humu.22301>



- Cai, L.-J., Tu, L., Huang, X.-M., Huang, J., Qiu, N., Xie, G.-H., Liao, J.-X., Du, W., Zhang, Y.-Y., & Tian, J.-Y. (2020). LncRNA MALAT1 facilitates inflammasome activation via epigenetic suppression of Nrf2 in Parkinson's disease. *Molecular Brain*, 13(1), 130. <https://doi.org/10.1186/s13041-020-00656-8>
- Cai, M., Kolluru, G. K., & Ahmed, A. (2017). Small Molecule, Big Prospects: MicroRNA in Pregnancy and Its Complications. *Journal of Pregnancy*, 2017, 6972732. <https://doi.org/10.1155/2017/6972732>
- Carp, R. I., Meeker, H. C., Chung, R., Kozak, C. A., Hosokawa, M., & Fujisawa, H. (2002). Murine leukemia virus in organs of senescence-prone and -resistant mouse strains. *Mechanisms of Ageing and Development*, 123(6), 575–584. [https://doi.org/10.1016/s0047-6374\(01\)00377-3](https://doi.org/10.1016/s0047-6374(01)00377-3)
- Chang, S.-H., Feng, D., Nagy, J. A., Sciuto, T. E., Dvorak, A. M., & Dvorak, H. F. (2009). Vascular permeability and pathological angiogenesis in caveolin-1-null mice. *The American Journal of Pathology*, 175(4), 1768–1776. <https://doi.org/10.2353/ajpath.2009.090171>
- Chatterjee, A., Macaulay, E. C., Rodger, E. J., Stockwell, P. A., Parry, M. F., Roberts, H. E., Slatter, T. L., Hung, N. A., Devenish, C. J., & Morison, I. M. (2016). Placental Hypomethylation Is More Pronounced in Genomic Loci Devoid of Retroelements. *G3: Genes|Genomes|Genetics*, 6(7), 1911–1921. <https://doi.org/10.1534/g3.116.030379>
- Chen, V. S., Morrison, J. P., Southwell, M. F., Foley, J. F., Bolon, B., & Elmore, S. A. (2017). Histology Atlas of the Developing Prenatal and Postnatal Mouse Central

- Nervous System, with Emphasis on Prenatal Days E7.5 to E18.5. *Toxicologic Pathology*, 45(6), 705–744. <https://doi.org/10.1177/0192623317728134>
- Chen, Y., Pal, B., Visvader, J. E., & Smyth, G. K. (2018). Differential methylation analysis of reduced representation bisulfite sequencing experiments using edgeR. *F1000Research*, 6. <https://doi.org/10.12688/f1000research.13196.2>
- Chew, Y. C., Guo, W., Yang, X., Jin, M., Booher, K., Horvath, S., & Jia, X. Y. (2018). A High-throughput Targeted Bisulfite Sequencing-based Analysis for Epigenetic Age Quantification and Monitoring. *The FASEB Journal*, 32(S1), 674.8-674.8. [https://doi.org/10.1096/fasebj.2018.32.1\\_supplement.674.8](https://doi.org/10.1096/fasebj.2018.32.1_supplement.674.8)
- Choi, K.-H., Kim, H.-S., Park, M.-S., Kim, J.-T., Kim, J.-H., Cho, K.-A., Lee, M.-C., Lee, H.-J., & Cho, K.-H. (2016). Regulation of Caveolin-1 Expression Determines Early Brain Edema After Experimental Focal Cerebral Ischemia. *Stroke*, 47(5), 1336–1343. <https://doi.org/10.1161/STROKEAHA.116.013205>
- Clayton, J. A. (2016). Sex influences in neurological disorders: Case studies and perspectives. *Dialogues in Clinical Neuroscience*, 18(4), 357–360.
- Coffey, C. E., Lucke, J. F., Saxton, J. A., Ratcliff, G., Unitas, L. J., Billig, B., & Bryan, R. N. (1998). Sex differences in brain aging: A quantitative magnetic resonance imaging study. *Archives of Neurology*, 55(2), 169–179. <https://doi.org/10.1001/archneur.55.2.169>
- Coninx, E., Chew, Y. C., Yang, X., Guo, W., Coolkens, A., Baatout, S., Moons, L., Verslegers, M., & Quintens, R. (2020). Hippocampal and cortical tissue-specific epigenetic clocks indicate an increased epigenetic age in a mouse model for

- Alzheimer's disease. *Aging (Albany NY)*, 12(20), 20817–20834.  
<https://doi.org/10.18632/aging.104056>
- Conway, M. E. (2020). Alzheimer's disease: Targeting the glutamatergic system. *Biogerontology*, 21(3), 257–274. <https://doi.org/10.1007/s10522-020-09860-4>
- Copper, R. L., Goldenberg, R. L., Cliver, S. P., DuBard, M. B., Hoffman, H. J., & Davis, R. O. (1993). Anthropometric assessment of body size differences of full-term male and female infants. *Obstetrics and Gynecology*, 81(2), 161–164.
- Cortes, L. R., Cisternas, C. D., & Forger, N. G. (2019). Does Gender Leave an Epigenetic Imprint on the Brain? *Frontiers in Neuroscience*, 13.  
<https://doi.org/10.3389/fnins.2019.00173>
- Costantino, S., & Paneni, F. (2020). Sex-related differences in the ageing brain: Time for precision medicine? *Cardiovascular Research*, 116(7), 1246–1248.  
<https://doi.org/10.1093/cvr/cvaa014>
- Cottarelli, A., Corada, M., Beznoussenko, G. V., Mironov, A. A., Globisch, M. A., Biswas, S., Huang, H., Dimberg, A., Magnusson, P. U., Agalliu, D., Lampugnani, M. G., & Dejana, E. (2020). Fgfbp1 promotes blood-brain barrier development by regulating collagen IV deposition and maintaining Wnt/ $\beta$ -catenin signaling. *Development (Cambridge, England)*, 147(16), dev185140.  
<https://doi.org/10.1242/dev.185140>
- Cui, H., Nishiguchi, N., Yanagi, M., Fukutake, M., Mouri, K., Kitamura, N., Hashimoto, T., Shirakawa, O., & Hishimoto, A. (2010). A putative cis-acting polymorphism in the NOS1 gene is associated with schizophrenia and NOS1 immunoreactivity

in the postmortem brain. *Schizophrenia Research*, 121(1–3), 172–178.

<https://doi.org/10.1016/j.schres.2010.05.003>

Curcio, C. A., & Drucker, D. N. (1993). Retinal ganglion cells in Alzheimer's disease and aging. *Annals of Neurology*, 33(3), 248–257.

<https://doi.org/10.1002/ana.410330305>

Damiani, C., Maspero, D., Di Filippo, M., Colombo, R., Pescini, D., Graudenzi, A., Westerhoff, H. V., Alberghina, L., Vanoni, M., & Mauri, G. (2019). Integration of single-cell RNA-seq data into population models to characterize cancer metabolism. *PLoS Computational Biology*, 15(2).

<https://doi.org/10.1371/journal.pcbi.1006733>

de Lucia, C., Piedepalumbo, M., Wang, L., Carnevale Neto, F., Raftery, D., Gao, E., Praticò, D., Promislow, D. E. L., & Koch, W. J. (2021). Effects of myocardial ischemia/reperfusion injury on plasma metabolomic profile during aging. *Aging Cell*, 20(1), e13284. <https://doi.org/10.1111/accel.13284>

de Magalhães, J. P., & Church, G. M. (2005). Genomes optimize reproduction: Aging as a consequence of the developmental program. *Physiology (Bethesda, Md.)*, 20, 252–259. <https://doi.org/10.1152/physiol.00010.2005>

Dearden, L., Bouret, S. G., & Ozanne, S. E. (2018). Sex and gender differences in developmental programming of metabolism. *Molecular Metabolism*, 15, 8–19.

<https://doi.org/10.1016/j.molmet.2018.04.007>

Decato, B. E., Lopez-Tello, J., Sferruzzi-Perri, A. N., Smith, A. D., & Dean, M. D. (2017). DNA Methylation Divergence and Tissue Specialization in the

Developing Mouse Placenta. *Molecular Biology and Evolution*, 34(7), 1702–1712. <https://doi.org/10.1093/molbev/msx112>

Denisova, E. I., Kozhevnikova, V. V., Bazhan, N. M., & Makarova, E. N. (2020). Sex-specific effects of leptin administration to pregnant mice on the placentae and the metabolic phenotypes of offspring. *FEBS Open Bio*, 10(1), 96–106.

<https://doi.org/10.1002/2211-5463.12757>

Dhakal, P., & Soares, M. J. (2017). Single-step PCR-based genetic sex determination of rat tissues and cells. *BioTechniques*, 62(5), 232–233.

<https://doi.org/10.2144/000114548>

Dhakal, P., Strawn, M., Samal, A., & Behura, S. K. (2021a). Fetal Brain Elicits Sexually Conflicting Transcriptional Response to the Ablation of Uterine Forkhead Box A2 (Foxa2) in Mice. *International Journal of Molecular Sciences*, 22(18), 9693.

<https://doi.org/10.3390/ijms22189693>

Dhakal, P., Strawn, M., Samal, A., & Behura, S. K. (2021b). Fetal Brain Elicits Sexually Conflicting Transcriptional Response to the Ablation of Uterine Forkhead Box A2 (Foxa2) in Mice. *International Journal of Molecular Sciences*, 22(18), 9693.

<https://doi.org/10.3390/ijms22189693>

Dilman, V. M. (1971a). Age-associated elevation of hypothalamic, threshold to feedback control, and its role in development, ageing, and disease. *Lancet (London, England)*, 1(7711), 1211–1219. [https://doi.org/10.1016/s0140-6736\(71\)91721-1](https://doi.org/10.1016/s0140-6736(71)91721-1)

- Dilman, V. M. (1971b). Age-associated elevation of hypothalamic, threshold to feedback control, and its role in development, ageing, and disease. *Lancet (London, England)*, *1*(7711), 1211–1219. [https://doi.org/10.1016/s0140-6736\(71\)91721-1](https://doi.org/10.1016/s0140-6736(71)91721-1)
- Dilman, V. M. (1971c). Age-associated elevation of hypothalamic, threshold to feedback control, and its role in development, ageing, and disease. *Lancet (London, England)*, *1*(7711), 1211–1219. [https://doi.org/10.1016/s0140-6736\(71\)91721-1](https://doi.org/10.1016/s0140-6736(71)91721-1)
- DiPietro, J. A., & Voegtline, K. M. (2017). The gestational foundation of sex differences in development and vulnerability. *Neuroscience*, *342*, 4–20. <https://doi.org/10.1016/j.neuroscience.2015.07.068>
- Dobin, A., Davis, C. A., Schlesinger, F., Drenkow, J., Zaleski, C., Jha, S., Batut, P., Chaisson, M., & Gingeras, T. R. (2013). STAR: Ultrafast universal RNA-seq aligner. *Bioinformatics*, *29*(1), 15–21. <https://doi.org/10.1093/bioinformatics/bts635>
- Docherty, S. J., Davis, O. S., Haworth, C. M., Plomin, R., & Mill, J. (2009). Bisulfite-based epityping on pooled genomic DNA provides an accurate estimate of average group DNA methylation. *Epigenetics & Chromatin*, *2*(1), 3. <https://doi.org/10.1186/1756-8935-2-3>
- dos Reis, M., Inoue, J., Hasegawa, M., Asher, R. J., Donoghue, P. C. J., & Yang, Z. (2012). Phylogenomic datasets provide both precision and accuracy in estimating the timescale of placental mammal phylogeny. *Proceedings. Biological Sciences*, *279*(1742), 3491–3500. <https://doi.org/10.1098/rspb.2012.0683>

- Du, P., Zhang, X., Huang, C.-C., Jafari, N., Kibbe, W. A., Hou, L., & Lin, S. M. (2010). Comparison of Beta-value and M-value methods for quantifying methylation levels by microarray analysis. *BMC Bioinformatics*, *11*(1), 587. <https://doi.org/10.1186/1471-2105-11-587>
- Dyke, J. U. V., Brandley, M. C., & Thompson, M. B. (2014). The evolution of viviparity: Molecular and genomic data from squamate reptiles advance understanding of live birth in amniotes. *Reproduction*, *147*(1), R15–R26. <https://doi.org/10.1530/REP-13-0309>
- Edde, M., Leroux, G., Altena, E., & Chanraud, S. (2021). Functional brain connectivity changes across the human life span: From fetal development to old age. *Journal of Neuroscience Research*, *99*(1), 236–262. <https://doi.org/10.1002/jnr.24669>
- Edgar, R. D., Jones, M. J., Meaney, M. J., Turecki, G., & Kobor, M. S. (2017). BECon: A tool for interpreting DNA methylation findings from blood in the context of brain. *Translational Psychiatry*, *7*(8), e1187. <https://doi.org/10.1038/tp.2017.171>
- Entringer, S., de Punder, K., Buss, C., & Wadhwa, P. D. (2018). The fetal programming of telomere biology hypothesis: An update. *Philosophical Transactions of the Royal Society B: Biological Sciences*, *373*(1741). <https://doi.org/10.1098/rstb.2017.0151>
- Eriksson, J. G., Kajantie, E., Osmond, C., Thornburg, K., & Barker, D. J. P. (2010). Boys live dangerously in the womb. *American Journal of Human Biology: The Official Journal of the Human Biology Council*, *22*(3), 330–335. <https://doi.org/10.1002/ajhb.20995>

- Evers, T. M. J., Hochane, M., Tans, S. J., Heeren, R. M. A., Semrau, S., Nemes, P., & Mashaghi, A. (2019). Deciphering Metabolic Heterogeneity by Single-Cell Analysis. *Analytical Chemistry*, *91*(21), 13314–13323.  
<https://doi.org/10.1021/acs.analchem.9b02410>
- Everson, T. M., O’Shea, T. M., Burt, A., Hermetz, K., Carter, B. S., Helderman, J., Hofheimer, J. A., McGowan, E. C., Neal, C. R., Pastyrnak, S. L., Smith, L. M., Soliman, A., DellaGrotta, S. A., Dansereau, L. M., Padbury, J. F., Lester, B. M., & Marsit, C. J. (2020). Serious neonatal morbidities are associated with differences in DNA methylation among very preterm infants. *Clinical Epigenetics*, *12*(1), 151. <https://doi.org/10.1186/s13148-020-00942-1>
- Fabbri, E., Zoli, M., Gonzalez-Freire, M., Salive, M. E., Studenski, S. A., & Ferrucci, L. (2015). Aging and Multimorbidity: New Tasks, Priorities, and Frontiers for Integrated Gerontological and Clinical Research. *Journal of the American Medical Directors Association*, *16*(8), 640–647.  
<https://doi.org/10.1016/j.jamda.2015.03.013>
- Fan, Y., Vilgalys, T. P., Sun, S., Peng, Q., Tung, J., & Zhou, X. (2019). IMAGE: High-powered detection of genetic effects on DNA methylation using integrated methylation QTL mapping and allele-specific analysis. *Genome Biology*, *20*(1), 220. <https://doi.org/10.1186/s13059-019-1813-1>
- Farré, P., Jones, M. J., Meaney, M. J., Emberly, E., Turecki, G., & Kobor, M. S. (2015). Concordant and discordant DNA methylation signatures of aging in human blood



and brain. *Epigenetics & Chromatin*, 8, 19. <https://doi.org/10.1186/s13072-015-0011-y>

- Farrell, C. M., Goldfarb, T., Rangwala, S. H., Astashyn, A., Ermolaeva, O. D., Hem, V., Katz, K. S., Kodali, V. K., Ludwig, F., Wallin, C. L., Pruitt, K. D., & Murphy, T. D. (2022). RefSeq Functional Elements as experimentally assayed nongenic reference standards and functional interactions in human and mouse. *Genome Research*, 32(1), 175–188. <https://doi.org/10.1101/gr.275819.121>
- Fayed, N., Modrego, P. J., Rojas-Salinas, G., & Aguilar, K. (2011). Brain glutamate levels are decreased in Alzheimer's disease: A magnetic resonance spectroscopy study. *American Journal of Alzheimer's Disease and Other Dementias*, 26(6), 450–456. <https://doi.org/10.1177/1533317511421780>
- Feltes, B. C., de Faria Poloni, J., & Bonatto, D. (2015a). Development and aging: Two opposite but complementary phenomena. *Interdisciplinary Topics in Gerontology*, 40, 74–84. <https://doi.org/10.1159/000364932>
- Feltes, B. C., de Faria Poloni, J., & Bonatto, D. (2015b). Development and aging: Two opposite but complementary phenomena. *Interdisciplinary Topics in Gerontology*, 40, 74–84. <https://doi.org/10.1159/000364932>
- Feng, L., Liao, W.-X., Luo, Q., Zhang, H.-H., Wang, W., Zheng, J., & Chen, D.-B. (2012). Caveolin-1 orchestrates fibroblast growth factor 2 signaling control of angiogenesis in placental artery endothelial cell caveolae. *Journal of Cellular Physiology*, 227(6), 2480–2491. <https://doi.org/10.1002/jcp.22984>

- Finney, C. A., Delerue, F., & Shvetcov, A. (2022). *Artificial intelligence-driven meta-analysis of brain gene expression data identifies novel gene candidates in Alzheimer's Disease* [Preprint]. *Genetic and Genomic Medicine*.  
<https://doi.org/10.1101/2022.02.02.22270347>
- Flurkey, K., Mcurrer, J., & Harrison, D. (2007). Mouse Models in Aging Research. In *The Mouse in Biomedical Research: Vol. III* (pp. 637–672). Elsevier.  
<https://doi.org/10.1016/B978-012369454-6/50074-1>
- Folgueras, A. R., Freitas-Rodríguez, S., Velasco, G., & López-Otín, C. (2018). Mouse Models to Disentangle the Hallmarks of Human Aging. *Circulation Research*, *123*(7), 905–924. <https://doi.org/10.1161/CIRCRESAHA.118.312204>
- Franceschi, C., Garagnani, P., Morsiani, C., Conte, M., Santoro, A., Grignolio, A., Monti, D., Capri, M., & Salvioli, S. (2018). The Continuum of Aging and Age-Related Diseases: Common Mechanisms but Different Rates. *Frontiers in Medicine*, *5*.  
<https://doi.org/10.3389/fmed.2018.00061>
- Franchini, L. F., & Pollard, K. S. (2015). Can a few non-coding mutations make a human brain? *BioEssays: News and Reviews in Molecular, Cellular and Developmental Biology*, *37*(10), 1054–1061. <https://doi.org/10.1002/bies.201500049>
- Franzén, O., Gan, L.-M., & Björkegren, J. L. M. (2019). PanglaoDB: A web server for exploration of mouse and human single-cell RNA sequencing data. *Database*, *2019*. <https://doi.org/10.1093/database/baz046>
- Fujino, Y., Kasai, T., Kitani-Morii, F., Ohmichi, T., Shinomoto, M., Menjo, K., & Mizuno, T. (2021). Impaired age-dependent increases in phosphoglycerate kinase

- activity in red blood cells of Parkinson's disease patients. *Parkinsonism & Related Disorders*, *91*, 128–134. <https://doi.org/10.1016/j.parkreldis.2021.09.016>
- Fushan, A. A., Turanov, A. A., Lee, S.-G., Kim, E. B., Lobanov, A. V., Yim, S. H., Buffenstein, R., Lee, S.-R., Chang, K.-T., Rhee, H., Kim, J.-S., Yang, K.-S., & Gladyshev, V. N. (2015a). Gene expression defines natural changes in mammalian lifespan. *Aging Cell*, *14*(3), 352–365. <https://doi.org/10.1111/accel.12283>
- Fushan, A. A., Turanov, A. A., Lee, S.-G., Kim, E. B., Lobanov, A. V., Yim, S. H., Buffenstein, R., Lee, S.-R., Chang, K.-T., Rhee, H., Kim, J.-S., Yang, K.-S., & Gladyshev, V. N. (2015b). Gene expression defines natural changes in mammalian lifespan. *Aging Cell*, *14*(3), 352–365. <https://doi.org/10.1111/accel.12283>
- Gage, S. H., Munafò, M. R., & Davey Smith, G. (2016). Causal Inference in Developmental Origins of Health and Disease (DOHaD) Research. *Annual Review of Psychology*, *67*, 567–585. <https://doi.org/10.1146/annurev-psych-122414-033352>
- Gagnon, R. (2003). Placental insufficiency and its consequences. *European Journal of Obstetrics & Gynecology and Reproductive Biology*, *110*, S99–S107. [https://doi.org/10.1016/S0301-2115\(03\)00179-9](https://doi.org/10.1016/S0301-2115(03)00179-9)
- Gao, W., Sun, Y.-B., Zhou, W.-W., Xiong, Z.-J., Chen, L., Li, H., Fu, T.-T., Xu, K., Xu, W., Ma, L., Chen, Y.-J., Xiang, X.-Y., Zhou, L., Zeng, T., Zhang, S., Jin, J.-Q., Chen, H.-M., Zhang, G., Hillis, D. M., ... Che, J. (2019). Genomic and

- transcriptomic investigations of the evolutionary transition from oviparity to viviparity. *Proceedings of the National Academy of Sciences of the United States of America*, 116(9), 3646–3655. <https://doi.org/10.1073/pnas.1816086116>
- Geirsdottir, L., David, E., Keren-Shaul, H., Weiner, A., Bohlen, S. C., Neuber, J., Balic, A., Giladi, A., Sheban, F., Dutertre, C.-A., Pfeifle, C., Peri, F., Raffo-Romero, A., Vizioli, J., Matiassek, K., Scheiwe, C., Meckel, S., Mätz-Rensing, K., van der Meer, F., ... Prinz, M. (2019). Cross-Species Single-Cell Analysis Reveals Divergence of the Primate Microglia Program. *Cell*, 179(7), 1609-1622.e16. <https://doi.org/10.1016/j.cell.2019.11.010>
- Gião, T., Teixeira, T., Almeida, M. R., & Cardoso, I. (2022). Choroid Plexus in Alzheimer's Disease-The Current State of Knowledge. *Biomedicines*, 10(2), 224. <https://doi.org/10.3390/biomedicines10020224>
- Gimse, K. E., O'Riordan, K., & Burger, C. (2019). Induction of Metabotropic Glutamate Receptor-Mediated Long-Term Depression in the Hippocampal Schaffer Collateral Pathway of Aging Rats. In C. Burger & M. J. Velardo (Eds.), *Glutamate Receptors* (Vol. 1941, pp. 93–105). Springer New York. [https://doi.org/10.1007/978-1-4939-9077-1\\_8](https://doi.org/10.1007/978-1-4939-9077-1_8)
- Gjoneska, E., Pfenning, A. R., Mathys, H., Quon, G., Kundaje, A., Tsai, L.-H., & Kellis, M. (2015). Conserved epigenomic signals in mice and humans reveal immune basis of Alzheimer's disease. *Nature*, 518(7539), 365–369. <https://doi.org/10.1038/nature14252>

- Glasgow, S. D., Wong, E. W., Thompson-Steckel, G., Marcal, N., Séguéla, P., Ruthazer, E. S., & Kennedy, T. E. (2020). Pre- and post-synaptic roles for DCC in memory consolidation in the adult mouse hippocampus. *Molecular Brain, 13*(1), 56.  
<https://doi.org/10.1186/s13041-020-00597-2>
- Gluckman, P. D., Hanson, M. A., Cooper, C., & Thornburg, K. L. (2008). Effect of In Utero and Early-Life Conditions on Adult Health and Disease. *The New England Journal of Medicine, 359*(1), 61–73. <https://doi.org/10.1056/NEJMra0708473>
- Gontarz, P., Fu, S., Xing, X., Liu, S., Miao, B., Bazylianska, V., Sharma, A., Madden, P., Cates, K., Yoo, A., Moszczynska, A., Wang, T., & Zhang, B. (2020). Comparison of differential accessibility analysis strategies for ATAC-seq data. *Scientific Reports, 10*(1), 10150. <https://doi.org/10.1038/s41598-020-66998-4>
- Gopalakrishnan, V. (2009). REST and the RESTless: In stem cells and beyond. *Future Neurology, 4*(3), 317–329. <https://doi.org/10.2217/fnl.09.1>
- Gorski, R. A. (1985). Sexual dimorphisms of the brain. *Journal of Animal Science, 61* Suppl 3, 38–61. [https://doi.org/10.1093/ansci/61.supplement\\_3.38](https://doi.org/10.1093/ansci/61.supplement_3.38)
- Goyal, M. S., Blazey, T. M., Su, Y., Couture, L. E., Durbin, T. J., Bateman, R. J., Benzinger, T. L.-S., Morris, J. C., Raichle, M. E., & Vlassenko, A. G. (2019a). Persistent metabolic youth in the aging female brain. *Proceedings of the National Academy of Sciences of the United States of America, 116*(8), 3251–3255.  
<https://doi.org/10.1073/pnas.1815917116>
- Goyal, M. S., Blazey, T. M., Su, Y., Couture, L. E., Durbin, T. J., Bateman, R. J., Benzinger, T. L.-S., Morris, J. C., Raichle, M. E., & Vlassenko, A. G. (2019b).

- Persistent metabolic youth in the aging female brain. *Proceedings of the National Academy of Sciences*, 116(8), 3251–3255.  
<https://doi.org/10.1073/pnas.1815917116>
- Greene, N. D. E., & Copp, A. J. (2014). Neural tube defects. *Annual Review of Neuroscience*, 37, 221–242. <https://doi.org/10.1146/annurev-neuro-062012-170354>
- Grillari, J., & Grillari-Voglauer, R. (2010). Novel modulators of senescence, aging, and longevity: Small non-coding RNAs enter the stage. *Experimental Gerontology*, 45(4), 302–311. <https://doi.org/10.1016/j.exger.2010.01.007>
- Gruzieva, O., Merid, S. K., Chen, S., Mukherjee, N., Hedman, A. M., Almqvist, C., Andolf, E., Jiang, Y., Kere, J., Scheynius, A., Söderhäll, C., Ullemar, V., Karmaus, W., Melén, E., Arshad, S. H., & Pershagen, G. (2019). DNA Methylation Trajectories During Pregnancy. *Epigenetics Insights*, 12, 2516865719867090. <https://doi.org/10.1177/2516865719867090>
- Guebel, D. V., & Torres, N. V. (2016). Sexual Dimorphism and Aging in the Human Hippocampus: Identification, Validation, and Impact of Differentially Expressed Genes by Factorial Microarray and Network Analysis. *Frontiers in Aging Neuroscience*, 8, 229. <https://doi.org/10.3389/fnagi.2016.00229>
- Gupta, S. K., Gressens, P., & Mani, S. (2009). NRSF downregulation induces neuronal differentiation in mouse embryonic stem cells. *Differentiation; Research in Biological Diversity*, 77(1), 19–28. <https://doi.org/10.1016/j.diff.2008.09.001>

- Hägg, S., & Jylhävä, J. (2021). Sex differences in biological aging with a focus on human studies. *ELife*, *10*, e63425. <https://doi.org/10.7554/eLife.63425>
- Handl, L., Jalali, A., Scherer, M., Eggeling, R., & Pfeifer, N. (2019). Weighted elastic net for unsupervised domain adaptation with application to age prediction from DNA methylation data. *Bioinformatics (Oxford, England)*, *35*(14), i154–i163. <https://doi.org/10.1093/bioinformatics/btz338>
- Hannibal, L. (2016). Nitric Oxide Homeostasis in Neurodegenerative Diseases. *Current Alzheimer Research*, *13*(2), 135–149. <https://doi.org/10.2174/1567205012666150921101250>
- Hannon, E., Mansell, G., Walker, E., Nabais, M. F., Burrage, J., Kepa, A., Best-Lane, J., Rose, A., Heck, S., Moffitt, T. E., Caspi, A., Arseneault, L., & Mill, J. (2021). Assessing the co-variability of DNA methylation across peripheral cells and tissues: Implications for the interpretation of findings in epigenetic epidemiology. *PLOS Genetics*, *17*(3), e1009443. <https://doi.org/10.1371/journal.pgen.1009443>
- Hanson, M. A., & Gluckman, P. D. (2014). Early Developmental Conditioning of Later Health and Disease: Physiology or Pathophysiology? *Physiological Reviews*, *94*(4), 1027–1076. <https://doi.org/10.1152/physrev.00029.2013>
- Harrison, T. M., Weintraub, S., Mesulam, M.-M., & Rogalski, E. (2012). Superior memory and higher cortical volumes in unusually successful cognitive aging. *Journal of the International Neuropsychological Society: JINS*, *18*(6), 1081–1085. <https://doi.org/10.1017/S1355617712000847>

- Hart, B., Morgan, E., & Alejandro, E. U. (2019). Nutrient sensor signaling pathways and cellular stress in fetal growth restriction. *Journal of Molecular Endocrinology*, 62(2), R155–R165. <https://doi.org/10.1530/JME-18-0059>
- Hattori, C., Asai, M., Onishi, H., Sasagawa, N., Hashimoto, Y., Saïdo, T. C., Maruyama, K., Mizutani, S., & Ishiura, S. (2006). BACE1 interacts with lipid raft proteins. *Journal of Neuroscience Research*, 84(4), 912–917. <https://doi.org/10.1002/jnr.20981>
- Hayder, H., O'Brien, J., Nadeem, U., & Peng, C. (2018). MicroRNAs: Crucial regulators of placental development. *Reproduction (Cambridge, England)*, 155(6), R259–R271. <https://doi.org/10.1530/REP-17-0603>
- Head, B. P., Peart, J. N., Panneerselvam, M., Yokoyama, T., Pearn, M. L., Niesman, I. R., Bonds, J. A., Schilling, J. M., Miyanochara, A., Headrick, J., Ali, S. S., Roth, D. M., Patel, P. M., & Patel, H. H. (2010a). Loss of caveolin-1 accelerates neurodegeneration and aging. *PloS One*, 5(12), e15697. <https://doi.org/10.1371/journal.pone.0015697>
- Head, B. P., Peart, J. N., Panneerselvam, M., Yokoyama, T., Pearn, M. L., Niesman, I. R., Bonds, J. A., Schilling, J. M., Miyanochara, A., Headrick, J., Ali, S. S., Roth, D. M., Patel, P. M., & Patel, H. H. (2010b). Loss of caveolin-1 accelerates neurodegeneration and aging. *PloS One*, 5(12), e15697. <https://doi.org/10.1371/journal.pone.0015697>
- Head, B. P., Peart, J. N., Panneerselvam, M., Yokoyama, T., Pearn, M. L., Niesman, I. R., Bonds, J. A., Schilling, J. M., Miyanochara, A., Headrick, J., Ali, S. S., Roth,



- D. M., Patel, P. M., & Patel, H. H. (2010c). Loss of caveolin-1 accelerates neurodegeneration and aging. *PloS One*, 5(12), e15697.  
<https://doi.org/10.1371/journal.pone.0015697>
- Heindel, J. J., & Vandenberg, L. N. (2015). Developmental Origins of Health and Disease: A Paradigm for Understanding Disease Etiology and Prevention. *Current Opinion in Pediatrics*, 27(2), 248–253.  
<https://doi.org/10.1097/MOP.0000000000000191>
- Herr, W., & Gilbert, W. (1982). Germ-line MuLV reintegrations in AKR/J mice. *Nature*, 296(5860), 865–868. <https://doi.org/10.1038/296865a0>
- Hess, D. C., Hill, W. D., Martin-Studdard, A., Carroll, J., Brailer, J., & Carothers, J. (2002). Bone marrow as a source of endothelial cells and NeuN-expressing cells After stroke. *Stroke*, 33(5), 1362–1368.  
<https://doi.org/10.1161/01.str.0000014925.09415.c3>
- Hirabayashi, K., Shiota, K., & Yagi, S. (2013). DNA methylation profile dynamics of tissue-dependent and differentially methylated regions during mouse brain development. *BMC Genomics*, 14, 82. <https://doi.org/10.1186/1471-2164-14-82>
- Horvath, S. (2013). DNA methylation age of human tissues and cell types. *Genome Biology*, 14(10), R115. <https://doi.org/10.1186/gb-2013-14-10-r115>
- Howerton, C. L., & Bale, T. L. (2014). Targeted placental deletion of OGT recapitulates the prenatal stress phenotype including hypothalamic mitochondrial dysfunction. *Proceedings of the National Academy of Sciences*, 111(26), 9639–9644.  
<https://doi.org/10.1073/pnas.1401203111>

- Howerton, C. L., Morgan, C. P., Fischer, D. B., & Bale, T. L. (2013). O-GlcNAc transferase (OGT) as a placental biomarker of maternal stress and reprogramming of CNS gene transcription in development. *Proceedings of the National Academy of Sciences of the United States of America*, *110*(13), 5169–5174.  
<https://doi.org/10.1073/pnas.1300065110>
- Hu, G., Li, J., & Wang, G.-Z. (2020). Significant Evolutionary Constraints on Neuron Cells Revealed by Single-Cell Transcriptomics. *Genome Biology and Evolution*, *12*(4), 300–308. <https://doi.org/10.1093/gbe/evaa054>
- Hur, J. H., Stork, D. A., & Walker, D. W. (2014). Complex-I-ty in aging. *Journal of Bioenergetics and Biomembranes*, *46*(4), 329–335.  
<https://doi.org/10.1007/s10863-014-9553-0>
- Hutchison, J. B., Beyer, C., Hutchison, R. E., & Wozniak, A. (1995). Sexual dimorphism in the developmental regulation of brain aromatase. *The Journal of Steroid Biochemistry and Molecular Biology*, *53*(1–6), 307–313.  
[https://doi.org/10.1016/0960-0760\(95\)00068-b](https://doi.org/10.1016/0960-0760(95)00068-b)
- Islam, M., Strawn, M., & Behura, S. K. (2022). *Fetal origin of sex-bias brain aging* (p. 2022.02.02.478867). bioRxiv. <https://doi.org/10.1101/2022.02.02.478867>
- Jänes, J., Dong, Y., Schoof, M., Serizay, J., Appert, A., Cerrato, C., Woodbury, C., Chen, R., Gemma, C., Huang, N., Kissiov, D., Stempor, P., Steward, A., Zeiser, E., Sauer, S., & Ahringer, J. (2018). Chromatin accessibility dynamics across *C. elegans* development and ageing. *ELife*, *7*, e37344.  
<https://doi.org/10.7554/eLife.37344>

- Jansson, T., & Powell, T. L. (2013). Role of placental nutrient sensing in developmental programming. *Clinical Obstetrics and Gynecology*, *56*(3), 591–601.  
<https://doi.org/10.1097/GRF.0b013e3182993a2e>
- Jasmin, J.-F., Malhotra, S., Singh Dhallu, M., Mercier, I., Rosenbaum, D. M., & Lisanti, M. P. (2007). Caveolin-1 Deficiency Increases Cerebral Ischemic Injury. *Circulation Research*, *100*(5), 721–729.  
<https://doi.org/10.1161/01.RES.0000260180.42709.29>
- Jensen Peña, C., Monk, C., & Champagne, F. A. (2012). Epigenetic effects of prenatal stress on 11 $\beta$ -hydroxysteroid dehydrogenase-2 in the placenta and fetal brain. *PloS One*, *7*(6), e39791. <https://doi.org/10.1371/journal.pone.0039791>
- Jeong, B. H., Jin, J. K., Choi, E. K., Lee, E. Y., Meeker, H. C., Kozak, C. A., Carp, R. I., & Kim, Y. S. (2002). Analysis of the expression of endogenous murine leukemia viruses in the brains of senescence-accelerated mice (SAMP8) and the relationship between expression and brain histopathology. *Journal of Neuropathology and Experimental Neurology*, *61*(11), 1001–1012.  
<https://doi.org/10.1093/jnen/61.11.1001>
- Jin, S., Lee, Y. K., Lim, Y. C., Zheng, Z., Lin, X. M., Ng, D. P. Y., Holbrook, J. D., Law, H. Y., Kwek, K. Y. C., Yeo, G. S. H., & Ding, C. (2013). Global DNA hypermethylation in down syndrome placenta. *PLoS Genetics*, *9*(6), e1003515.  
<https://doi.org/10.1371/journal.pgen.1003515>
- Johnson, A. A., Akman, K., Calimport, S. R. G., Wuttke, D., Stolzing, A., & de Magalhães, J. P. (2012). The Role of DNA Methylation in Aging, Rejuvenation,

and Age-Related Disease. *Rejuvenation Research*, 15(5), 483–494.

<https://doi.org/10.1089/rej.2012.1324>

Jones, M. J., Goodman, S. J., & Kobor, M. S. (2015). DNA methylation and healthy human aging. *Aging Cell*, 14(6), 924–932. <https://doi.org/10.1111/accel.12349>

Jové, M., Pradas, I., Dominguez-Gonzalez, M., Ferrer, I., & Pamplona, R. (2019). Lipids and lipoxidation in human brain aging. Mitochondrial ATP-synthase as a key lipoxidation target. *Redox Biology*, 23, 101082.

<https://doi.org/10.1016/j.redox.2018.101082>

Kalisch-Smith, J. I., Simmons, D. G., Pantaleon, M., & Moritz, K. M. (2017). Sex differences in rat placental development: From pre-implantation to late gestation. *Biology of Sex Differences*, 8, 17. <https://doi.org/10.1186/s13293-017-0138-6>

Kanton, S., Boyle, M. J., He, Z., Santel, M., Weigert, A., Sanchís-Calleja, F., Guijarro, P., Sidow, L., Fleck, J. S., Han, D., Qian, Z., Heide, M., Huttner, W. B., Khaitovich, P., Pääbo, S., Treutlein, B., & Camp, J. G. (2019). Organoid single-cell genomic atlas uncovers human-specific features of brain development.

*Nature*, 574(7778), 418–422. <https://doi.org/10.1038/s41586-019-1654-9>

Kim, D., Langmead, B., & Salzberg, S. L. (2015). HISAT: A fast spliced aligner with low memory requirements. *Nature Methods*, 12(4), 357–360.

<https://doi.org/10.1038/nmeth.3317>

Kim, H., Jang, W. Y., Kang, M.-C., Jeong, J., Choi, M., Sung, Y., Park, S., Kwon, W., Jang, S., Kim, M. O., Kim, S. H., & Ryoo, Z. Y. (2016). TET1 contributes to neurogenesis onset time during fetal brain development in mice. *Biochemical and*

*Biophysical Research Communications*, 471(4), 437–443.

<https://doi.org/10.1016/j.bbrc.2016.02.060>

Kim, S. S., & Lee, S.-J. V. (2019). Non-Coding RNAs in *Caenorhabditis elegans* Aging. *Molecules and Cells*, 42(5), 379–385.

<https://doi.org/10.14348/molcells.2019.0077>

Klauck, S. M., Felder, B., Kolb-Kokocinski, A., Schuster, C., Chiocchetti, A., Schupp, I., Wellenreuther, R., Schmötzer, G., Poustka, F., Breitenbach-Koller, L., & Poustka, A. (2006). Mutations in the ribosomal protein gene RPL10 suggest a novel modulating disease mechanism for autism. *Molecular Psychiatry*, 11(12), 1073–1084. <https://doi.org/10.1038/sj.mp.4001883>

Klein, M. O., Battagello, D. S., Cardoso, A. R., Hauser, D. N., Bittencourt, J. C., & Correa, R. G. (2019). Dopamine: Functions, Signaling, and Association with Neurological Diseases. *Cellular and Molecular Neurobiology*, 39(1), 31–59.

<https://doi.org/10.1007/s10571-018-0632-3>

Klemm, S. L., Shipony, Z., & Greenleaf, W. J. (2019). Chromatin accessibility and the regulatory epigenome. *Nature Reviews. Genetics*, 20(4), 207–220.

<https://doi.org/10.1038/s41576-018-0089-8>

Kobak, D., & Berens, P. (2019). The art of using t-SNE for single-cell transcriptomics. *Nature Communications*, 10(1), 5416. <https://doi.org/10.1038/s41467-019-13056->

x

- Konstantinides, N., Degabriel, S., & Desplan, C. (2018). Neuro-evo-devo in the single cell sequencing era. *Current Opinion in Systems Biology*, *11*, 32–40. <https://doi.org/10.1016/j.coisb.2018.08.001>
- Koohy, H., Bolland, D. J., Matheson, L. S., Schoenfelder, S., Stellato, C., Dimond, A., Várnai, C., Chovanec, P., Chessa, T., Denizot, J., Manzano Garcia, R., Wingett, S. W., Freire-Pritchett, P., Nagano, T., Hawkins, P., Stephens, L., Elderkin, S., Spivakov, M., Fraser, P., ... Varga-Weisz, P. D. (2018). Genome organization and chromatin analysis identify transcriptional downregulation of insulin-like growth factor signaling as a hallmark of aging in developing B cells. *Genome Biology*, *19*(1), 126. <https://doi.org/10.1186/s13059-018-1489-y>
- Koukoura, O., Sifakis, S., & Spandidos, D. A. (2012). DNA methylation in the human placenta and fetal growth (review). *Molecular Medicine Reports*, *5*(4), 883–889. <https://doi.org/10.3892/mmr.2012.763>
- Kozak, C. A., & Rowe, W. P. (1980). Genetic mapping of the ecotropic virus-inducing locus Akv-2 of the AKR mouse. *The Journal of Experimental Medicine*, *152*(5), 1419–1423. <https://doi.org/10.1084/jem.152.5.1419>
- Kratimenos, P., & Penn, A. A. (2019a). Placental programming of neuropsychiatric disease. *Pediatric Research*, *86*(2), 157–164. <https://doi.org/10.1038/s41390-019-0405-9>
- Kratimenos, P., & Penn, A. A. (2019b). Placental programming of neuropsychiatric disease. *Pediatric Research*, *86*(2), 157–164. <https://doi.org/10.1038/s41390-019-0405-9>

- Kratimenos, P., & Penn, A. A. (2019c). Placental programming of neuropsychiatric disease. *Pediatric Research*, *86*(2), 157–164. <https://doi.org/10.1038/s41390-019-0405-9>
- Kreisman, M. J., Song, C. I., Yip, K., Natale, B. V., Natale, D. R., & Breen, K. M. (2017). Androgens Mediate Sex-Dependent Gonadotropin Expression During Late Prenatal Development in the Mouse. *Endocrinology*, *158*(9), 2884–2894. <https://doi.org/10.1210/en.2017-00285>
- Krueger, F., & Andrews, S. R. (2011). Bismark: A flexible aligner and methylation caller for Bisulfite-Seq applications. *Bioinformatics (Oxford, England)*, *27*(11), 1571–1572. <https://doi.org/10.1093/bioinformatics/btr167>
- Kuningas, M., Altmäe, S., Uitterlinden, A. G., Hofman, A., van Duijn, C. M., & Tiemeier, H. (2011). The relationship between fertility and lifespan in humans. *Age (Dordrecht, Netherlands)*, *33*(4), 615–622. <https://doi.org/10.1007/s11357-010-9202-4>
- Kuntz, E. M., Baquero, P., Michie, A. M., Dunn, K., Tardito, S., Holyoake, T. L., Helgason, G. V., & Gottlieb, E. (2017). Targeting mitochondrial oxidative phosphorylation eradicates therapy-resistant chronic myeloid leukemia stem cells. *Nature Medicine*, *23*(10), 1234–1240. <https://doi.org/10.1038/nm.4399>
- Kverková, K., Polonyiová, A., Kubička, L., & Němec, P. (2020). Individual and age-related variation of cellular brain composition in a squamate reptile. *Biology Letters*, *16*(9), 20200280. <https://doi.org/10.1098/rsbl.2020.0280>

- Kwak, S., Kim, H., Chey, J., & Youm, Y. (2018). Feeling How Old I Am: Subjective Age Is Associated With Estimated Brain Age. *Frontiers in Aging Neuroscience, 10*. <https://www.frontiersin.org/article/10.3389/fnagi.2018.00168>
- Langlois, M.-A., Kemmerich, K., Rada, C., & Neuberger, M. S. (2009). The AKV Murine Leukemia Virus Is Restricted and Hypermutated by Mouse APOBEC3. *Journal of Virology, 83*(22), 11550–11559. <https://doi.org/10.1128/JVI.01430-09>
- Langmead, B., & Salzberg, S. L. (2012). Fast gapped-read alignment with Bowtie 2. *Nature Methods, 9*(4), 357–359. <https://doi.org/10.1038/nmeth.1923>
- Lau, S.-F., Cao, H., Fu, A. K. Y., & Ip, N. Y. (2020). Single-nucleus transcriptome analysis reveals dysregulation of angiogenic endothelial cells and neuroprotective glia in Alzheimer’s disease. *Proceedings of the National Academy of Sciences of the United States of America, 117*(41), 25800–25809. <https://doi.org/10.1073/pnas.2008762117>
- Lau, S.-F., Chen, C., Fu, W.-Y., Qu, J. Y., Cheung, T. H., Fu, A. K. Y., & Ip, N. Y. (2020). IL-33-PU.1 Transcriptome Reprogramming Drives Functional State Transition and Clearance Activity of Microglia in Alzheimer’s Disease. *Cell Reports, 31*(3), 107530. <https://doi.org/10.1016/j.celrep.2020.107530>
- Laufer, B. I., Neier, K. E., Valenzuela, A. E., Yasui, D. H., Schmidt, R. J., Lein, P. J., & LaSalle, J. M. (2021). Genome-Wide DNA Methylation Profiles of Neurodevelopmental Disorder Genes in Mouse Placenta and Fetal Brain Following Prenatal Exposure to Polychlorinated Biphenyls. *BioRxiv, 2021.05.27.446011*. <https://doi.org/10.1101/2021.05.27.446011>



- Lazzari, E., Ramalingam, P., Poulos, M. G., & Butler, J. M. (2018). Aging of the Vascular Niche Enhances Leukemia-Initiating Cell Metabolic Switch. *Blood*, *132*(Supplement 1), 871. <https://doi.org/10.1182/blood-2018-99-115019>
- Le Douce, J., Maugard, M., Veran, J., Matos, M., Jégo, P., Vigneron, P.-A., Faivre, E., Toussay, X., Vandenberghe, M., Balbastre, Y., Piquet, J., Guiot, E., Tran, N. T., Taverna, M., Marinesco, S., Koyanagi, A., Furuya, S., Gaudin-Guérif, M., Goutal, S., ... Bonvento, G. (2020). Impairment of Glycolysis-Derived l-Serine Production in Astrocytes Contributes to Cognitive Deficits in Alzheimer's Disease. *Cell Metabolism*, *31*(3), 503-517.e8. <https://doi.org/10.1016/j.cmet.2020.02.004>
- Lee, E. A., Angka, L., Rota, S.-G., Hanlon, T., Mitchell, A., Hurren, R., Wang, X. M., Gronda, M., Boyaci, E., Bojko, B., Minden, M., Sriskanthadevan, S., Datti, A., Wrana, J. L., Edginton, A., Pawliszyn, J., Joseph, J. W., Quadrilatero, J., Schimmer, A. D., & Spagnuolo, P. A. (2015). Targeting Mitochondria with Avocatin B Induces Selective Leukemia Cell Death. *Cancer Research*, *75*(12), 2478–2488. <https://doi.org/10.1158/0008-5472.CAN-14-2676>
- Lee, Y., Choufani, S., Weksberg, R., Wilson, S. L., Yuan, V., Burt, A., Marsit, C., Lu, A. T., Ritz, B., Bohlin, J., Gjessing, H. K., Harris, J. R., Magnus, P., Binder, A. M., Robinson, W. P., Jugessur, A., & Horvath, S. (2019). Placental epigenetic clocks: Estimating gestational age using placental DNA methylation levels. *Aging*, *11*(12), 4238–4253. <https://doi.org/10.18632/aging.102049>

- Leiser, R., & Dantzer, V. (1988). Structural and functional aspects of porcine placental microvasculature. *Anatomy and Embryology*, 177(5), 409–419.  
<https://doi.org/10.1007/BF00304738>
- Li, H., & Durbin, R. (2009). Fast and accurate short read alignment with Burrows-Wheeler transform. *Bioinformatics (Oxford, England)*, 25(14), 1754–1760.  
<https://doi.org/10.1093/bioinformatics/btp324>
- Li, L., Maire, C. L., Bilenky, M., Carles, A., Heravi-Moussavi, A., Hong, C., Tam, A., Kamoh, B., Cho, S., Cheung, D., Li, I., Wong, T., Nagarajan, R. P., Mungall, A. J., Moore, R., Wang, T., Kleinman, C. L., Jabado, N., Jones, S. J., ... Hirst, M. (2020). Epigenomic programming in early fetal brain development. *Epigenomics*, 12(12), 1053–1070. <https://doi.org/10.2217/epi-2019-0319>
- Li, L., Zhao, L., Man, J., & Liu, B. (2021). CXCL2 benefits acute myeloid leukemia cells in hypoxia. *International Journal of Laboratory Hematology*, 43(5), 1085–1092.  
<https://doi.org/10.1111/ijlh.13512>
- Liao, Y., Smyth, G. K., & Shi, W. (2014). featureCounts: An efficient general purpose program for assigning sequence reads to genomic features. *Bioinformatics (Oxford, England)*, 30(7), 923–930. <https://doi.org/10.1093/bioinformatics/btt656>
- Liddel, S. A. (2015). Development of the choroid plexus and blood-CSF barrier. *Frontiers in Neuroscience*, 9.  
<https://www.frontiersin.org/article/10.3389/fnins.2015.00032>
- Lilue, J., Doran, A. G., Fiddes, I. T., Abrudan, M., Armstrong, J., Bennett, R., Chow, W., Collins, J., Collins, S., Czechanski, A., Danecek, P., Diekhans, M., Dolle, D.-D.,

- Dunn, M., Durbin, R., Earl, D., Ferguson-Smith, A., Flicek, P., Flint, J., ... Keane, T. M. (2018). Sixteen diverse laboratory mouse reference genomes define strain-specific haplotypes and novel functional loci. *Nature Genetics*, *50*(11), 1574–1583. <https://doi.org/10.1038/s41588-018-0223-8>
- Lim, Y. C., Li, J., Ni, Y., Liang, Q., Zhang, J., Yeo, G. S. H., Lyu, J., Jin, S., & Ding, C. (2017). A complex association between DNA methylation and gene expression in human placenta at first and third trimesters. *PloS One*, *12*(7), e0181155. <https://doi.org/10.1371/journal.pone.0181155>
- Lin, D., Chen, J., Ehrlich, S., Bustillo, J. R., Perrone-Bizzozero, N., Walton, E., Clark, V. P., Wang, Y.-P., Sui, J., Du, Y., Ho, B. C., Schulz, C. S., Calhoun, V. D., & Liu, J. (2018). Cross-Tissue Exploration of Genetic and Epigenetic Effects on Brain Gray Matter in Schizophrenia. *Schizophrenia Bulletin*, *44*(2), 443–452. <https://doi.org/10.1093/schbul/sbx068>
- Lissemore, J. I., Bhandari, A., Mulsant, B. H., Lenze, E. J., Reynolds, C. F., Karp, J. F., Rajji, T. K., Noda, Y., Zomorodi, R., Sibille, E., Daskalakis, Z. J., & Blumberger, D. M. (2018). Reduced GABAergic cortical inhibition in aging and depression. *Neuropsychopharmacology: Official Publication of the American College of Neuropsychopharmacology*, *43*(11), 2277–2284. <https://doi.org/10.1038/s41386-018-0093-x>
- Liu, B.-C., Liu, F.-Y., Gao, X.-Y., Chen, Y.-L., Meng, Q.-Q., Song, Y.-L., Li, X.-H., & Bao, S.-Q. (2021). Global Transcriptional Analyses of the Wnt-Induced Development of Neural Stem Cells from Human Pluripotent Stem Cells.

*International Journal of Molecular Sciences*, 22(14), 7473.

<https://doi.org/10.3390/ijms22147473>

Liu, N., Sun, H., Li, X., Cao, W., Peng, A., Dong, S., & Yu, Z. (2021). Downregulation of lncRNA KCNQ1OT1 relieves traumatic brain injury induced neurological deficits via promoting “M2” microglia polarization. *Brain Research Bulletin*, 171, 91–102. <https://doi.org/10.1016/j.brainresbull.2021.03.004>

López-Otín, C., Blasco, M. A., Partridge, L., Serrano, M., & Kroemer, G. (2013). The hallmarks of aging. *Cell*, 153(6), 1194–1217.

<https://doi.org/10.1016/j.cell.2013.05.039>

MacInnes, A. W. (2016). The role of the ribosome in the regulation of longevity and lifespan extension. *Wiley Interdisciplinary Reviews. RNA*, 7(2), 198–212.

<https://doi.org/10.1002/wrna.1325>

Magwene, P. M., Willis, J. H., & Kelly, J. K. (2011). The statistics of bulk segregant analysis using next generation sequencing. *PLoS Computational Biology*, 7(11), e1002255. <https://doi.org/10.1371/journal.pcbi.1002255>

Maklakov, A. A., Simpson, S. J., Zajitschek, F., Hall, M. D., Dessmann, J., Clissold, F., Raubenheimer, D., Bonduriansky, R., & Brooks, R. C. (2008). Sex-specific fitness effects of nutrient intake on reproduction and lifespan. *Current Biology: CB*, 18(14), 1062–1066. <https://doi.org/10.1016/j.cub.2008.06.059>

Mardones, M. D., Andaur, G. A., Varas-Godoy, M., Henriquez, J. F., Salech, F., Behrens, M. I., Couve, A., Inestrosa, N. C., & Varela-Nallar, L. (2016). Frizzled-1 receptor

regulates adult hippocampal neurogenesis. *Molecular Brain*, 9, 29.

<https://doi.org/10.1186/s13041-016-0209-3>

Marioni, J. C., & Arendt, D. (2017). How Single-Cell Genomics Is Changing Evolutionary and Developmental Biology. *Annual Review of Cell and Developmental Biology*, 33, 537–553. <https://doi.org/10.1146/annurev-cellbio-100616-060818>

Martin, E., Smeester, L., Bommarito, P. A., Grace, M. R., Boggess, K., Kuban, K., Karagas, M. R., Marsit, C. J., O’Shea, T. M., & Fry, R. C. (2017). Sexual epigenetic dimorphism in the human placenta: Implications for susceptibility during the prenatal period. *Epigenomics*, 9(3), 267–278. <https://doi.org/10.2217/epi-2016-0132>

McCarthy, M. M. (2016a). Sex differences in the developing brain as a source of inherent risk. *Dialogues in Clinical Neuroscience*, 18(4), 361–372.

McCarthy, M. M. (2016b). Sex differences in the developing brain as a source of inherent risk. *Dialogues in Clinical Neuroscience*, 18(4), 361–372.

Meer, M. V., Podolskiy, D. I., Tyshkovskiy, A., & Gladyshev, V. N. (2018). A whole lifespan mouse multi-tissue DNA methylation clock. *ELife*, 7. <https://doi.org/10.7554/eLife.40675>

Melamed, P., Haj, M., Yosefzon, Y., Rudnizky, S., Wijeweera, A., Pnueli, L., & Kaplan, A. (2018). Multifaceted Targeting of the Chromatin Mediates Gonadotropin-Releasing Hormone Effects on Gene Expression in the Gonadotrope. *Frontiers in Endocrinology*, 9. <https://www.frontiersin.org/article/10.3389/fendo.2018.00058>

- Meyer, P. E., Lafitte, F., & Bontempi, G. (2008). minet: A R/Bioconductor package for inferring large transcriptional networks using mutual information. *BMC Bioinformatics*, *9*, 461. <https://doi.org/10.1186/1471-2105-9-461>
- Meyers, C. A., Albitar, M., & Estey, E. (2005). Cognitive impairment, fatigue, and cytokine levels in patients with acute myelogenous leukemia or myelodysplastic syndrome. *Cancer*, *104*(4), 788–793. <https://doi.org/10.1002/cncr.21234>
- Miranda, R. C. (2012). MicroRNAs and Fetal Brain Development: Implications for Ethanol Teratology during the Second Trimester Period of Neurogenesis. *Frontiers in Genetics*, *3*, 77. <https://doi.org/10.3389/fgene.2012.00077>
- Mitchell, S. J., Matute, J. M., Scheibye-Knudsen, M., Fang, E., Aon, M., González-Reyes, J. A., Cortassa, S., Kaushik, S., Gonzalez-Freire, M., Patel, B., Wahl, D., Ali, A., Calvo-Rubio, M., Burón, M. I., Guitierrez, V., Ward, T. M., Palacios, H. H., Cai, H., Frederick, D. W., ... de Cabo, R. (2016). Effects of Sex, Strain, and Energy Intake on Hallmarks of Aging in Mice. *Cell Metabolism*, *23*(6), 1093–1112. <https://doi.org/10.1016/j.cmet.2016.05.027>
- Mohanty, S., Anderson, C. L., & Robinson, J. M. (2010). The expression of caveolin-1 and the distribution of caveolae in the murine placenta and yolk sac: Parallels to the human placenta. *Placenta*, *31*(2), 144–150. <https://doi.org/10.1016/j.placenta.2009.11.007>
- Molnár, Z., & Clowry, G. (2012). Cerebral cortical development in rodents and primates. *Progress in Brain Research*, *195*, 45–70. <https://doi.org/10.1016/B978-0-444-53860-4.00003-9>

- Monstein, H. J., Folkesson, R., & Terenius, L. (1986). Proenkephalin A-like mRNA in human leukemia leukocytes and CNS-tissues. *Life Sciences*, 39(23), 2237–2241. [https://doi.org/10.1016/0024-3205\(86\)90402-9](https://doi.org/10.1016/0024-3205(86)90402-9)
- Moore, L. D., Le, T., & Fan, G. (2013). DNA Methylation and Its Basic Function. *Neuropsychopharmacology*, 38(1), 23–38. <https://doi.org/10.1038/npp.2012.112>
- Mori, H., Funahashi, Y., Yoshino, Y., Kumon, H., Ozaki, Y., Yamazaki, K., Ochi, S., Tachibana, A., Yoshida, T., Shimizu, H., Mori, T., Iga, J., & Ueno, S. (n.d.). Blood CDKN2A Gene Expression in Aging and Neurodegenerative Diseases. *Journal of Alzheimer's Disease*, 82(4), 1737–1744. <https://doi.org/10.3233/JAD-210483>
- Mortazavi, A., Williams, B. A., McCue, K., Schaeffer, L., & Wold, B. (2008). Mapping and quantifying mammalian transcriptomes by RNA-Seq. *Nature Methods*, 5(7), 621–628. <https://doi.org/10.1038/nmeth.1226>
- Mouillet, J.-F., Ouyang, Y., Coyne, C. B., & Sadovsky, Y. (2015). MicroRNAs in placental health and disease. *American Journal of Obstetrics and Gynecology*, 213(4 Suppl), S163-172. <https://doi.org/10.1016/j.ajog.2015.05.057>
- Moussa, M., & Măndoiu, I. I. (2018). Single cell RNA-seq data clustering using TF-IDF based methods. *BMC Genomics*, 19(Suppl 6). <https://doi.org/10.1186/s12864-018-4922-4>
- Müller, H.-G., Chiou, J.-M., Carey, J. R., & Wang, J.-L. (2002). Fertility and Life SpanLate Children Enhance Female Longevity. *The Journals of Gerontology: Series A*, 57(5), B202–B206. <https://doi.org/10.1093/gerona/57.5.B202>

- Muraleva, N. A., Kolosova, N. G., & Stefanova, N. A. (2019). P38 MAPK-dependent alphaB-crystallin phosphorylation in Alzheimer's disease-like pathology in OXYS rats. *Experimental Gerontology*, *119*, 45–52.  
<https://doi.org/10.1016/j.exger.2019.01.017>
- Murphy, C. T. (2010). Aging: MiRacles of longevity? *Current Biology: CB*, *20*(24), R1076-1078. <https://doi.org/10.1016/j.cub.2010.11.018>
- Navarro-Escalante, L., Zhao, C., Shukle, R., & Stuart, J. (2020). BSA-Seq Discovery and Functional Analysis of Candidate Hessian Fly (*Mayetiola destructor*) Avirulence Genes. *Frontiers in Plant Science*, *11*.  
<https://www.frontiersin.org/article/10.3389/fpls.2020.00956>
- Neild, G. H. (2001). Multi-organ renal failure in the elderly. *International Urology and Nephrology*, *32*(4), 559–565. <https://doi.org/10.1023/a:1014474305423>
- Nelissen, E. C. M., van Montfoort, A. P. A., Dumoulin, J. C. M., & Evers, J. L. H. (2011). Epigenetics and the placenta. *Human Reproduction Update*, *17*(3), 397–417. <https://doi.org/10.1093/humupd/dmq052>
- Nelson, M. A., McLaughlin, K. L., Hagen, J. T., Coalson, H. S., Schmidt, C., Kassai, M., Kew, K. A., McClung, J. M., Neuffer, P. D., Brophy, P., Vohra, N. A., Liles, D., Cabot, M. C., & Fisher-Wellman, K. H. (2021). Intrinsic OXPHOS limitations underlie cellular bioenergetics in leukemia. *ELife*, *10*, e63104.  
<https://doi.org/10.7554/eLife.63104>
- Niculescu, M. D., Craciunescu, C. N., & Zeisel, S. H. (2006). Dietary choline deficiency alters global and gene-specific DNA methylation in the developing hippocampus



of mouse fetal brains. *FASEB Journal: Official Publication of the Federation of American Societies for Experimental Biology*, 20(1), 43–49.

<https://doi.org/10.1096/fj.05-4707com>

Nitta, K., Okada, K., Yanai, M., & Takahashi, S. (2013). Aging and chronic kidney disease. *Kidney & Blood Pressure Research*, 38(1), 109–120.

<https://doi.org/10.1159/000355760>

Nugent, B. M., Wright, C. L., Shetty, A. C., Hodes, G. E., Lenz, K. M., Mahurkar, A., Russo, S. J., Devine, S. E., & McCarthy, M. M. (2015). Brain feminization requires active repression of masculinization via DNA methylation. *Nature Neuroscience*, 18(5), 690–697.

<https://doi.org/10.1038/nn.3988>

Numata, S., Ye, T., Hyde, T. M., Guitart-Navarro, X., Tao, R., Wininger, M., Colantuoni, C., Weinberger, D. R., Kleinman, J. E., & Lipska, B. K. (2012). DNA Methylation Signatures in Development and Aging of the Human Prefrontal Cortex. *American Journal of Human Genetics*, 90(2), 260–272.

<https://doi.org/10.1016/j.ajhg.2011.12.020>

Nwanaji-Enwerem, J. C., Colicino, E., Gao, X., Wang, C., Vokonas, P., Boyer, E. W., Baccarelli, A. A., & Schwartz, J. (2021). Associations of Plasma Folate and Vitamin B6 With Blood DNA Methylation Age: An Analysis of One-Carbon Metabolites in the VA Normative Aging Study. *The Journals of Gerontology. Series A, Biological Sciences and Medical Sciences*, 76(5), 760–769.

<https://doi.org/10.1093/gerona/glaa257>

- Ooi, L., & Wood, I. C. (2007). Chromatin crosstalk in development and disease: Lessons from REST. *Nature Reviews. Genetics*, 8(7), 544–554.  
<https://doi.org/10.1038/nrg2100>
- Ori, A., Toyama, B. H., Harris, M. S., Bock, T., Iskar, M., Bork, P., Ingolia, N. T., Hetzer, M. W., & Beck, M. (2015). Integrated Transcriptome and Proteome Analyses Reveal Organ-Specific Proteome Deterioration in Old Rats. *Cell Systems*, 1(3), 224–237. <https://doi.org/10.1016/j.cels.2015.08.012>
- Ostrovsky, A. N., Lidgard, S., Gordon, D. P., Schwaha, T., Genikhovich, G., & Ereskovsky, A. V. (2016). Matrotrophy and placentation in invertebrates: A new paradigm. *Biological Reviews of the Cambridge Philosophical Society*, 91(3), 673–711. <https://doi.org/10.1111/brv.12189>
- Palmer, G., Lipsky, B. P., Smithgall, M. D., Meininger, D., Siu, S., Talabot-Ayer, D., Gabay, C., & Smith, D. E. (2008). The IL-1 receptor accessory protein (AcP) is required for IL-33 signaling and soluble AcP enhances the ability of soluble ST2 to inhibit IL-33. *Cytokine*, 42(3), 358–364.  
<https://doi.org/10.1016/j.cyto.2008.03.008>
- Pandolfi, E. C., Tonsfeldt, K. J., Hoffmann, H. M., & Mellon, P. L. (2019). Deletion of the Homeodomain Protein Six6 From GnRH Neurons Decreases GnRH Gene Expression, Resulting in Infertility. *Endocrinology*, 160(9), 2151–2164.  
<https://doi.org/10.1210/en.2019-00113>
- Park, D. S., Cohen, A. W., Frank, P. G., Razani, B., Lee, H., Williams, T. M., Chandra, M., Shirani, J., De Souza, A. P., Tang, B., Jelicks, L. A., Factor, S. M., Weiss, L.

- M., Tanowitz, H. B., & Lisanti, M. P. (2003). Caveolin-1 null (-/-) mice show dramatic reductions in life span. *Biochemistry*, *42*(51), 15124–15131.  
<https://doi.org/10.1021/bi0356348>
- Park, D. S., Lee, H., Frank, P. G., Razani, B., Nguyen, A. V., Parlow, A. F., Russell, R. G., Hult, J., Pestell, R. G., & Lisanti, M. P. (2002). Caveolin-1-deficient Mice Show Accelerated Mammary Gland Development During Pregnancy, Premature Lactation, and Hyperactivation of the Jak-2/STAT5a Signaling Cascade. *Molecular Biology of the Cell*, *13*(10), 3416–3430.  
<https://doi.org/10.1091/mbc.02-05-0071>
- Park, S. Y., Kang, J. Y., Lee, T., Nam, D., Jeon, C.-J., & Kim, J. B. (2020). SPON1 Can Reduce Amyloid Beta and Reverse Cognitive Impairment and Memory Dysfunction in Alzheimer’s Disease Mouse Model. *Cells*, *9*(5), E1275.  
<https://doi.org/10.3390/cells9051275>
- Pavanello, S., Campisi, M., Fabozzo, A., Cibir, G., Tarzia, V., Toscano, G., & Gerosa, G. (2020). The biological age of the heart is consistently younger than chronological age. *Scientific Reports*, *10*(1), 10752. <https://doi.org/10.1038/s41598-020-67622-1>
- Pembroke, W. G., Hartl, C. L., & Geschwind, D. H. (2021). Evolutionary conservation and divergence of the human brain transcriptome. *Genome Biology*, *22*(1), 52.  
<https://doi.org/10.1186/s13059-020-02257-z>
- Penkler, M., Hanson, M., Biesma, R., & Müller, R. (2019). DOHaD in science and society: Emergent opportunities and novel responsibilities. *Journal of*

*Developmental Origins of Health and Disease*, 10(3), 268–273.

<https://doi.org/10.1017/S2040174418000892>

Petanjek, Z., & Kostović, I. (2012). Epigenetic regulation of fetal brain development and neurocognitive outcome. *Proceedings of the National Academy of Sciences of the United States of America*, 109(28), 11062–11063.

<https://doi.org/10.1073/pnas.1208085109>

Peters, R. (2006). Ageing and the brain. *Postgraduate Medical Journal*, 82(964), 84–88.

<https://doi.org/10.1136/pgmj.2005.036665>

Pidsley, R., Viana, J., Hannon, E., Spiers, H., Troakes, C., Al-Saraj, S., Mechawar, N., Turecki, G., Schalkwyk, L. C., Bray, N. J., & Mill, J. (2014). Methylomic profiling of human brain tissue supports a neurodevelopmental origin for schizophrenia. *Genome Biology*, 15(10), 483. <https://doi.org/10.1186/s13059-014-0483-2>

Plass, M., Solana, J., Wolf, F. A., Ayoub, S., Misios, A., Glažar, P., Obermayer, B., Theis, F. J., Kocks, C., & Rajewsky, N. (2018). Cell type atlas and lineage tree of a whole complex animal by single-cell transcriptomics. *Science (New York, N.Y.)*, 360(6391). <https://doi.org/10.1126/science.aaq1723>

Premoli, A., Paschetta, E., Hvalryg, M., Spandre, M., Bo, S., & Durazzo, M. (2009).

Characteristics of liver diseases in the elderly: A review. *Minerva Gastroenterologica E Dietologica*, 55(1), 71–78.

Premratanachai, A., Suwanjang, W., Govitrapong, P., Chetsawang, J., & Chetsawang, B. (2020). Melatonin prevents calcineurin-activated the nuclear translocation of

- nuclear factor of activated T-cells in human neuroblastoma SH-SY5Y cells undergoing hydrogen peroxide-induced cell death. *Journal of Chemical Neuroanatomy*, *106*, 101793. <https://doi.org/10.1016/j.jchemneu.2020.101793>
- Quinlan, A. R., & Hall, I. M. (2010). BEDTools: A flexible suite of utilities for comparing genomic features. *Bioinformatics*, *26*(6), 841–842. <https://doi.org/10.1093/bioinformatics/btq033>
- Rachdaoui, N., & Sarkar, D. K. (2014). Transgenerational epigenetics and brain disorders. *International Review of Neurobiology*, *115*, 51–73. <https://doi.org/10.1016/B978-0-12-801311-3.00002-0>
- Radovic, M., Ghalwash, M., Filipovic, N., & Obradovic, Z. (2017). Minimum redundancy maximum relevance feature selection approach for temporal gene expression data. *BMC Bioinformatics*, *18*. <https://doi.org/10.1186/s12859-016-1423-9>
- Räikkönen, K., Pesonen, A.-K., Roseboom, T. J., & Eriksson, J. G. (2012). Early determinants of mental health. *Best Practice & Research. Clinical Endocrinology & Metabolism*, *26*(5), 599–611. <https://doi.org/10.1016/j.beem.2012.03.001>
- Rallis, A., Navarro, J. A., Rass, M., Hu, A., Birman, S., Schneuwly, S., & Thérond, P. P. (2020). Hedgehog Signaling Modulates Glial Proteostasis and Lifespan. *Cell Reports*, *30*(8), 2627-2643.e5. <https://doi.org/10.1016/j.celrep.2020.02.006>
- Rath, P. C., & Kanungo, M. S. (1989). Methylation of repetitive DNA sequences in the brain during aging of the rat. *FEBS Letters*, *244*(1), 193–198. [https://doi.org/10.1016/0014-5793\(89\)81191-3](https://doi.org/10.1016/0014-5793(89)81191-3)

- Ratnu, V. S., Emami, M. R., & Bredy, T. W. (2017). Genetic and epigenetic factors underlying sex differences in the regulation of gene expression in the brain. *Journal of Neuroscience Research*, 95(1–2), 301–310.  
<https://doi.org/10.1002/jnr.23886>
- Razani, B., Engelman, J. A., Wang, X. B., Schubert, W., Zhang, X. L., Marks, C. B., Macaluso, F., Russell, R. G., Li, M., Pestell, R. G., Di Vizio, D., Hou, H., Kneitz, B., Lagaud, G., Christ, G. J., Edelman, W., & Lisanti, M. P. (2001). Caveolin-1 null mice are viable but show evidence of hyperproliferative and vascular abnormalities. *The Journal of Biological Chemistry*, 276(41), 38121–38138.  
<https://doi.org/10.1074/jbc.M105408200>
- Renaud, L., Picher-Martel, V., Codron, P., & Julien, J.-P. (2019). Key role of UBQLN2 in pathogenesis of amyotrophic lateral sclerosis and frontotemporal dementia. *Acta Neuropathologica Communications*, 7(1), 103.  
<https://doi.org/10.1186/s40478-019-0758-7>
- Reyahi, A., Nik, A. M., Ghiami, M., Gritli-Linde, A., Pontén, F., Johansson, B. R., & Carlsson, P. (2015). Foxf2 Is Required for Brain Pericyte Differentiation and Development and Maintenance of the Blood-Brain Barrier. *Developmental Cell*, 34(1), 19–32. <https://doi.org/10.1016/j.devcel.2015.05.008>
- Riedmiller, M. (1994). *Advanced Supervised Learning in Multi-layer Perceptrons—From Backpropagation to Adaptive Learning Algorithms*.

- Ristow, M., & Schmeisser, S. (2011). Extending life span by increasing oxidative stress. *Free Radical Biology & Medicine*, *51*(2), 327–336.  
<https://doi.org/10.1016/j.freeradbiomed.2011.05.010>
- Roberts, R. M., Green, J. A., & Schulz, L. C. (2016). The Evolution of the Placenta. *Reproduction (Cambridge, England)*, *152*(5), R179–R189.  
<https://doi.org/10.1530/REP-16-0325>
- Rogalski, E. J., Gefen, T., Shi, J., Samimi, M., Bigio, E., Weintraub, S., Geula, C., & Mesulam, M.-M. (2013). Youthful Memory Capacity in Old Brains: Anatomic and Genetic Clues from the Northwestern SuperAging Project. *Journal of Cognitive Neuroscience*, *25*(1), 29–36. [https://doi.org/10.1162/jocn\\_a\\_00300](https://doi.org/10.1162/jocn_a_00300)
- Rojas, M., Mora, A. L., Kapetanaki, M., Weathington, N., Gladwin, M., & Eickelberg, O. (2015). Aging and Lung Disease. Clinical Impact and Cellular and Molecular Pathways. *Annals of the American Thoracic Society*, *12*(12), S222–S227.  
<https://doi.org/10.1513/AnnalsATS.201508-484PL>
- Rosenfeld, C. S. (2015). Sex-Specific Placental Responses in Fetal Development. *Endocrinology*, *156*(10), 3422–3434. <https://doi.org/10.1210/en.2015-1227>
- Rosenfeld, C. S. (2020). Placental serotonin signaling, pregnancy outcomes, and regulation of fetal brain development†. *Biology of Reproduction*, *102*(3), 532–538. <https://doi.org/10.1093/biolre/ioz204>
- Rothwell, E. S., Workman, K. P., Wang, D., & Lacreuse, A. (2022). Sex differences in cognitive aging: A 4-year longitudinal study in marmosets. *Neurobiology of Aging*, *109*, 88–99. <https://doi.org/10.1016/j.neurobiolaging.2021.09.015>

- Rowe, W. P., Hartley, J. W., & Bremner, T. (1972). Genetic mapping of a murine leukemia virus-inducing locus of AKR mice. *Science (New York, N.Y.)*, *178*(4063), 860–862. <https://doi.org/10.1126/science.178.4063.860>
- Sachkova, M., & Burkhardt, P. (2019). Exciting times to study the identity and evolution of cell types. *Development*, *146*(18). <https://doi.org/10.1242/dev.178996>
- Salehi, F., Scheithauer, B. W., Sharma, S., Kovacs, K., Lloyd, R. V., Cusimano, M. D., & Munoz, D. G. (2013). Immunohistochemical expression of PTTG in brain tumors. *Anticancer Research*, *33*(1), 119–122.
- Sarnowski, C., Ghanbari, M., Bis, J. C., Logue, M., Fornage, M., Mishra, A., Ahmad, S., Beiser, A. S., Boerwinkle, E., Bouteloup, V., Chouraki, V., Cupples, L. A., Damotte, V., DeCarli, C. S., DeStefano, A. L., Djoussé, L., Fohner, A. E., Franz, C. E., Kautz, T. F., ... Seshadri, S. (2022). Meta-analysis of genome-wide association studies identifies ancestry-specific associations underlying circulating total tau levels. *Communications Biology*, *5*(1), 336. <https://doi.org/10.1038/s42003-022-03287-y>
- Sasaki, K., & Norwitz, E. R. (2011). Gonadotropin-releasing hormone/gonadotropin-releasing hormone receptor signaling in the placenta. *Current Opinion in Endocrinology, Diabetes, and Obesity*, *18*(6), 401–408. <https://doi.org/10.1097/MED.0b013e32834cd3b0>
- Schachtschneider, K. M., Schook, L. B., Meudt, J. J., Shanmuganayagam, D., Zoller, J. A., Haghani, A., Li, C. Z., Zhang, J., Yang, A., Raj, K., & Horvath, S. (2020).



Epigenetic clock and DNA methylation analysis of porcine models of aging and obesity. *BioRxiv*, 2020.09.29.319509. <https://doi.org/10.1101/2020.09.29.319509>

Schaum, N., Lehallier, B., Hahn, O., Pálovics, R., Hosseinzadeh, S., Lee, S. E., Sit, R., Lee, D. P., Losada, P. M., Zardeneta, M. E., Fehlmann, T., Webber, J. T., McGeever, A., Calcuttawala, K., Zhang, H., Berdnik, D., Mathur, V., Tan, W., Zee, A., ... Wyss-Coray, T. (2020). Ageing hallmarks exhibit organ-specific temporal signatures. *Nature*, 583(7817), 596–602. <https://doi.org/10.1038/s41586-020-2499-y>

Schaum, N., Lehallier, B., Hahn, O., Pálovics, R., Hosseinzadeh, S., Lee, S. E., Sit, R., Lee, D. P., Losada, P. M., Zardeneta, M. E., Fehlmann, T., Webber, J. T., McGeever, A., Calcuttawala, K., Zhang, H., Berdnik, D., Mathur, V., Tan, W., Zee, A., ... Wyss-Coray, T. (2020). Ageing hallmarks exhibit organ-specific temporal signatures. *Nature*, 583(7817), 596–602. <https://doi.org/10.1038/s41586-020-2499-y>

Schlotz, W., & Phillips, D. I. W. (2009). Fetal origins of mental health: Evidence and mechanisms. *Brain, Behavior, and Immunity*, 23(7), 905–916. <https://doi.org/10.1016/j.bbi.2009.02.001>

Schroeder, D. I., Jayashankar, K., Douglas, K. C., Thirkill, T. L., York, D., Dickinson, P. J., Williams, L. E., Samollow, P. B., Ross, P. J., Bannasch, D. L., Douglas, G. C., & LaSalle, J. M. (2015). Early Developmental and Evolutionary Origins of Gene Body DNA Methylation Patterns in Mammalian Placentas. *PLoS Genetics*, 11(8), e1005442. <https://doi.org/10.1371/journal.pgen.1005442>

- Sebé-Pedrós, A., Chomsky, E., Pang, K., Lara-Astiaso, D., Gaiti, F., Mukamel, Z., Amit, I., Hejnal, A., Degnan, B. M., & Tanay, A. (2018). Early metazoan cell type diversity and the evolution of multicellular gene regulation. *Nature Ecology & Evolution*, *2*(7), 1176–1188. <https://doi.org/10.1038/s41559-018-0575-6>
- Shah, R., Courtiol, E., Castellanos, F. X., & Teixeira, C. M. (2018). Abnormal Serotonin Levels During Perinatal Development Lead to Behavioral Deficits in Adulthood. *Frontiers in Behavioral Neuroscience*, *12*, 114. <https://doi.org/10.3389/fnbeh.2018.00114>
- Shen, J., & Tower, J. (2009). Programmed cell death and apoptosis in aging and life span regulation. *Discovery Medicine*, *8*(43), 223–226.
- Sierra, M. I., Fernández, A. F., & Fraga, M. F. (2015). Epigenetics of Aging. *Current Genomics*, *16*(6), 435–440. <https://doi.org/10.2174/1389202916666150817203459>
- Singh, S. K., Kagalwala, M. N., Parker-Thornburg, J., Adams, H., & Majumder, S. (2008). REST maintains self-renewal and pluripotency of embryonic stem cells. *Nature*, *453*(7192), 223–227. <https://doi.org/10.1038/nature06863>
- Soares, M. J., Varberg, K. M., & Iqbal, K. (2018). Hemochorial placentation: Development, function, and adaptations. *Biology of Reproduction*, *99*(1), 196–211. <https://doi.org/10.1093/biolre/i0y049>
- Somel, M., Franz, H., Yan, Z., Lorenc, A., Guo, S., Giger, T., Kelso, J., Nickel, B., Dannemann, M., Bahn, S., Webster, M. J., Weickert, C. S., Lachmann, M., Pääbo, S., & Khaitovich, P. (2009). Transcriptional neoteny in the human brain.

*Proceedings of the National Academy of Sciences*, 106(14), 5743–5748.

<https://doi.org/10.1073/pnas.0900544106>

Song, Z., Li, B., Li, M.-Y., Luo, J.-M., Hong, Y.-Q., He, Y.-Y., Chen, S.-T., Yang, Z.-S., Liang, C., & Yang, Z.-M. (2022). Caveolin-1 Regulation and Function in Mouse Uterus during Early Pregnancy and under Human In Vitro Decidualization.

*International Journal of Molecular Sciences*, 23(7), 3699.

<https://doi.org/10.3390/ijms23073699>

Spiers, H., Hannon, E., Schalkwyk, L. C., Smith, R., Wong, C. C. Y., O'Donovan, M. C., Bray, N. J., & Mill, J. (2015). Methyloomic trajectories across human fetal brain development. *Genome Research*, 25(3), 338–352.

<https://doi.org/10.1101/gr.180273.114>

Sriskantheadavan, S., Jeyaraju, D. V., Chung, T. E., Prabha, S., Xu, W., Skrtic, M., Jhas, B., Hurren, R., Gronda, M., Wang, X., Jitkova, Y., Sukhai, M. A., Lin, F.-H., Maclean, N., Laister, R., Goard, C. A., Mullen, P. J., Xie, S., Penn, L. Z., ... Schimmer, A. D. (2015). AML cells have low spare reserve capacity in their respiratory chain that renders them susceptible to oxidative metabolic stress.

*Blood*, 125(13), 2120–2130. <https://doi.org/10.1182/blood-2014-08-594408>

Steenman, M., & Lande, G. (2017). Cardiac aging and heart disease in humans.

*Biophysical Reviews*, 9(2), 131–137. <https://doi.org/10.1007/s12551-017-0255-9>

Stefanatos, R., & Sanz, A. (2018). The role of mitochondrial ROS in the aging brain.

*FEBS Letters*, 592(5), 743–758. <https://doi.org/10.1002/1873-3468.12902>

- Steuer, R., Kurths, J., Daub, C. O., Weise, J., & Selbig, J. (2002a). The mutual information: Detecting and evaluating dependencies between variables. *Bioinformatics (Oxford, England)*, *18 Suppl 2*, S231-240. [https://doi.org/10.1093/bioinformatics/18.suppl\\_2.s231](https://doi.org/10.1093/bioinformatics/18.suppl_2.s231)
- Steuer, R., Kurths, J., Daub, C. O., Weise, J., & Selbig, J. (2002b). The mutual information: Detecting and evaluating dependencies between variables. *Bioinformatics (Oxford, England)*, *18 Suppl 2*, S231-240. [https://doi.org/10.1093/bioinformatics/18.suppl\\_2.s231](https://doi.org/10.1093/bioinformatics/18.suppl_2.s231)
- Strawn, M., Moraes, J. G. N., Safranski, T. J., & Behura, S. K. (2021). Sexually Dimorphic Transcriptomic Changes of Developing Fetal Brain Reveal Signaling Pathways and Marker Genes of Brain Cells in Domestic Pigs. *Cells*, *10(9)*, 2439. <https://doi.org/10.3390/cells10092439>
- Stuart, T., Srivastava, A., Lareau, C., & Satija, R. (2020). Multimodal single-cell chromatin analysis with Signac. *BioRxiv*, 2020.11.09.373613. <https://doi.org/10.1101/2020.11.09.373613>
- Stubbs, T. M., Bonder, M. J., Stark, A.-K., Krueger, F., BI Ageing Clock Team, von Meyenn, F., Stegle, O., & Reik, W. (2017a). Multi-tissue DNA methylation age predictor in mouse. *Genome Biology*, *18(1)*, 68. <https://doi.org/10.1186/s13059-017-1203-5>
- Stubbs, T. M., Bonder, M. J., Stark, A.-K., Krueger, F., BI Ageing Clock Team, von Meyenn, F., Stegle, O., & Reik, W. (2017b). Multi-tissue DNA methylation age

predictor in mouse. *Genome Biology*, 18(1), 68. <https://doi.org/10.1186/s13059-017-1203-5>

- Suganuma, K., Miwa, H., Imai, N., Shikami, M., Gotou, M., Goto, M., Mizuno, S., Takahashi, M., Yamamoto, H., Hiramatsu, A., Wakabayashi, M., Watarai, M., Hanamura, I., Imamura, A., Mihara, H., & Nitta, M. (2010). Energy metabolism of leukemia cells: Glycolysis *versus* oxidative phosphorylation. *Leukemia & Lymphoma*, 51(11), 2112–2119. <https://doi.org/10.3109/10428194.2010.512966>
- Takayasu, Y., Takeuchi, K., Kumari, R., Bennett, M. V. L., Zukin, R. S., & Francesconi, A. (2010). Caveolin-1 knockout mice exhibit impaired induction of mGluR-dependent long-term depression at CA3-CA1 synapses. *Proceedings of the National Academy of Sciences*, 107(50), 21778–21783. <https://doi.org/10.1073/pnas.1015553107>
- Tamnes, C. K., Walhovd, K. B., Dale, A. M., Østby, Y., Grydeland, H., Richardson, G., Westlye, L. T., Roddey, J. C., Hagler, D. J., Due-Tønnessen, P., Holland, D., Fjell, A. M., & Alzheimer’s Disease Neuroimaging Initiative. (2013). Brain development and aging: Overlapping and unique patterns of change. *NeuroImage*, 68, 63–74. <https://doi.org/10.1016/j.neuroimage.2012.11.039>
- Tang, W., Huang, L., Bu, S., Zhang, X., & Wu, W. (2018). Estimation of QTL heritability based on pooled sequencing data. *Bioinformatics (Oxford, England)*, 34(6), 978–984. <https://doi.org/10.1093/bioinformatics/btx703>
- Tarashansky, A. J., Musser, J. M., Khariton, M., Li, P., Arendt, D., Quake, S. R., & Wang, B. (2020). Mapping single-cell atlases throughout Metazoa unravels cell

type evolution. *BioRxiv*, 2020.09.28.317784.

<https://doi.org/10.1101/2020.09.28.317784>

Tekola-Ayele, F., Workalemahu, T., Gorf, G., Shrestha, D., Tycko, B., Wapner, R., Zhang, C., & Louis, G. M. B. (2019a). Sex differences in the associations of placental epigenetic aging with fetal growth. *Aging*, *11*(15), 5412–5432.

<https://doi.org/10.18632/aging.102124>

Tekola-Ayele, F., Workalemahu, T., Gorf, G., Shrestha, D., Tycko, B., Wapner, R., Zhang, C., & Louis, G. M. B. (2019b). Sex differences in the associations of placental epigenetic aging with fetal growth. *Aging*, *11*(15), 5412–5432.

<https://doi.org/10.18632/aging.102124>

Templeman, N. M., & Murphy, C. T. (2018). Regulation of reproduction and longevity by nutrient-sensing pathways. *The Journal of Cell Biology*, *217*(1), 93–106.

<https://doi.org/10.1083/jcb.201707168>

Teschendorff, A. E., Zhu, T., Breeze, C. E., & Beck, S. (2020). EPISCORE: Cell type deconvolution of bulk tissue DNA methylomes from single-cell RNA-Seq data. *Genome Biology*, *21*(1), 221. <https://doi.org/10.1186/s13059-020-02126-9>

Thibaut, F. (2016a). The role of sex and gender in neuropsychiatric disorders. *Dialogues in Clinical Neuroscience*, *18*(4), 351–352.

Thibaut, F. (2016b). The role of sex and gender in neuropsychiatric disorders. *Dialogues in Clinical Neuroscience*, *18*(4), 351–352.

Tiku, V., & Antebi, A. (2018). Nucleolar Function in Lifespan Regulation. *Trends in Cell Biology*, *28*(8), 662–672. <https://doi.org/10.1016/j.tcb.2018.03.007>

- Tognini, P., Napoli, D., & Pizzorusso, T. (2015). Dynamic DNA methylation in the brain: A new epigenetic mark for experience-dependent plasticity. *Frontiers in Cellular Neuroscience*, 9, 331. <https://doi.org/10.3389/fncel.2015.00331>
- Tsuneura, Y., Sawahata, M., Itoh, N., Miyajima, R., Mori, D., Kohno, T., Hattori, M., Sobue, A., Nagai, T., Mizoguchi, H., Nabeshima, T., Ozaki, N., & Yamada, K. (2021). Analysis of Reelin signaling and neurodevelopmental trajectory in primary cultured cortical neurons with RELN deletion identified in schizophrenia. *Neurochemistry International*, 144, 104954. <https://doi.org/10.1016/j.neuint.2020.104954>
- Turlejski, K. (1996). Evolutionary ancient roles of serotonin: Long-lasting regulation of activity and development. *Acta Neurobiologiae Experimentalis*, 56(2), 619–636.
- Tylee, D. S., Kawaguchi, D. M., & Glatt, S. J. (2013). On the outside, looking in: A review and evaluation of the comparability of blood and brain “-omes.” *American Journal of Medical Genetics Part B: Neuropsychiatric Genetics*, 162(7), 595–603. <https://doi.org/10.1002/ajmg.b.32150>
- Ucar, D., Márquez, E. J., Chung, C.-H., Marches, R., Rossi, R. J., Uyar, A., Wu, T.-C., George, J., Stitzel, M. L., Palucka, A. K., Kuchel, G. A., & Banchereau, J. (2017). The chromatin accessibility signature of human immune aging stems from CD8+ T cells. *The Journal of Experimental Medicine*, 214(10), 3123–3144. <https://doi.org/10.1084/jem.20170416>
- Vaiserman, A. (Ed.). (2019a). *Early Life Origins of Ageing and Longevity*. Springer International Publishing. <https://doi.org/10.1007/978-3-030-24958-8>

- Vaiserman, A. (Ed.). (2019b). *Early Life Origins of Ageing and Longevity* (Vol. 9). Springer International Publishing. <https://doi.org/10.1007/978-3-030-24958-8>
- Van der Auwera, G. A., Carneiro, M. O., Hartl, C., Poplin, R., Del Angel, G., Levy-Moonshine, A., Jordan, T., Shakir, K., Roazen, D., Thibault, J., Banks, E., Garimella, K. V., Altshuler, D., Gabriel, S., & DePristo, M. A. (2013). From FastQ data to high confidence variant calls: The Genome Analysis Toolkit best practices pipeline. *Current Protocols in Bioinformatics*, *43*, 11.10.1-11.10.33. <https://doi.org/10.1002/0471250953.bi1110s43>
- van Helmond, Z. K., Miners, J. S., Bednall, E., Chalmers, K. A., Zhang, Y., Wilcock, G. K., Love, S., & Kehoe, P. G. (2007). Caveolin-1 and -2 and their relationship to cerebral amyloid angiopathy in Alzheimer's disease. *Neuropathology and Applied Neurobiology*, *33*(3), 317–327. <https://doi.org/10.1111/j.1365-2990.2006.00815.x>
- Vandamme, T. (2014). Use of rodents as models of human diseases. *Journal of Pharmacy and Bioallied Sciences*, *6*(1), 2. <https://doi.org/10.4103/0975-7406.124301>
- Vanni, S., Zattoni, M., Moda, F., Giaccone, G., Tagliavini, F., Haïk, S., Deslys, J.-P., Zanusso, G., Ironside, J. W., Carmona, M., Ferrer, I., Kovacs, G. G., & Legname, G. (2018). Hemoglobin mRNA Changes in the Frontal Cortex of Patients with Neurodegenerative Diseases. *Frontiers in Neuroscience*, *12*, 8. <https://doi.org/10.3389/fnins.2018.00008>



- Velasquez, J. C., Goeden, N., & Bonnin, A. (2013). Placental serotonin: Implications for the developmental effects of SSRIs and maternal depression. *Frontiers in Cellular Neuroscience*, 7. <https://doi.org/10.3389/fncel.2013.00047>
- Vidal-Pineiro, D., Wang, Y., Krogsrud, S. K., Amlien, I. K., Baaré, W. F., Bartres-Faz, D., Bertram, L., Brandmaier, A. M., Drevon, C. A., Düzel, S., Ebmeier, K., Henson, R. N., Junqué, C., Kievit, R. A., Kühn, S., Leonardsen, E., Lindenberger, U., Madsen, K. S., Magnussen, F., ... Fjell, A. (2021). Individual variations in 'brain age' relate to early-life factors more than to longitudinal brain change. *eLife*, 10, e69995. <https://doi.org/10.7554/eLife.69995>
- von Bernhardt, R. (2007). Glial cell dysregulation: A new perspective on Alzheimer disease. *Neurotoxicity Research*, 12(4), 215–232. <https://doi.org/10.1007/BF03033906>
- Von Bernhardt, R. (2007). Glial cell dysregulation: A new perspective on Alzheimer disease. *Neurotoxicity Research*, 12(4), 215–232. <https://doi.org/10.1007/BF03033906>
- Wadhwa, P. D. (2005). Psychoneuroendocrine processes in human pregnancy influence fetal development and health. *Psychoneuroendocrinology*, 30(8), 724–743. <https://doi.org/10.1016/j.psyneuen.2005.02.004>
- Wadhwa, P. D., Buss, C., Entringer, S., & Swanson, J. M. (2009). Developmental Origins of Health and Disease: Brief History of the Approach and Current Focus on Epigenetic Mechanisms. *Seminars in Reproductive Medicine*, 27(5), 358–368. <https://doi.org/10.1055/s-0029-1237424>

- Walton, E., Hass, J., Liu, J., Roffman, J. L., Bernardoni, F., Roessner, V., Kirsch, M., Schackert, G., Calhoun, V., & Ehrlich, S. (2016). Correspondence of DNA Methylation Between Blood and Brain Tissue and Its Application to Schizophrenia Research. *Schizophrenia Bulletin*, *42*(2), 406–414. <https://doi.org/10.1093/schbul/sbv074>
- Wang, F., Cao, Y., Ma, L., Pei, H., Rausch, W. D., & Li, H. (2018). Dysfunction of Cerebrovascular Endothelial Cells: Prelude to Vascular Dementia. *Frontiers in Aging Neuroscience*, *10*. <https://www.frontiersin.org/article/10.3389/fnagi.2018.00376>
- Wang, L., Chadwick, W., Park, S.-S., Zhou, Y., Silver, N., Martin, B., & Maudsley, S. (2010). Gonadotropin-releasing hormone receptor system: Modulatory role in aging and neurodegeneration. *CNS & Neurological Disorders Drug Targets*, *9*(5), 651–660. <https://doi.org/10.2174/187152710793361559>
- Wei, X., Zhang, L., & Zeng, Y. (2020). DNA methylation in Alzheimer’s disease: In brain and peripheral blood. *Mechanisms of Ageing and Development*, *191*, 111319. <https://doi.org/10.1016/j.mad.2020.111319>
- Weinstock, M. (2005). The potential influence of maternal stress hormones on development and mental health of the offspring. *Brain, Behavior, and Immunity*, *19*(4), 296–308. <https://doi.org/10.1016/j.bbi.2004.09.006>
- Wei, A. L., Meijer, M., Budeus, B., Pauper, M., Hakobjan, M., Groothuismink, J., Shi, Y., Neveling, K., Buitelaar, J. K., Hoogman, M., Franke, B., & Klein, M. (2021). DNA methylation associated with persistent ADHD suggests TARBP1 as novel

candidate. *Neuropharmacology*, 184, 108370.

<https://doi.org/10.1016/j.neuropharm.2020.108370>

Williams, A. M., van Wijngaarden, E., Seplaki, C. L., Heckler, C., Weber, M. T., Barr, P. M., Zent, C. S., & Janelins, M. C. (2020). Cognitive Function in Patients with Chronic Lymphocytic Leukemia: A Cross-Sectional Study Examining Effects of Disease and Treatment. *Leukemia & Lymphoma*, 61(7), 1627–1635.

<https://doi.org/10.1080/10428194.2020.1728748>

Workman, A. D., Charvet, C. J., Clancy, B., Darlington, R. B., & Finlay, B. L. (2013). Modeling transformations of neurodevelopmental sequences across mammalian species. *The Journal of Neuroscience: The Official Journal of the Society for Neuroscience*, 33(17), 7368–7383. <https://doi.org/10.1523/JNEUROSCI.5746-12.2013>

World, N. R. C. (US) P. on a R. A. and N. D. for an A. (2001). Our Aging World. In *Preparing for an Aging World: The Case for Cross-National Research*. National Academies Press (US). <https://www.ncbi.nlm.nih.gov/books/NBK98375/>

Wu, C., Gong, Q., Xu, X., Fang, P., Wang, C., Yu, J.-Y., Wang, X.-X., Fang, S.-H., Chen, W.-J., Lou, H.-F., Liu, Y.-H., Wang, L., Liu, Y.-J., Chen, W., & Wang, X.-D. (2022a). Disrupted presynaptic nectin1-based neuronal adhesion in the entorhinal-hippocampal circuit contributes to early-life stress-induced memory deficits. *Translational Psychiatry*, 12(1), 141. <https://doi.org/10.1038/s41398-022-01908-y>

- Wu, C., Gong, Q., Xu, X., Fang, P., Wang, C., Yu, J.-Y., Wang, X.-X., Fang, S.-H., Chen, W.-J., Lou, H.-F., Liu, Y.-H., Wang, L., Liu, Y.-J., Chen, W., & Wang, X.-D. (2022b). Disrupted presynaptic nectin1-based neuronal adhesion in the entorhinal-hippocampal circuit contributes to early-life stress-induced memory deficits. *Translational Psychiatry*, *12*(1), 141. <https://doi.org/10.1038/s41398-022-01908-y>
- Wu, F., Zhang, C., Cai, J., Yang, F., Liang, T., Yan, X., Wang, H., Wang, W., Chen, J., & Jiang, T. (2017). Upregulation of long noncoding RNA HOXA-AS3 promotes tumor progression and predicts poor prognosis in glioma. *Oncotarget*, *8*(32), 53110–53123. <https://doi.org/10.18632/oncotarget.18162>
- Wu, W.-L., Hsiao, E. Y., Yan, Z., Mazmanian, S. K., & Patterson, P. H. (2017). The placental interleukin-6 signaling controls fetal brain development and behavior. *Brain, Behavior, and Immunity*, *62*, 11–23. <https://doi.org/10.1016/j.bbi.2016.11.007>
- Wyller, S. C., Lord, C. C., Lee, S., Elmquist, J. K., & Liu, C. (2017). Serotonergic Control of Metabolic Homeostasis. *Frontiers in Cellular Neuroscience*, *11*, 277. <https://doi.org/10.3389/fncel.2017.00277>
- Xia, Y., Won, S., Du, X., Lin, P., Ross, C., La Vine, D., Wiltshire, S., Leiva, G., Vidal, S. M., Whittle, B., Goodnow, C. C., Koziol, J., Moresco, E. M. Y., & Beutler, B. (2010). Bulk segregation mapping of mutations in closely related strains of mice. *Genetics*, *186*(4), 1139–1146. <https://doi.org/10.1534/genetics.110.121160>

- Yabut, J. M., Crane, J. D., Green, A. E., Keating, D. J., Khan, W. I., & Steinberg, G. R. (2019). Emerging Roles for Serotonin in Regulating Metabolism: New Implications for an Ancient Molecule. *Endocrine Reviews*, *40*(4), 1092–1107. <https://doi.org/10.1210/er.2018-00283>
- Yang, Y., Zhao, H., Boomsma, D. I., Ligthart, L., Belin, A. C., Smith, G. D., Esko, T., Freilinger, T. M., Hansen, T. F., Ikram, M. A., Kallela, M., Kubisch, C., Paraskevi, C., Strachan, D. P., Wessman, M., International Headache Genetics Consortium, van den Maagdenberg, A. M. J. M., Terwindt, G. M., & Nyholt, D. R. (2018). Molecular genetic overlap between migraine and major depressive disorder. *European Journal of Human Genetics: EJHG*, *26*(8), 1202–1216. <https://doi.org/10.1038/s41431-018-0150-2>
- Yankner, B. A., Lu, T., & Loerch, P. (2008). The Aging Brain. *Annual Review of Pathology: Mechanisms of Disease*, *3*(1), 41–66. <https://doi.org/10.1146/annurev.pathmechdis.2.010506.092044>
- Yeo, E.-J. (2019). Hypoxia and aging. *Experimental & Molecular Medicine*, *51*(6), 1–15. <https://doi.org/10.1038/s12276-019-0233-3>
- Ying, W. (2008). NAD<sup>+</sup>/NADH and NADP<sup>+</sup>/NADPH in cellular functions and cell death: Regulation and biological consequences. *Antioxidants & Redox Signaling*, *10*(2), 179–206. <https://doi.org/10.1089/ars.2007.1672>
- Young, L. J., & Pfaff, D. W. (2014). Sex differences in neurological and psychiatric disorders. *Frontiers in Neuroendocrinology*, *35*(3), 253–254. <https://doi.org/10.1016/j.yfrne.2014.05.005>

- Yuan, R., Tsaih, S.-W., Petkova, S. B., de Evsikova, C. M., Xing, S., Marion, M. A., Bogue, M. A., Mills, K. D., Peters, L. L., Bult, C. J., Rosen, C. J., Sundberg, J. P., Harrison, D. E., Churchill, G. A., & Paigen, B. (2009). Aging in inbred strains of mice: Study design and interim report on median lifespans and circulating IGF1 levels. *Aging Cell*, 8(3), 277–287. <https://doi.org/10.1111/j.1474-9726.2009.00478.x>
- Zeltser, L. M., & Leibel, R. L. (2011). Roles of the placenta in fetal brain development. *Proceedings of the National Academy of Sciences of the United States of America*, 108(38), 15667–15668. <https://doi.org/10.1073/pnas.1112239108>
- Zhang, D., Jiang, H., Ye, J., Gao, M., Wang, X., Lu, E., Yang, H., Wang, L., & Zhao, S. (2021). A novel lncRNA, RPL34-AS1, promotes proliferation and angiogenesis in glioma by regulating VEGFA. *Journal of Cancer*, 12(20), 6189–6197. <https://doi.org/10.7150/jca.59337>
- Zhang, H., Chen, W., Tan, Z., Zhang, L., Dong, Z., Cui, W., Zhao, K., Wang, H., Jing, H., Cao, R., Kim, C., Safar, J. G., Xiong, W.-C., & Mei, L. (2020). A Role of Low-Density Lipoprotein Receptor-Related Protein 4 (LRP4) in Astrocytic A $\beta$  Clearance. *The Journal of Neuroscience*, 40(28), 5347–5361. <https://doi.org/10.1523/JNEUROSCI.0250-20.2020>
- Zhang, J., & Panthee, D. R. (2020). PyBSASeq: A simple and effective algorithm for bulked segregant analysis with whole-genome sequencing data. *BMC Bioinformatics*, 21(1), 99. <https://doi.org/10.1186/s12859-020-3435-8>

- Zhang, L.-Y., Lin, P., Pan, J., Ma, Y., Wei, Z., Jiang, L., Wang, L., Song, Y., Wang, Y., Zhang, Z., Jin, K., Wang, Q., & Yang, G.-Y. (2018). CLARITY for High-resolution Imaging and Quantification of Vasculature in the Whole Mouse Brain. *Aging and Disease*, *9*(2), 262. <https://doi.org/10.14336/AD.2017.0613>
- Zhu, C., Preissl, S., & Ren, B. (2020). Single-cell multimodal omics: The power of many. *Nature Methods*, *17*(1), 11–14. <https://doi.org/10.1038/s41592-019-0691-5>
- Zhu, Q., Song, L., Peng, G., Sun, N., Chen, J., Zhang, T., Sheng, N., Tang, W., Qian, C., Qiao, Y., Tang, K., Han, J.-D. J., Li, J., & Jing, N. (2014). The transcription factor Pou3f1 promotes neural fate commitment via activation of neural lineage genes and inhibition of external signaling pathways. *ELife*, *3*, e02224. <https://doi.org/10.7554/eLife.02224>
- Zhu, R., Pan, Y.-H., Sun, L., Zhang, T., Wang, C., Ye, S., Yang, N., Lu, T., Wisniewski, T., Dang, S., & Zhang, W. (2019). ADAMTS18 Deficiency Affects Neuronal Morphogenesis and Reduces the Levels of Depression-like Behaviors in Mice. *Neuroscience*, *399*, 53–64. <https://doi.org/10.1016/j.neuroscience.2018.12.025>
- Zhuang, X., Yang, Z., & Cordes, D. (2020). A technical review of canonical correlation analysis for neuroscience applications. *Human Brain Mapping*, *41*(13), 3807–3833. <https://doi.org/10.1002/hbm.25090>
- Zou, R., Zhang, D., Lv, L., Shi, W., Song, Z., Yi, B., Lai, B., Chen, Q., Yang, S., & Hua, P. (2019). Bioinformatic gene analysis for potential biomarkers and therapeutic targets of atrial fibrillation-related stroke. *Journal of Translational Medicine*, *17*(1), 45. <https://doi.org/10.1186/s12967-019-1790-x>

- Zullo, J. M., Drake, D., Aron, L., O'Hern, P., Dhamne, S. C., Davidsohn, N., Mao, C.-A., Klein, W. H., Rotenberg, A., Bennett, D. A., Church, G. M., Colaiácovo, M. P., & Yankner, B. A. (2019). Regulation of lifespan by neural excitation and REST. *Nature*, *574*(7778), 359–364. <https://doi.org/10.1038/s41586-019-1647-8>
- Zuloaga, D. G., Puts, D. A., Jordan, C. L., & Breedlove, S. M. (2008). The Role of Androgen Receptors in the Masculinization of Brain and Behavior: What we've learned from the Testicular Feminization Mutation. *Hormones and Behavior*, *53*(5), 613–626. <https://doi.org/10.1016/j.yhbeh.2008.01.013>